OPTIMIZATION OF APHANAMIXIS BASED BIODIESEL AND ITS COMBUSTION CHARACTERISTICS

MD. RUHUL AMIN

DESSERTATION SUBMITTED IN FULFILMENT OF THE REQUIREMENTS FOR THE DEGREE OF MASTER OF ENGINEERING SCIENCES

FACULTY OF ENGINEERING
UNIVERSITY OF MALAYA
KUALA LUMPUR

2017

UNIVERSITY OF MALAYA

ORIGINAL LITERARY WORK DECLARATION

Name of Candidate: **Md. Ruhul Amin**

Registration/Matric No: **KGA 140020**

Name of Degree: **Master of Engineering Science**

Title of Dissertation: **Optimization of *Aphanamixis* based biodiesel and its combustion characteristics**

Field of Study: **Energy**

I do solemnly and sincerely declare that:

(1) I am the sole author/writer of this Work;
(2) This Work is original;
(3) Any use of any work in which copyright exists was done by way of fair dealing and for permitted purposes and any excerpt or extract from, or reference to or reproduction of any copyright work has been disclosed expressly and sufficiently and the title of the Work and its authorship have been acknowledged in this Work;
(4) I do not have any actual knowledge nor do I ought reasonably to know that the making of this work constitutes an infringement of any copyright work;
(5) I hereby assign all and every rights in the copyright to this work to the University of Malaya ("UM"), who henceforth shall be owner of the copyright in this Work and that any reproduction or use in any form or by any means whatsoever is prohibited without the written consent of UM having been first had and obtained;
(6) I am fully aware that if in the course of making this Work I have infringed any copyright whether intentionally or otherwise, I may be subject to legal action or any other action as may be determined by UM.

Candidate's Signature Date:

Subscribed and solemnly declared before,

Witness's Signature Date:

Name:

Designation:

ABSTRACT

A non-edible vegetable oil source "Pithraj" widely known as "*Aphanamixis polystachya*" (AP) was chosen in the current study considering the high price of edible oil sources and food security. Main forces of this study were to optimize the biodiesel production process from low-quality vegetable oil employing waste eggshell extracted heterogeneous catalyst and evaluate fuel feasibility in an unmodified diesel engine.

A heterogeneous catalyst was extracted and confirmed its activity as a catalyst by various characterization like thermogravimetric analysis (TGA), Fourier transform infrared (FTIR) spectroscopy analysis, scanning electron microscope (SEM), energy dispersive X-ray (EDX) spectroscopy and X-ray powder diffraction (XRD) analysis. The basic strength of the Egg CaO catalyst found to be 9.8<H_<10.1 which is very close to commercially available Pure CaO. This heterogeneous catalyst was introduced at the transesterification step to produce biodiesel which is cost effective as well as eco-friendly. Both the esterification and transesterification chemical process for biodiesel yield was optimized through response surface methodology (RSM). Product yield after degumming stage, esterification and transesterification stage were found 97.12%, 96.53% and 97.5% respectively, which is 91.4% of crude oil. When optimal reaction condition for esterification was 152.79 % (v/v of oil) methanol, 0.80% (v/v of oil) catalyst loading and 60.29 °C reaction temperature for 3 hours. The optimal condition for transesterification was found at 35.59 % (v/v of esterified oil) methanol, 1.46% (w/w of esterified oil) catalyst loading and 65.10 °C reaction temperature for 2 hours. Properties of the biodiesel and its blends with diesel conform the ASTM specification.

Finally, the produced biodiesel blends were tested in a single cylinder diesel engine at various operating condition such as (a) constant torque, variable engine speed (b) constant speed, variable torque and (c) constant speed with advancing and retarding

injection timing. Combustion, performance and exhaust gas emission characteristics were investigated by 20% (v/v) and 30% (v/v) biodiesel-diesel blends and compared with ordinary diesel (OD) as well as the corresponding blends of "*Millettia pinnata"* biodiesel. AP diesel-biodiesel blends provide slightly decreased brake power (BP), brake thermal efficiency (1.22-0.33%) and increased brake specific fuel consumption (about 1.17-2.09%) compared to OD. In-cylinder pressure (ICP), heat release rate (HRR), mass fraction burned (MFB) and ignition delay (ID) were found to inferior in quality for AP on OD. The average CO and HC emissions were reduced to an extent of 13.90-14.27% and 4.03-10.09% for AP biodiesel blends, whereas NO, CO_2 emission was found to be 2.93-5.47% and 8.61-17.23% respectively, higher than OD.

ABSTRAK

Selain itu, ia boleh dicampurkan dengan diesel dalam apa-apa nisbah dan boleh digunakan tanpa mengubah reka bentuk enjin. Satu sumber minyak sayuran, Pitraj, yang tidak boleh dimakan dikenali sebagai "*Aphanamixis polystachya*" (AP) telah dipilih dalam kajian semasa memandangkan harag sumber minyak yang boleh dimakan adalah tinggi beserta keselamatan makanan. Fokus utama kajian ini adalah untuk mengoptimumkan proses pengeluaran biodiesel dari minyak sayuran berkualiti rendah yang menggunakan pemangkin heterogen daripada ekstrak kulit telur terbuang dan menilai kebolehlaksanaan minyak dalam enjin diesel yang tidak diubahsuai. Satu pemangkin heterogen telah diekstrak dan disahkan keaktifannya sebagai satu pemangkin oleh pelbagai ujian pencirian seperti analisis Termogravimetri (TGA), analisis spektroskopi inframerah transformasi Fourier (FTIR), mikroskop elektron imbasan (SEM), analisis spektroskopi serakan tenaga sinar-X (EDX) dan pembelauan serbuk sinar-X (XRD). Kekuatan alkali bagi pemangkin kalsium oksida kulit telur telah direkodkan pada nilai 9.8 <H_<10.1 di mana nilainya hampir sama dengan kalsium oksida asli komersial. Pemangkin heterogen ini telah digunakan pada langkah transesterifikasi untuk menghasilkan biodiesel pada kos yang efektif dan mesra alam. Kedua-dua proses kimia esterifikasi dan transesterifikasi untuk menghasilkan biodiesel ini telah dioptimumkan melalui kaedah gerak balas permukaan (RSM). Produk terhasil daripada proses penyahgaman, esterifikasi dan transesterifikasi adalah 97.12%, 96.53% dan 97.5%, dimana 91.4% adalah minyak mentah. Keadaan tindak balas optimum untuk esterifikasi adalah 152.79% (v/v minyak) metanol, pemuatan pemangkin 0.80% (v/v minyak) dan suhu tindakbalas pada 60.29 ^{o}C selama 3 jam. Keadaan tindak balas optimum untuk transesterifikasi adalah 35.59% (v/v minyak telah diester) metanol, pemuatan pemangkin 1.46% (v/v minyak telah diester) dan suhu tindakbalas pada 65.10

^{o}C selama 2 jam. Sifat-sifat biodiesel dan campurannya bersama diesel telah dikenalpasti dengan piawai ASTM.

Akhir sekali, campuran biodiesel yang terhasil telah diuji menggunakan sebuah enjin diesel satu silinder pada keadaan operasi yang berbeza seperti (a) tork malar, kelajuan enjin berbeza, (b) kelajuan eenjin malar, tork berbeza (c) kelajuan enjin malar dengan pemasaan pancitan terlajak dan terencat. Pembakaran, prestasi dan ciri-ciri pelepasan pencemar ekzos telah dikaji menggunakan campuran diesel-biodiesel 20% (v/v) dan 30% (v/v) dan dibandingkan dengan diesel tulen (OD) bersama campuran biodiesel "*Millettia pinnata"*. Campuran diesel- biodiesel AP menunjukkan sedikit pengurangan pada kuasa brek (BP), kecekapan haba brek (1.22-0.33%) dan meningkatkan penggunaan bahan api tentu brek (iaitu 1.17-2.09%) jika dibandingkan dengan OD. Tekanan silinder dalaman (ICP), kadar pelepasan haba (HRR), pecahan jisim terbakar (MFB) dan lengah pencucuhan (ID) didapati lebih rendah dalam kualiti untuk AP pada OD. Purata pelepasan karbon mono-oksida dan hidrokarbon telah berkurangan, masing-masing kepada tahap 13.90-14.27% dan 4.03-10.09% untuk campuran biodiesel AP, manakala pelepasan nitrogen monoksida dan karbon dioksida telah meningkat berbanding OD, masing-masing pada 2.93-5.47% dan 8.61-17.23%.

ACKNOWLEDGEMENTS

At first Alhamdulillah and thank you to the Almighty Allah for giving the ability and strength to complete this thesis regardless of many problems faced throughout the period of my study.

I would like to express my sincere gratitude to my supervisor (s), Professor Ir. Dr. Masjuki Bin Haji Hassan and Associate Professor Dr. Md. Abul Kalam for their constant guidance, valuable advice, and inspiration throughout the progress of this project. Without their direct support and persistent involvement in this work, completion of research and thesis would not be an easy task.

I would also like to extend my gratitude to all faculty members in the Department of Mechanical Engineering of the University of Malaya, Kuala Lumpur and all my colleagues. In particular, I would like to thank I. M. Rizwanul Fattah, Shancita Islam, Ali Shahir Shawkat and Yew Heng Teoh for their assistance during my laboratory work. I also would like to thank my colleagues of Centre for Energy Sciences (CFES) for their encouragement. I wish to express my special thanks to my beloved parents, my siblings, for their endless love and encouragement. My heartfelt appreciation goes to those who have indirectly contributed to this research.

I would like to express my gratitude to Ministry of Higher Education (MOHE) for financial support from the University of Malaya through project High Impact Research (HIR) grant (UM.C/HIR/MOHE/ENG/07). Last but by no means the least, I would like to thank the government of the People's Republic of Bangladesh for providing me high-quality education from primary school to university as well as fostering my stay overseas to pursue this research.

TABLE OF CONTENTS

LIST OF FIGURES

LIST OF TABLES

LIST OF ACRONYMS

ANOVA	:	Analysis of Variance
AP	:	*Aphanamixis polystachya*
AP20	:	20:80 (v/v) *Aphanamixis polystachya* biodiesel to Diesel
AP30	:	30:70 (v/v) *Aphanamixis polystachya* biodiesel to Diesel
APME	:	*Aphanamixis polystachya* Methyl Ester
ASEAN	:	Association of Southeast Asian Nations
ASTM	:	American Society of Testing Materials
aTDC	:	After Top Dade Center
AV	:	Acid Value
BDC	:	Bottom Dead Centre
BET	:	Brunauer–Emmett–Teller
BMW	:	Bayerische Motoren Werke
BP	:	Brake Power
BSFC	:	Brake Specific Fuel Consumption
bTDC	:	Before Top Dade Center
BTE	:	Brake Thermal Efficiency
CAPO	:	Crude *Aphanamixis polystachya* Oil
CAPO	:	Crude *Aphanamixis polystachya* Oil
CCD	:	Central Composite Design
CCI	:	Calculated Cenatne Index
CFPP	:	Cold Filter Plugging Point
CI	:	Compression Ignition
CMPO	:	Crude *Millettia pinnata* Oil
CN	:	Cetane Number
CO	:	Carbon Monoxide
CO_2	:	Carbon Dioxide
COV	:	Coefficient of Variance
CP	:	Cloud Point
CV	:	Calorific Value
DAQ	:	Data Acquisition
DI	:	Direct Injection
DoE	:	Design of Experiment
EDX	:	Energy Dispersive X-ray spectroscopy

EGT	:	Exhaust Gas Temperature
FAC	:	Fatty Acid Composition
FAEE	:	Fatty Acid Ethyl Ester
FAME	:	Fatty Acid Methyl Ester
FFA	:	Free Fatty Acid
FP	:	Flash Point
FTIR	:	Fourier Transform Infrared Spectroscopy
GC	:	Gas Chromatographer
Gt	:	Gigatonnes
h	:	Hour
HC	:	Unburned Hydrocarbon
HHV	:	Higher Heating Value
HRR	:	Heat Release Rate
IC	:	Internal Combustion
ICP	:	In-cylinder Pressure
ID	:	Ignition Delay
IEA	:	International Energy Agency
IGT	:	Injection Timing
IUPAC	:	International Union of Pure and Applied Chemistry
IV	:	Iodine Value
kW	:	Kilo Watt
LHV	:	Lower Heating Value
Max.	:	Maximum
MFB	:	Mass Fraction Burned
Min.	:	Minimum
ml	:	Milliliter
MP	:	*Millettia pinnata*
MP20	:	20:80 (v/v) *Millettia pinnata* biodiesel to Diesel
MP30	:	30:70 (v/v) *Millettia pinnata* biodiesel to Diesel
MPME	:	*Millettia pinnata* Methyl Ester
Mtoe	:	Million tons of oil equivalent
NO	:	Nitric Oxide
NO_2	:	Nitrogen Dioxide
NO_X	:	Oxides of Nitrogen
OD	:	Ordinary Diesel or Fossil Diesel

OECD	:	Organization for Economic Co-operation and Development
PM		Particulate Matter
PP	:	Pour Point
ppm	:	Parts per Million
PRESS	:	Predicted Residual Error Sum of Squares
rpm	:	Revolution per Minute
RSM	:	Response Surface Methodology
SAE	:	Society of Automotive Engineers
SEM	:	Scanning Electron Microscope
SN	:	Saponification Number
SOC	:	Start of Combustion
SOI	:	Start of Injection
tcm	:	Trillion Cubic Metres
TGA	:	Thermogravimetric Analysis
XRD	:	X-ray Powder Diffraction
°C	:	Degree Celsius
°CA	:	Degree Crank Angle
µm	:	Micrometer
v/v	:	Volume percentage
w/w	:	Weight percentage
g/kWh	:	Gram per Kilo Watt Hour
cc	:	Cubic Centimeter
mb/d	:	Million Barrels per Day
mboe/d	:	Million Barrels of Oil Equivalent per Day

CHAPTER 1: INTRODUCTION

1.1 Overview

Energy is an essential part of our daily life activities and the main driving force of socio-economic development. The rapid growth of population, as well as the modernization of society, increase the consumption of energy. World population will add another 1.8 billion to its current figure by 2040 and will reach approximately 9 billion Selin (2013). The gross domestic product (GDP) will be around 140% in 2040 compared with 2010 because of the projected global population growth. Considering to this tendency, the predicted global energy demand will increase by around 35% in 2040 compared to the demand in 2010 which is equivalent to 1.1% of average growth (Selin, 2013). ASEAN regional total primary energy consumption was around 444 Mtoe in the year of 2011 and the projected consumption will increase to 1186 Mtoe by 2040. Malaysia and Thailand population growth will slow down from 2025; their primary energy consumption rate will be slower than other ASEAN countries. The graphical representation of ASEAN primary energy consumption by country and Malaysia energy consumption with corresponding sectors are illustrated in Figure 1.1. However, the total energy resources are limited regarding petroleum fuel reservation. To fulfill additional energy demands for the growing people, additional and alternative resources are needed to be discovered to supply energy for human consumption and civilization. Figure 1.2 (a) shows the world historical and projected energy consumption and projection till 2040 for both OECD and Non-OECD countries and Figure 1.2 (b) represents the consumptions and projections by energy sources. Coal demand growth is driven by the stringency of carbon policies and for that, it rises at a slower rate about 0.5% per year between 2012 to 2040.According to world energy outlook, in the New Policies Scenario, the demand grows by 37% to 2040 on planned policies of which demand of oil rising by 14 mb/d, to

reach 104 mb/d, the demand of gas consumption is 5.4 tcm. In the New Policies Scenario, world electricity demand increases by almost 80% over the period 2012-2040. Fossil fuels continue to dominate the power sector, although their share of generation declines from 68% in 2012 to 55% in 2040 (Sieminski, 2014).

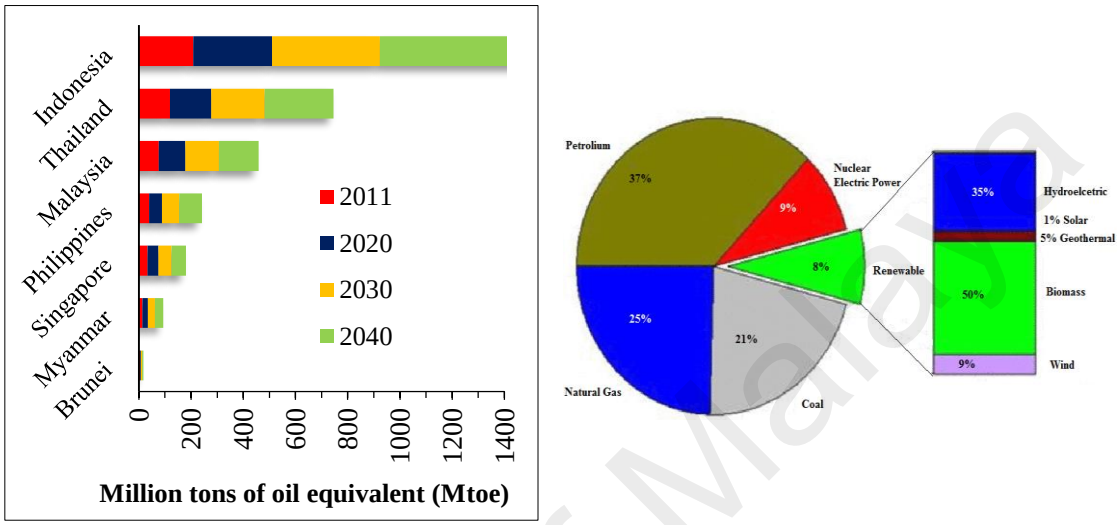

Figure 1.1: ASEAN primary energy consumption (a) projection by country (b) Malaysia energy consumption

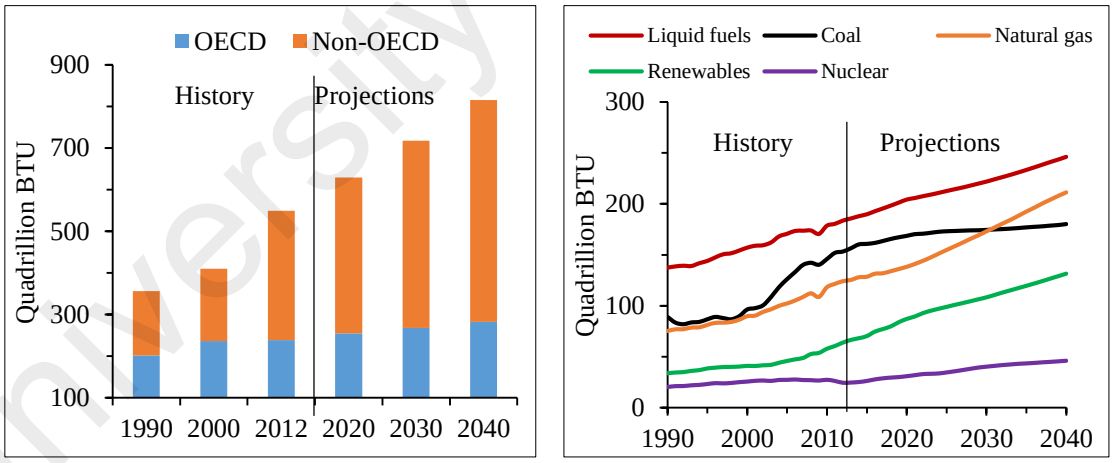

Figure 1.2: World energy consumption by (a) origin (b) energy source [International Energy Outlook-2016]

Classification of energy sources and their contribution towards global energy consumption in different sectors in ASEAN can be illustrated by the Figure 1.3.

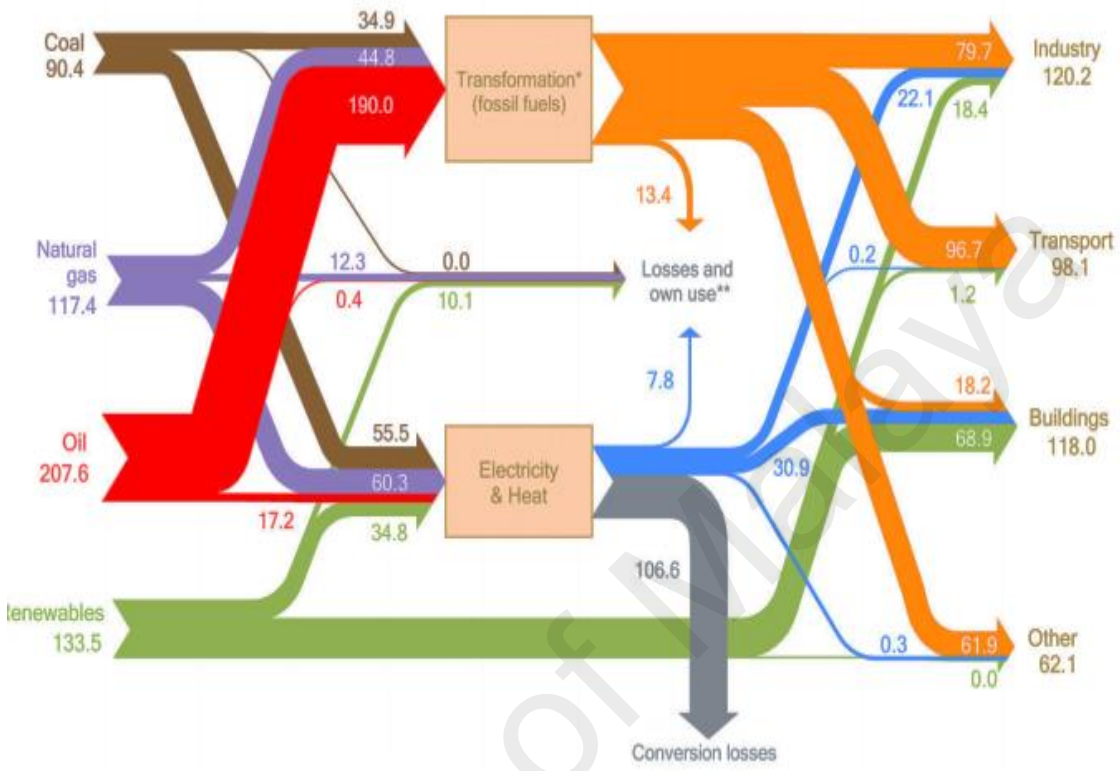

Figure 1.3: ASEAN primary system (in Mtoe)
[International Energy Agency, 2015]

According to Navigant report, more than 1.2 billion vehicles are on the world's roads today, with nearly 98% being powered by blends of gasoline or diesel. In 2004, transport energy use amounted to 26% of total world energy use and world transport energy use is projected to increase at the rate of about 2% per year (Ribeiro & Zhou, 2007). Fossil fuels are the main contributor of carbon dioxide (CO_2), nitrogen oxide (NO_x), volatile organic compounds (VOC) and hydrocarbons (HC). In 2004, the transport sector produced 6.3 Gt CO_2 emissions (23% of world energy-related CO_2 emissions), but now road transport is liable for about 74% of total transport CO_2 (Ribeiro & Zhou, 2007). CO_2 emissions from the power sector rise from 13.2 Gt in 2012 to 15.4 Gt in 2040, retaining a share of around 40% of global emissions over the period (U. S. Energy Information Administration, September 9, 2014). According to world energy outlook 2014, the

emission will rise by 20%. This alarming situation is putting the world on track for a long-term global temperature increase of 3.6°C. Moreover, it is believed that climate change, acid rain and smog are currently the most pressing global environmental problems that are attributed to burning fossil fuels. According to world energy outlook 2014, the share of renewables in total power generation rises from 21% in 2012 to 33% in 2040. Biofuels use more than tripled, rising from 1.3 million barrels of oil equivalent per day (mboe/d) in 2012 to 4.6 mboe/d in 2040, by which time it represents 8% of road-transport fuel demand. Moreover, the IEA assesses that biofuels – liquid and gaseous fuels derived from biomass (organic material derived from plants and animals).As it is one of the key technologies to reduce CO_2 emissions and reduce dependency on liquid transport fuels.The predicted global share of biofuel in total transport fuel would grow from 2% today to 27% in 2050.

Nowadays, the most compelling technological concern of both energy demand and supplying issues are establishing the successor of fossil fuel-derived energy resources. Thus, biofuels especially, biodiesels are receiving significant attention because of these environmental as well as energy concerns. The use of biodiesel is becoming popular due to its adaptation with current transportation infrastructure and requires modification of minimal for its use. Today, biofuels provide around 3% of total road transport fuel globally (on an energy basis), and considerably higher shares are achieved in certain countries as reported by International Energy Agency (IEA) (Miller, 2011).

1.2 Background of the research

Biodiesel, which refers to the fatty acid alkyl esters (FAAEs), are derived from lipid substances originated from resources like vegetable oil, animal fats, waste greases, recycled cooking oils, etc. However, their use raises many concerns such as food versus fuel crisis, major environmental problems such as serious destruction of vital soil resources, deforestation and usage of much of the available arable land. Moreover, in the

last ten years, the prices of vegetable oil plants have increased dramatically which will affect the economic viability of biodiesel industry (Balat, 2011b; Balat & Balat, 2010; Deng et al., 2011).

Biodiesel has recently become a popular research field because of its renewability, biodegradability, nontoxicity, and carbon neutrality. The application is growing with the energy and the proclivity demand of energy consumption through modernization has encountered a serious threat due to the waning character of fossil fuels. Various sectors, for instance, industry, transport, agriculture, domestic, etc. require energy from sources like wood, coal, petroleum products, nuclear power, solar, wind, etc. (Kumar & Chauhan, 2013). Currently, more than 80% energy demand largely depends on fossil fuels (Atabani et al., 2013). The deep concerned about fossil fuels is its toxic pollutants generation that linked to global warming, climate change and even some impasse diseases (Aransiola et al., 2014). A myriad of research has been actuated by researchers to compete for this critical situation as an alternative to fossil fuels and eco-friendly condition.

Current world energy situation combined with its adverse effect on the environment. Biodiesel is becoming increasingly popular in Southeast Asian countries as a replacement for petroleum-based diesel in transportation and power generation. Malaysia and Indonesia are the two largest biofuel producers in Asia. The Malaysian government started a palm oil biodiesel program in 1982 and has been trying to implement a B5 (5% processed palm oil and 95% diesel) blend for vehicles and industrial sectors. The countries, that have progressively embarked on higher biodiesel blends include Indonesia (B20), the United States (up to B10 in some states), Colombia (B10), Argentina (B10), Brazil (B8) and France (B8) ("Malaysian Biodiesel Association," Access date 29th December 2016). The five states will need only 200,000 tons of biodiesel per year to be implemented. This is about 40 % of the 500,000 tons per year of biodiesel required for nationwide implementation (www.mdv.com.my).

Statement by BMW Group Malaysia MD and CEO Alan Harris BMW Malaysia reported "B10 biodiesel not good for engines" although the modern diesel engines are suited to run on B7 biodiesel. Diesel passenger vehicles usually have a maximum B7 rating written on the fuel cap. B5 biodiesel was rolled out in Malaysia in June 2011 (Paultan.org, 2011). Currently, all diesel fuels sold in Malaysia carry a B7 biodiesel blend. It has been clarified by the Ministry which is subsequently backed up by BHPetrol and Petronas that even if the B10 biodiesel mandate comes into force, Euro 5 diesel will remain on the B7 blend as it is exempted from the mandate (Jonathan, 2017). It also said that when it does enter petrol stations, B10 biodiesel is set to bring about significant and impactful environmental benefits, particularly with regards to the reduction of greenhouse gas emissions. According to Malaysian Plantation Industries and Commodities Minister, "PB10 will be launched nationwide by 2017. They are formulating action plans with the help of Malaysian Palm Oil Board, which includes engine performance, emission, thermodynamics and tribology analysis of PB10 or higher blending ratio as required by the Original Equipment Manufacturers, especially on engine warranty. So, these are the reasons for choosing 20% and a higher blend of biodiesel.

1.3 Problem statement

Multiple research explicitly recognizes biodiesel that the utilization of biodiesel can be the complementary substitute of fossil diesel due to its eco-friendly nature. Biodiesel can be engendered from a wide variety of vegetable oils. All vegetable oil sources are not enough to meet the incremental energy demand. Statics shows only 6% of diesel demand would be satisfied by biodiesel if all U.S. soybean production were dedicated to producing biodiesel (Atabani et al., 2013). Only a few are commercially used among the vegetable oils because of low quality and availability of feedstock (Saxena et al., 2013b). More than 10% free fatty acid (FFA) and 3000 ppm water containing in crude oil are treated as a low-quality biodiesel feedstock in biodiesel technology. Water can cause poor reactions

and high soap content which leads to poor conversions and difficulty washing the fuel. Among the sources available such as edible and non-edible vegetable oils, waste or recycled oil animal fats (Madhu et al., 2014; Zeng et al., 2014) algae, halophytes, sewage sludge for biodiesel production, vegetable oils are found dominant because of numbers of oil-bearing crops about 350 are available in nature (Silitonga et al., 2013) and can be produced in large scale easily and the regional climate largely affects the feedstock available for biodiesel production. In this point of view, a new or low-quality biodiesel feedstock is considering as the high potential resource. Although the low-quality non-edible feedstocks are cheaper, compare to edible sources but still suffering from the production technology regarding processing cost i.e. chemical and energy consumption. However, the production process for the special sources needs to be upgraded consequently. Besides, the rapid use of chemical during the production process has an impact on the environment and the living organism on the earth. Thus bio-oil to engine fuel conversion from low-quality feedstocks is quite challenging task regarding the chemical utilization and reusability (Knothe, 2007). Therefore, research is still required for new and low-quality biodiesel feedstock which can contribute to energy demand.

1.4 Objectives of this study

The aim of the study is to utilize the waste material and minimize the use of the chemical in biodiesel production without sacrificing the production yield, from a non-edible, low-quality vegetable oil source. In this research work, two potential oil sources namely *Aphanamixis polystachya* (Pithraj) and *Millettia pinnata* (Karanja) have been considered and utilized as the promising and potential feedstock for biodiesel. A heterogeneous catalyst was extracted from waste eggshell and characterized its properties for confirming the catalytic activity. Production process parameter has been optimized from low-quality *Aphanamixis polystachya* feedstocks employing eggshell extracted catalyst. Physicochemical properties of produced biodiesel and their blends with diesel

have been measured. Finally, the biodiesel blends are evaluated and compared with diesel in the context of performance, combustion and emission characteristics in a diesel engine with the different operating condition. The considered aims of the study are listed as follows:

1. To extract and characterize a heterogeneous catalyst from the waste eggshell.
2. To optimize the biodiesel production yield from low-quality vegetable oil.
3. To study combustion and exhaust pollutant emission in an IC engine.

1.5 Scope of study

This study aims to utilize a waste material to wealth in biodiesel production technology from a non-edible feedstock which can minimize the production cost without sacrificing the food security. Based on the fact, this study is categorized as the catalyst extraction, process optimization and engine testing. The strength of the extracted catalyst has been confirmed through various characterization test. A useful process optimization tool namely response surface methodology (RSM) has been incorporated to maximize the production yield with minimum chemical consumption. Produced biodiesels major properties and have been measured and compared with fossil diesel. Finally the analysis of combustion parameter like in-cylinder pressure, heat release rate, combustion duration, mass burned fractions as well as the ignition delay discussed. The novelty of this study is the production process parameter optimization of the low-quality non-edible feedstock employing waste eggshell extracted heterogeneous catalyst. The quality was evaluated in the context of performance, combustion and emission characteristics in a diesel engine. Other aspects such as improvement of catalyst, techno-economic analysis, chemical recovery and catalyst reuse have not been covered in this research. Also, some uncontrolled emission not taken into account in this investigation.

1.6 Organization of thesis

This dissertation is comprised of five chapters. The organization of each chapter is set out as follows:

Chapter 1 presents a short overview of the research topic. It started with the overview of current and future energy scenario and followed by background research. Which refers the importance of utilization biodiesel as alternative and sustainable sources together with specific goals to be achieved. Finally, objectives and scopes of this study are discussed.

Chapter 2 gives a brief of utilization heterogeneous catalyst that associated with biodiesel production technology. This section also compares advantages and disadvantages of various production technology and challenges in biodiesel technology. Application of biodiesel as alternative fuel in the automotive engine has been discussed.

Chapter 3 explains in detail the materials and experimental techniques to achieve the objectives of this study. It including the heterogeneous catalyst development process, characterization, biodiesel process parameter optimization and physicochemical properties characterization. Subsequently, engine test bed preparation and other measuring procedure along with the calibration to evaluated the biodiesel sustainability in an unmodified direct injection diesel engine.

Chapter 4 is dedicated to showing all the results that have been obtained from the experimental work and present the findings of the study followed by a detailed discussion and analysis of these findings besides comparing them with the previous studies. It also includes a details an experimental design for response surface methodology (RSM) optimization process with statistical analysis for justifying the model adequacy and desirability.

Chapter 5 provides the conclusion of the findings in the light of the research objectives and puts recommendations for the future studies.

CHAPTER 2: LITERATURE REVIEW

2.1 Introduction

This chapter reviews major publications and reports that will provide insight and understanding about the topic and related issues. This section first introduced about concept about biodiesel, its available feedstock and different production technology available till to date. Based on this study several individual factors that are affecting the biodiesel production are discussed. The role of heterogeneous catalyst in biodiesel production technology is discussed. Then a large number of selective literature is reviewed regarding the production optimization process, especially on the selective biodiesel feedstocks. Finally, research on engine performance and emission fueled with biodiesel blends are discussed.

2.2 Biodiesel and its production technology

Biodiesel refers to a vegetable oil or animal fat-based diesel fuel consisting of long-chain alkyl (methyl, ethyl, or propyl) esters. It is made by chemically reacting lipids (e.g., vegetable oil, animal fat) with an alcohol producing fatty acid esters. Typically biodiesel contains long chain carbon molecules with hydrogen atoms similar to petroleum diesel with an additional ester functional group (-COOR) connected which is almost three times larger than petroleum diesel molecules. Biodiesel consists of hydrocarbon molecules that range in size from 8 to 21 carbon atoms. Because of its atomic size and structure vegetable oil becomes gels in cold weather and thus it becomes quite difficult to use directly in the engine. The molecular structure of (a) petroleum diesel (b) biodiesel and (c) vegetable oil is shown in Figure 2.1.

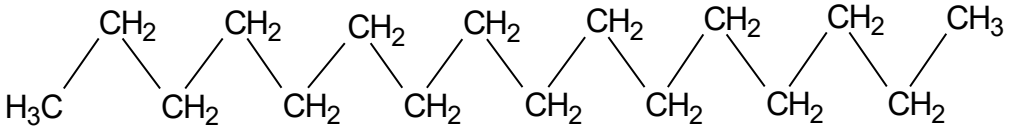

(a) Petroleum diesel

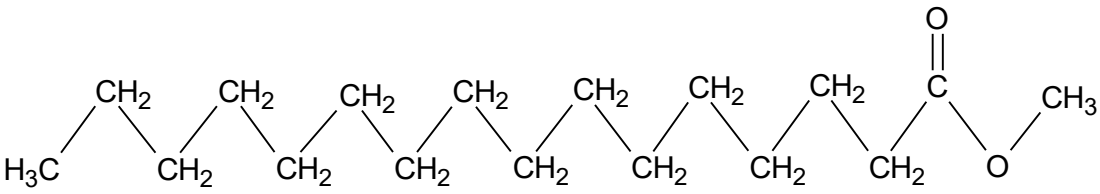

(b) Biodiesel

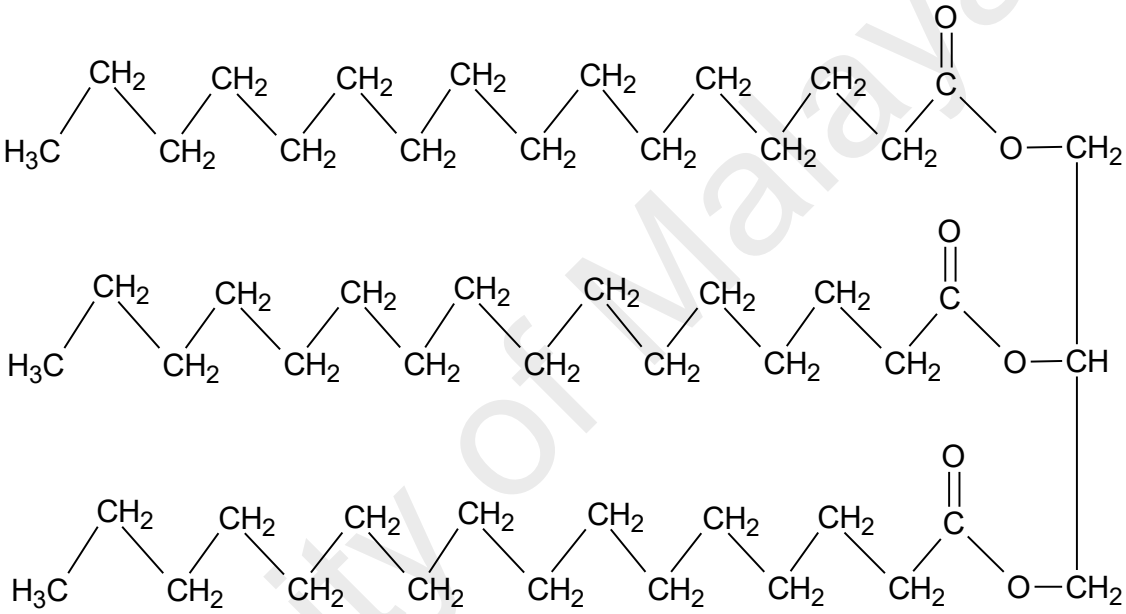

(c) Vegetable oil or Triglyceride

Figure 2.1: Molecular structure of (a) Petroleum diesel (b) Biodiesel (c) Vegetable oil

Petroleum diesel is obtained through the fractional distillation of crude oil whereas biodiesel obtained from the successive chemical reaction of triglycerides i.e. vegetable oil. Triglycerides are initially diminished to diglycerides, then monoglycerides and finally converted at long last lessened to fatty acid ester. The step by step reaction mechanism of producing the monoglycerides from triglycerides or vegetable oil is briefly showing in Figure 2.2 where R represents an alkyl group, R^1, R^2, R^3 fatty acid chain and k_1, k_2, k_3, k_4, k_5, k_6 represents catalyst.

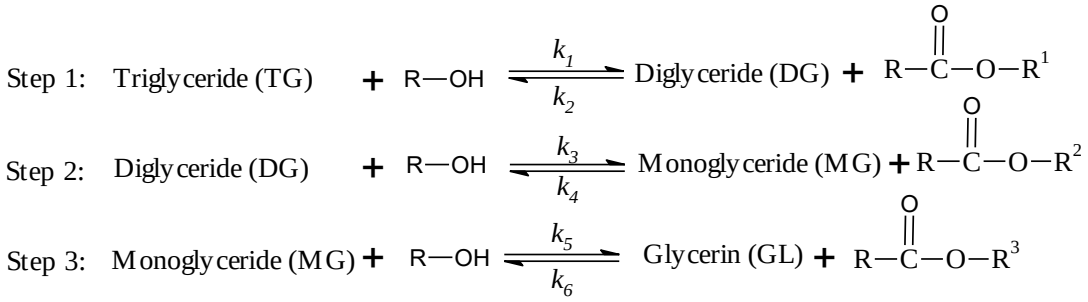

Figure 2.2: Step by step triglyceride to monoglycerides production of vegetable oils

2.3 Biodiesel production process

There are several techniques available for obtaining biodiesel from the different feedstock. For an example transesterification through radio frequency, microwave, ultra-sonication, alcohol reflex temperature & alcohol supercritical temperature. Extensively all of the biodiesel production techniques can be classified in pyrolysis or thermal cracking, esterification & transesterification process.

2.3.1 Thermal cracking (pyrolysis)

Pyrolysis indicates the shifting or transformation of one substance to another by employing heat. The catalyst is introduced to the process for minimizing conversion time. In other words, pyrolysis refers to the transformation of one organic material into another by thermal decomposition with the presence of desired catalyst and absence of air or oxygen (Sonntag, 1979). Vegetable oil, animal fats, natural fatty acids, or methyl ester of fatty acids may be used as pyrolysis material. Transformation of vegetable oil and animal fat into producible biodiesel feedstock is a potential technology using thermal cracking reaction. This innovation is particularly encouraging in areas where the hydro preparing industry is entrenched because this innovation is fundamentally the same as that of traditional petroleum refining (Maher & Bressler, 2007). Dissimilar lower hydrocarbons are obtained by pyrolysis of vegetable oil, which could be used as fuel. The properties of treated pyrolytic synthesis fuel derived from vegetable oil are significantly near to that of diesel fuel. Thus, numerous scientists have stated that this fuel is a suitable alternative for

diesel (Lappi & Alén, 2011; Maher & Bressler, 2007). Based on its operating conditions, the pyrolysis process can be classified (Atabani et al., 2013) as, conventional pyrolysis, fast pyrolysis, and flash pyrolysis. The mechanism of thermal decomposition of triglycerides is prone to complexity because of its various possible reaction and chemical structure, which depends on the reaction condition or pathway. A simple systematic reaction mechanism of thermal decomposition of triglyceride is represented in Figure 2.3. (Lima et al., 2004). Scientists have performed experiments on soybean, palm, and castor oils to determine the optimum distillation temperature, thereby obtaining fuel properties similar to those of petroleum-based fuel (Atabani et al., 2013). Comparing to the other conventional process on the yield the equipment used for thermal cracking and pyrolysis is costly. By contrast, this process sometimes produces low-value materials and more gasoline than diesel fuel (Ma & Hanna, 1999).

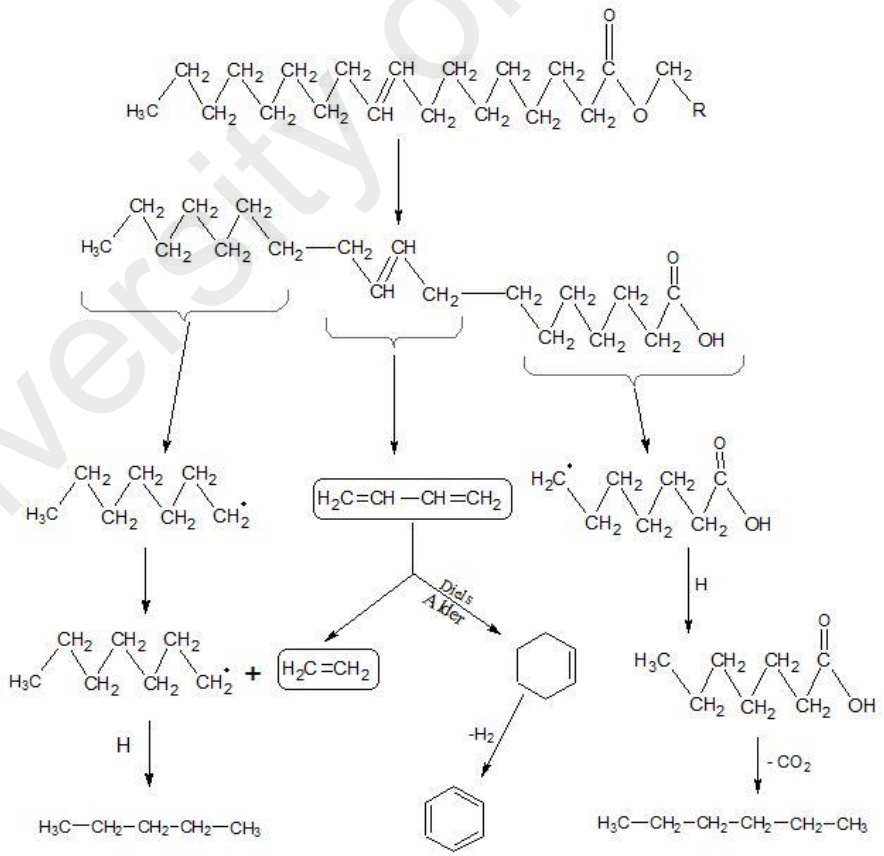

Figure 2.3: The mechanism of thermal decomposition of triglycerides

Nevertheless, pyrolysis process requires high temperatures ranging from approximately 300 °C to 500 °C and product characterization is difficult because of differences in the reaction pathway and products acquired from the reactants. Lima et al. (2004) employed zeolite as a catalyst during pyrolysis of soybean oil and found that the reaction temperature was approximately 400 °C in the N_2 flow. The obtained products were olefins, paraffin, carboxylic acids, and aldehydes. Şensöz et al. (2000) inspected the effect of particle size on the pyrolysis of rapeseed. By changing the particle size of rapeseed in the scope of 0.224–1.8 mm, they observed that the yields of products are not dependent on particle size. More than 30 compounds were detected from the pyrolysis of Macauba fruit, and a number of main products diminished by increasing the pyrolysis temperature (Fortes & Baugh, 2004).

2.3.2 Esterification

An esterification reaction is one where an ester is produced from one or two other organic substances. The most common method to produce ester is by chemically reacting an organic acid (carboxylic acid) and alcohol (methanol) with the help of an acid catalyst. Esterification can be performed on a vegetable oil or animal fat (triglyceride) with methanol or methanol (short chain alcohol) to produce biodiesel, especially where considerable quantities of free fatty acids (FFAs) are present. These include byproducts of waste oils, non-edible oils, animal oils, and refined vegetable oils. Such oils possess considerable quantities of saturated fatty acids, specifically stearic acid (IUPAC name: octadecanoic acid), which contains 18 carbon chains. In some cases, the homogeneous acid-catalyzed reaction is not viable because it may produce corrosion and environmental problems. By contrast, heterogeneous reactions do not show corrosive behavior. Also, heterogeneous reactions are easier to use for splitting products, diminishing wastewater quantity, and lowering process instrumentation, expenses, time, and environmental effects. Thus, the heterogeneous acid-catalyzed reaction is preferred for esterification

reactions. Such catalysis plays a significant role in producing cleaner and more profitable biodiesel by esterification. Thus chemical process employing heterogeneous catalyst is the most acceptable to researchers for creating biodiesel by esterification (Liu et al., 2015).

2.3.3 Transesterification

Producing biodiesel from the transesterification reaction with the help of a catalyst is a highly favored method. The transesterification reaction for biodiesel production can be performed using various methods and is broadly described as the addition of alcohol (generally methanol or ethanol) with lipids (vegetable oil, algal oil or animals fat) in the presence of a acid catalyst or base catalyst (Leung et al., 2010). Outlines of the transesterification reactions for fatty acid methyl ester (FAME) and fatty acid ethyl ester (FAEE) are shown in Figure 2.4 (a) and (b), respectively, where R^1, R^2, and R^3 represent mixture of long fatty acid chains (Park et al., 2010).

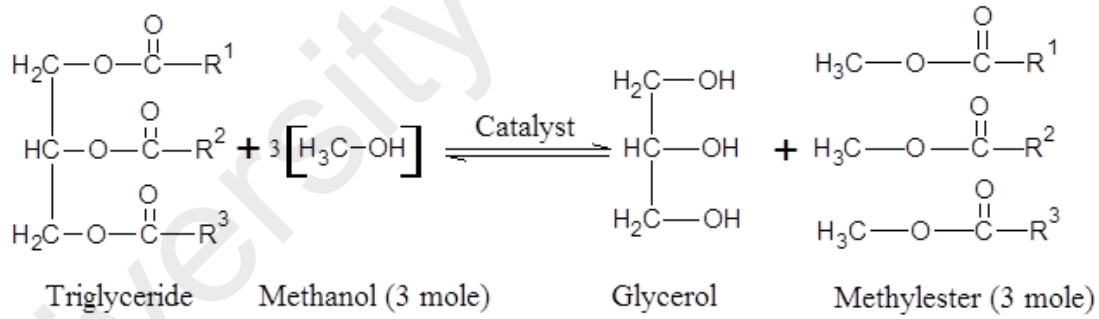

(a) Fatty acid methyl ester (FAME)

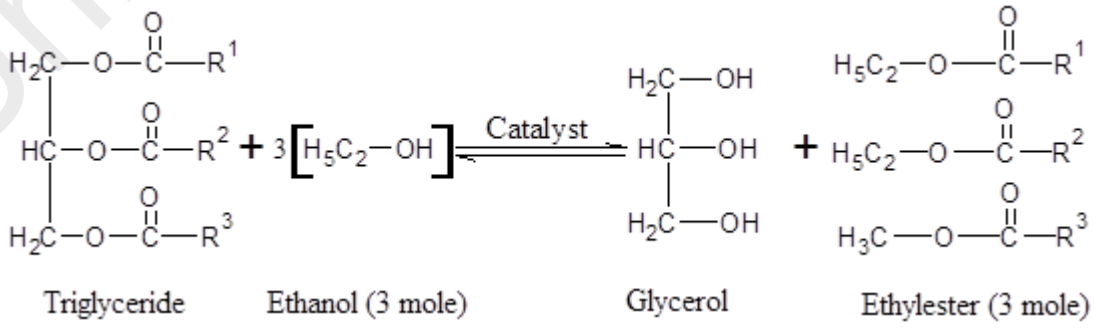

(b) Fatty acid ethyl ester (FAEE)

Figure 2.4: Chemistry of transesterification reaction for glyceride to biodiesel production. (a) FAME (b) FAEE.

Biodiesel could be produced in a single step or two step, depending upon its FFAs contains and water content in it. The higher FFAs content indicates the higher acid value of the feedstocks. Crude oil with a higher acid value is first esterified with an acid catalyst and then transesterified with the suitable base catalyst. A flow diagram of laboratory scale or fixed bed transesterification biodiesel production process is presented in Figure 2.5.

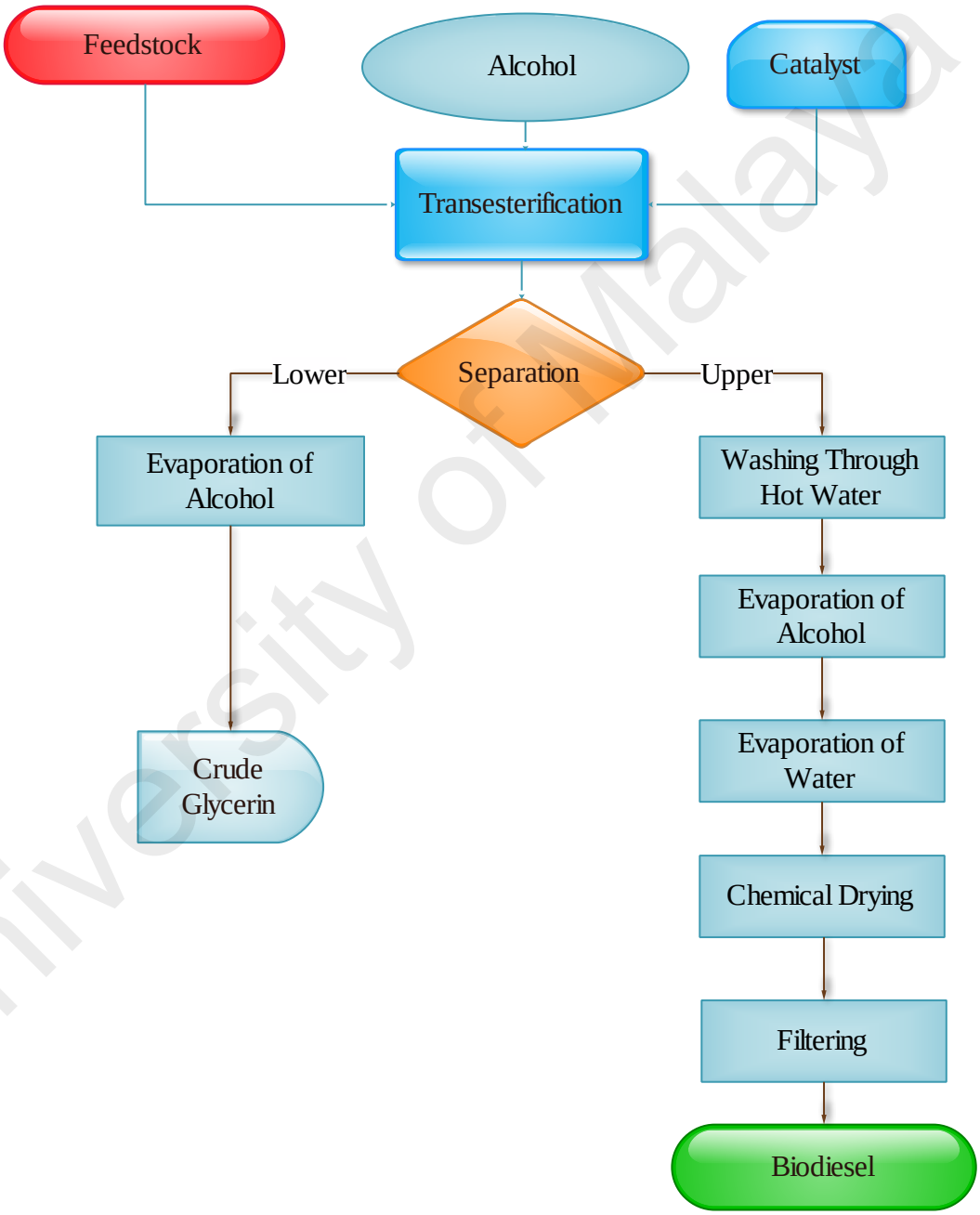

Figure 2.5: Biodiesel production flow chart for laboratory scale (Single Step)

2.3.4 Microwave-assisted transesterification technology

Microwave irradiation or microwave-assisted transesterification is a technique where an electromagnetic microwave is used to heat up the system. Electromagnetic wave frequencies ranging from 0.3 GHz to 300 GHz, which are relatively low in the electromagnetic spectrum, are used to produce energy (Kapilan & Baykov, 2014). During microwave irradiation, the bonds are neither formed nor broken. However, the energy is rapidly transferred to the sample. A microwave is integrated with the process after the mixture (methanol, feedstock, and catalyst) chamber. Utilization of electromagnetic microwaves has drawn significant attention (Teng et al., 2016) because these waves present some advantages over conventional heating in transesterification. A simple schematic of the microwave-assisted transesterification process (Ali et al., 2015) shown in Figure 2.6. Faster and uniform heat distribution, higher yields of cleaner product, less energy consumption, and reduction of the catalyst to methanol ratio are among the attractive features of this technique.

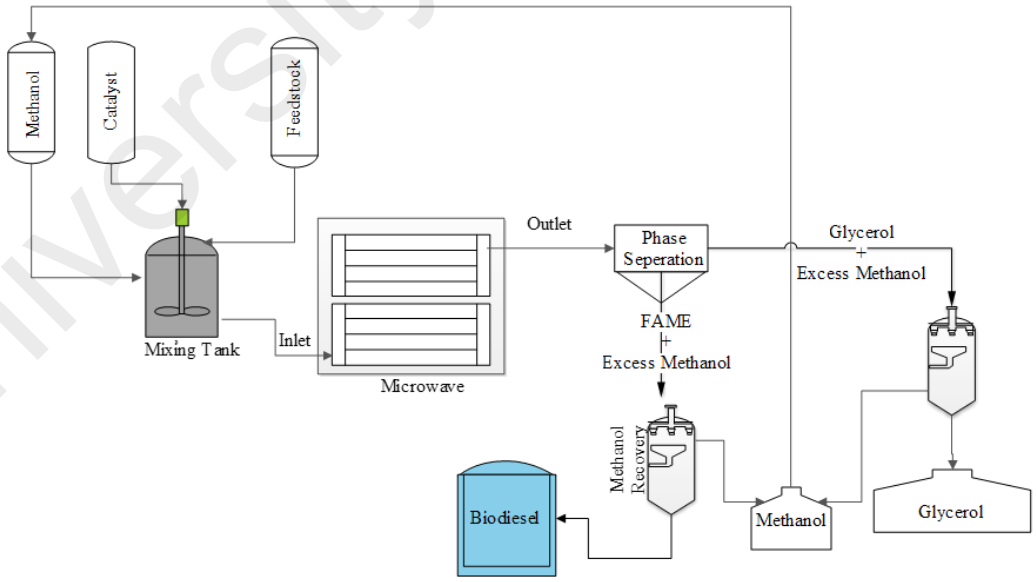

Figure 2.6: Microwave-assisted transesterification process

2.3.5 Ultrasonic technology

Ultrasonic technologies are typically used in a variety of biological and chemical reactions to enhance yield within a shorter reaction time. Ultrasonic technologies are an effective method to enhance the mass transfer rate between immiscible liquid–liquid phases within a heterogeneous catalyst (Ji et al., 2006). The audible range of human beings lies between 16 and 18 kHz (Vyas et al., 2010), whereas ultrasonic sound ranges lie between 20 kHz and 100 MHz. The principle of ultrasound action in biodiesel production is primarily based on the emulsification of immiscible liquid reactants by micro-turbulence generated by the radial motion of cavitation bubbles. Molecules in the medium continuously vibrate and create cavities by compressing and stretching the molecular spacing of the medium, which is developed by a high-frequency sound wave. As a result, micro-fine bubbles are formed by the sudden expansion and violent collapse, generating energy for chemical and mechanical effects (Colucci et al., 2005). This process allows a short reaction time and high yield because of the cavitation of the liquid–liquid immiscible system. Maneechakr et al. (2015) stated that ultrasonic-assisted transesterification shortens the reaction time and minimizes the molar ratio of alcohol to oil, and reduces energy consumption compared with the conventional mechanical stirring method. According to Lee et al. (2011), ultrasonic irradiation reduces reaction times by at least 30 min compared with the conventional method and produces the highest biodiesel yields.

Globally, there are many efforts to develop and improve the vegetable oil properties to approximate the properties of diesel fuel. It is well known that viscosity is the main barrier that prevents the use of direct vegetable oils in conventional diesel engines. Four methods can overcome these problems; pyrolysis, dilution with hydrocarbons blending, Micro-emulsion, and transesterification (Demirbas, 2009; Singh & Singh, 2010). Lin et

al. (2011) conduct a comparison between different approaches to utilizing biodiesel. This comparison is given in Table 2.1

Table 2.1: Comparison of biodiesel utilization approaches

Approaches	Advantage	Disadvantage
Dilution (direst blending or micro-emulsion	• Simple process	• High viscosity • Bad volatility • Bad stability
Pyrolysis	• Simple process • No-polluting	• High temperature is required • Equipment is expensive • Low purity
Transesterification	• Fuel properties is closer to diesel • High conversion Efficiency • Low cost • It is suitable for industrialized production	• Low free fatty acid and water content are required (for base catalyst) • Pollutants will be produced because products must be neutralized and washed • Accompanied by side reactions • Difficult reaction products separation
Supercritical methanol	• No catalyst • Short reaction time • High conversion • Good adaptability	• High temperature and pressure are required • Equipment cost is high • High energy consumption

2.4 Factors that are affecting biodiesel production

There are several factors that affect the biodiesel production yield. Especially they are associated used chemical purity, the amount used in the reaction, reaction environment or condition and the reaction time. The major factor that directly affects biodiesel conversion rate are discussed below:

2.4.1 Molar ratio of alcohol to oil and type of alcohol

The molar ratio of alcohol to oil is another important variable affecting the yield of biodiesel from oil (A molar ratio is a ratio between the amounts in moles of any two compounds involved in a chemical reaction, one mole of methanol equal 32 grams and one mole of oil = 900 grams). Based on reaction stoichiometry, only three moles of

alcohol required to transesterify a molecule of triglyceride and produce three moles of fatty acid alkyl esters (biodiesel) and a mole of glycerol. Generally, 100-200% excess alcohol is used, which drives the reaction in the forward direction and favors bio-diesel reduction. However, a very high molar ratio of alcohol to vegetable oil is avoided because it might interfere with the phase separation of biodiesel and glycerol post-transesterification reaction. Additionally, when high molar ratios are used, the reverse reaction is favored, lowering the yield of esters.

In a previous study, the transesterification of Cynara oil with ethanol as an alcohol was studied at molar ratios of alcohol to oil between 3:1 and 15:1. The conversion increased as the molar ratio increased up to a value of 12:1. The best conversions were obtained at molar ratios between 9:1 and 12:1. For lower molar ratios, the reaction was not completed, and for higher molar ratios, the yield of esters decreased because of improper phase separation (Encinar et al., 2002). However, the optimal molar ratio will vary from one oil source to another. Zhou et al. (2003) studied the effect of alcohol/oil molar ratio on the single-phase base catalyzed ethanolysis of sunflower oils. In that study, four molar ratios of ethanol to sunflower oil (6:1, 20:1, 25:1, and 30:1) were examined. The authors found that at ethanol/oil molar ratios of 20, 25, and 30:1, equilibrium was reached in 6 to 10 min at 23 ^{O}C when 1.4% of potassium hydroxide was used. While at the molar ratio of 6:1, equilibrium could not be reached even after 30 min. Increasing the molar ratio did favor the formation of esters, but the difference for the range of molar ratios from 25:1 to 20:1 was small. Meher et al. (2006) concluded that the reaction was faster with a higher molar ratio of methanol to oil whereas a longer time was required for a lower molar ratio (6:1) to get the same conversion. In their research, the molar ratio of methanol to oil, i.e., 6:1, 9:1, 12:1, and 24:1, were investigated for optimizing bio-diesel production from Karanja oil.

Canakci and Sanli (2008) investigated the effect of different alcohol types on transesterification. Methanol, ethanol, 2-propanol and 1-butanol were tested for a 48 h test period, with sulfuric acid catalyst concentration equal to 3% and the molar ratio of alcohol to oil at 6:1. The conversion was 87.8%, 95.8%, 92.9%, and 92.1% for methyl ester, ethyl ester, 2-propyl ester, and 1-butyl ester, respectively. A higher conversion rate was observed for the longer chain alcohols compared with methanol. The authors attributed this to the fact that higher reaction temperatures were chosen due to the higher boiling point of the long chain alcohols. Also, long chain alcohols can increase the solubility between the oil and alcohol since they are more nonpolar than shorter chain alcohols.

2.4.2 Effect of temperature and reaction time

Temperature influences the rate of the reaction and percentage conversion (Tomasevic & Siler-Marinkovic, 2003). In one study refined oil was transesterified with methanol, with a 6:1 molar ratio of methanol to oil, 1% (w/w) NaOH, and three different reaction temperatures (Alexander & Hurt, 2007). After 6 minutes, yields of 94, 87 and 64% were obtained respectively for 60, 45 and 32° C temperature. However, after an hour, yields were similar at 60 and 45° C and only slightly lower at 32° C. In the same study, the effect of reaction time on conversion was also studied. For cottonseed, soybean, sunflower and transesterified peanut oil, with methanol to oil molar ratio 6:1, 0.5% (w/w) sodium methoxide catalyst and 60° C reaction 58 temperature, an approximate percentage yield of 80% were obtained after a minute for sunflower and soybean oils. After 60 minutes, the yield was similar (93 to 98%) for all four oils studied (Freedman et al., 1984). With beef tallow, the reaction was slow during the first minute possibly due to initial mass transfer limitations of methanol in the beef tallow. However, the reaction proceeded at a faster rate from 1 to 5 minutes, with the highest conversion reached at about 15 minutes (Ma et al., 1999). The boiling point of methanol is 64.8° C. At reaction

temperatures higher than this the alcohol will burn, and this will cause reduced yield. Leung and Guo (2006) indicated that reaction temperature higher than 50° C had a negative impact on the product for neat oil.

2.4.3 Mixing intensity

Mixing is an important transesterification factor as low molecular weight alcohols like methanol and ethanol are immiscible with oil at the room temperature. Hence, the reaction mixtures are often agitated mechanically to facilitate mass transfer of alcohol into the oil. In a prior study, the effect of mixing on transesterification of beef tallow was studied (Gardner, 2003). The results showed that the reaction did not proceed without mixing the two reactants, however, when NaOH-methanol mixture was added to the melted beef tallow in the reactor with continuous mixing, stirring speed was found to be insignificant suggesting that the mixing speeds studied were way above the threshold requirement for mixing. A mixing speed of 600 rpm was concluded as optimum in some previous studies.

2.5 Feedstocks for biodiesel and properties

Biodiesel can be engendered from a wide variety of oils. These include virgin oil feedstocks, waste vegetable oils, animal fat (tallow, lard, yellow grease, chicken fat (Leonard, 2007)), algae, halophytes (*Salicomia bigelovii* (Edward P. Glenn)), sewage sludge (Casey, 2010), etc. Globally, more than 350 oil-bearing crops are identified as potential source of biodiesel (Silitonga et al., 2013). The regional climate largely affects the feedstock available for biodiesel production. Table 2.2 presents some important oil-bearing species (Kumar et al., 2013; Saxena et al., 2013a).

Table 2.2: Oil species for biodiesel production

Category	Source of oil
Edible oil	Sunflower, Rapeseed, Rice bran, Soybean, Coconut, Corn, Palm, Olive, Pistachia Palestine, Sesame seed, Peanut, Opium Poppy, Safflower oil, Amaranth, apricot, argan, artichoke, avocado, babassu, bay laurel, beech nut, ben, Borneo tallow nut, carob pod (algaroba), cohune, coriander seed, false flax, grape seed, hemp, kapok seed, lallemantia, lemon seed, macauba fruit (Acrocomia sclerocarpa), meadowfoam seed, mustard, okra seed (hibiscus seed), perilla seed, pequi,(Caryocar brasiliensis seed), pine nut, poppy seed, prune kernel, quinoa, ramtil (Guizotia abyssinica seed or Nigerpea), rice bran, tallow, tea (Camellia), thistle (Silybum marianum seed), and wheat germ etc.
Non-edible oil	Jatropha, Karanja or Pongamia, Neem, Jojoba, Cottonseed, Linseed, Mahua, Deccan hemp, Kusum, Orange, Rubber seed, Sea Mango, Karanja or Honge, milk bush, Nagchampa, Rubber seed tree, Tobacco seed oil, Algae, Halophytes and Xylocarpus moluccensis, etc.
Animal fats	Tallow, Yellow grease, chicken fat and by-products from fish oil, etc.

The quality of biodiesel are definite by physicochemical properties. Some of these properties include; cetane number, density (kg/m^3), viscosity (mm^2/s), cloud and pour points (°C), flash point (°C), acid value (mg KOH/g), ash content (%), copper corrosion, carbon residue, water content and sediment, sulfur content, glycerine (% m/m), phosphorus (mg/kg) and oxidation stability. The physical and chemical fuel properties of biodiesel depend on the type of feedstock and their fatty acids composition (Atadashi et al., 2010; Lin et al., 2009; Murugesan et al., 2009). A summary of physicochemical properties of diesel and biodiesel produced from different feedstock in ASTM D6751-13 and EN 14214 specifications are shown in Table 2.3

Table 2.3: ASTM, European (EN) and Malaysian biodiesel standard

		ASTM D6751		EN 14214		MS 2008:2008	
Properties	**Units**	**Limit**	**Test Method**	**Limit**	**Test Method**	**Limit**	**Test Method**
Density @15 ˚C	g/cm^3	-	-	0.86-0.90	EN ISO 3675 or 12185	0.86-0.90	ISO 3675 or 12185
Viscosity @40 ˚C	cSt	1.9-6.0	D445	3.50-5.00	EN ISO 3104	3.50-5.00	ISO 3104, MS 1831
CP	ºC	Report	D2500	-	-	-	
PP	ºC	-	D97	-	ISO 3016	-	
CFPP	ºC	-	D6371	Report	EN 116	-	
Flash point	°C	130 Min.	D93	120 Min.	EN ISO 3679	120	ISO 3679e, MS 686
Cetane number	-	47 Min.	D613	51 Min.	EN ISO 5165	51.0	ISO 5465, MS 1895
Sulfur content	mg/kg	15.0 Max.	D5453	10.0 Max.	EN ISO 20846 or 20884	10.0	ISO 20884, ASTM D5453
Phosphorus content	mg/kg	10.0 Max	D4951	10.0 max	EN ISO 14107	10.0 Max.	EN 14107, ASTM D4951
Water content	mg/kg	500 Max.	D2709	500 Max	EN ISO 12937	500 Max.	ISO 12937, ASTM D1160
Acid value	mgKOH/g	0.80 Max.	D664	0.50 Max.	EN 14104	0.50 Max.	EN 14104, MS 2011
Free glycerin	%mass	0.02 Max.	D6584	0.02 Max.	EN 14105 or 14106	0.02 Max.	EN 14105, ASTM D6584
Total glycerin	%mass	0.24 Max.	D6584	0.25 Max.	EN 14105	0.25 Max.	EN 14105, ASTM D6584
Monoglyceride	%mass	-	-	0.8	EN 14105		
Diglyceride	%mass	-	-	0.2	EN 14105		
Triglyceride	%mass	-	-	0.2	EN 14105		
Ester content	%mass	-	-	96.5 Min.	EN 14103	96.5 Min.	EN 14103
Carbon residue	%mass	0.05 Max.	D4530	0.30 Max.	EN 10370	0.30-0.50 Max.	EN 10370, ASTM D4530
Iodine value	I_2/100 g	-	-	120 Max.	EN 14111	110	EN 14111
Oxidation stability @110 ˚C	hour	3 Min.	EN 14112	6 Min.	EN 14112	6 Min.	EN 14112

2.5.1 Overview and previous research on selected feedstocks

Aphanamixis polystachya (AP) is a widespread species found in Indo-China and western Malaysia. It is native to Indonesia, Malaysia, Singapore and Taiwan. It is commonly known as 'Pithraj' in Bangladesh and 'Amoora' in India. Figure 2.7 represents the different parts i.e. a tree with leaf, fruit and seed of the *A. polystachya.* This non-edible oil has been reported to be a potential biodiesel feedstock by some researchers, and its use will be acceptable as it will not compete with food supply (Ferdous et al., 2014; Gowda, 2014; Palash et al., 2015)

In the published literature there are handful amount of articles which mainly deals with biodiesel production and its characterization. Gowda (2014) reported on Indian amoora oil, which had 4.62% free fatty acids (FFA) content. Two stage biodiesel production yield were employed for biodiesel production. In acid pretreatment step, the oil was treated with 5% H_2SO_4 and 40:1 methanol to FFA by the molar ratio to reduce FFA content. After that transesterification process was carried out with 1:6 oil to methanol in the presence of more than 3.5 g/L of NaOH at 60°C temperature which yielded 96% (v/v) biodiesel with 1 h reaction time. Ferdous et al. (2014) studied the Bangladeshi Pithraj oil which had FFA content of 7.5%. They also carried out two-step esterification-transesterification process. For esterification, 5% H_2SO_4 and a molar ratio of 1:6 (oil to methanol) were selected for 1 hour reaction time at 70°C. After that, with NaOH at 1 wt% of oil and 1:6 molar ratio of methanol, methyl ester conversion was complete within 1 hour at a temperature of 60°C.

Some physicochemical properties of crude *Aphanamixis polystachya* oil (CAPO) and the *Aphanamixis polystachya* methyl ester (APME) are measured and reported. The *Aphanamixis polystachya* (Pithraj) tree, is a species of tree in the family Meliaceae. It is native to India, Pakistan, Nepal, Bhutan, Bangladesh, Myanmar and Sri Lanka. It is a

widely used as a medicinal plant in Ayurveda. Oil is not edible and can be used as biodiesel and lighting.

(a) Tree (b) Fruit (C) Seed

Figure 2.7: *Aphanamixis polystachya* (a) tree (b) fruit and (c) seed

The *Millettia pinnata* (Karanja) is a species of tree in the Fabaceae family. It is often known by the synonym *Pongamia pinnata* as recently it was moved to the genus Millettia. Fabaceae, native to tropical and temperate Asia including parts of the Indian subcontinent, Bangladesh China, Japan, Australia and Pacific islands. Oil is not edible oil sources and can be used as the second generation biodiesel. Figure 2.8 represents the different parts i.e. a tree with leaf, fruit, and seed of the *M. pinnata.* In Table 2.4 biological nomenclature of the two non-edible feedstock source are presented.

(a) Tree (b) Fruit (c) Seed

Figure 2.8: *Millettia pinnata* (a) tree (b) fruit and (c) seed

Table 2.4: Botanical nomenclature of *A. polystachya* and *M. pinnata*

	Aphanamixis polystachya	***Millettia pinnata***
Kingdom	Plantae	Plantae
Order	Sapindales	Fabales
Family	Meliaceae	Fabaceae
Genus	*Aphanamixis*	*Millettia*
Species	*A. polystachya*	*M. pinnata*

2.6 Heterogeneous catalyst

The catalysts with a phase or state different from that of the reactants are considered heterogeneous catalysts. A heterogeneous catalyst is often a practical material that regularly creates active sites with its reactants under the reaction atmosphere. The application of a heterogeneous catalyst will result in simpler and less costly separation processes, as well as additional capital and energy costs. The disadvantages of heterogeneous catalysts include elevated temperatures and higher oil to alcohol ratios than those required in the homogeneous catalytic procedure. Some of these catalysts have demonstrated good performance even under the reaction conditions employed for homogeneous catalysts (Serio et al., 2007; Mittelbach & Remschmidt, 2004). The separation, purification, and reusability of the catalyst are among the more attractive features of the heterogeneous catalytic process. Carbonates and hydrocarbonates of alkaline metals, alkaline metal oxides, alkaline metal hydroxides anionic resins, and base zeolite may be used as heterogeneous catalysts. The basic mechanism of an acid catalyst is shown in Figure 2.9.

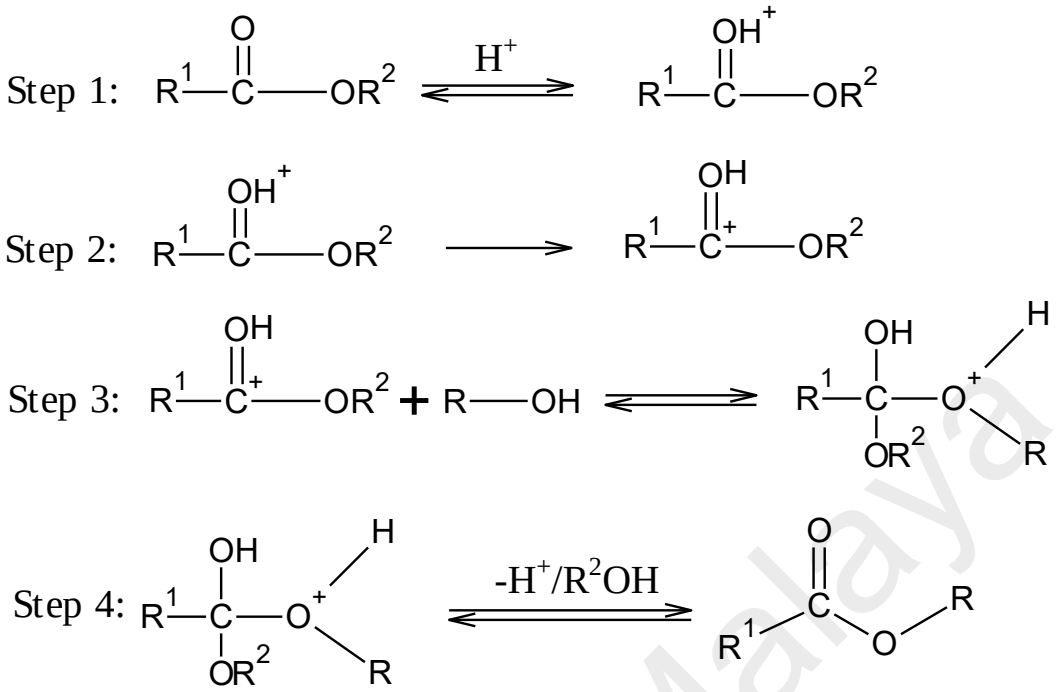

Figure 2.9: Basic reaction mechanism of an acid catalytic process

2.6.1 CaO as a heterogeneous base catalyst

CaO is the most commonly exploited alkaline earth metal oxide for transesterification. FAME yields of nearly were initially reported (Veljković et al., 2009). The ability to reutilize the catalyst is a major topic of concern. The modification of CaO to organic metallic nature, for example, $Ca(OCH_3)_2$ and $Ca(C_3H_7O_3)_2$, investigate the reutilization function. Collected works on biodiesel state that approximately 93% biodiesel yield may be obtained from a 20-cycle reaction. 95% $Ca(C_3H_7O_3)_2/CaCO_3$ has also been determined to be a capable heterogeneous catalyst with a reusability of 5 cycles and good FAME yield (Kouzu et al., 2008). The mechanics of transesterification introduced by Lam et al. (2010) used CaO as a heterogeneous base catalyst. CaO was reacted with FFAs, and a certain amount of the catalyst was transformed into Ca soap by rejoining with the FFAs, causing limited catalyst recovery. As a basic standard of biodiesel, the concentration of mineral matter should be less than 200 ppm. Kouzu et al. (2008) determined a Ca concentration of 3065 ppm in the reaction products, thus exceeding this standard.

Some investigators noted that CaO can remove soluble matter throughout transesterification. CaO slightly dissolves in methanol, thus transforming into soluble calcium diglyceroxide, where CaO reacts with glycerin during the transesterification of soybean oil with methanol (Kawashima et al., 2009). Stimulated CaO is used to study the function of H_2O and CO_2 in the loss of catalytic performance in the presence of O_2 during the transesterification of sunflower oils (Granados et al., 2007). In the above studies, CaO quickly hydrated and carbonated in the air. Stimulated CaO was affected because of surface activity, as well as absorption of CO_2 and H_2O on surface area. If CaO is exposed to deal at 700°C to eliminate carbonate groups from the surface, then the catalytic action of CaO might be restored. However, filtering or removing the catalyst from the product was noticeable in the transesterification reaction, whereas temperature dealing was occupied. Considering its low solubility in methanol, CaO results in high basic strength and fewer ecological effects. Furthermore, CaO can be produced from economic resources such as limestone and $Ca(OH)_2$.

KOH can use be used as an alternative of CaO. However, advantages of CaO over KOH include a lower price, lower solubility, higher basicity, and easier handling. In actual practice, the reaction rate is unsatisfactory during transesterification for relatively low activity. However, the reusable activity can be enhanced by washing and improving thermal activation treatment. Being nano-sized, CaO provides effective catalyst activity because of high surface area. A surface structure of a metal oxide is presented in Figure 2.10.

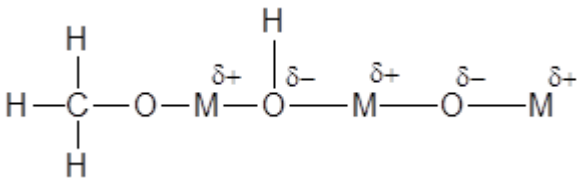

Figure 2.10: Surface structure of metal oxides compare with its acidic & basic sites.

2.6.2 Waste material as heterogeneous catalyst

Mainly calcium-enriched waste materials are used as catalysts synthesis sources, with mollusk shell, eggshell, and bones being the more common. Researchers examined some systems to remove misused atoms and change useable catalysis with high-cost viability. CaO force obtained from these waste materials could be a potential probability for biodiesel era. Chakraborty et al. (2011) reported that waste shells could be utilized for the transesterification of palm olein into methyl esters as a catalyst, which is an issue of CaO. Categorization consequences showed that the fundamental segment of the shell was $CaCO_3$, which changed into CaO when enacted over 700°C for 2 h. The economically produced catalyst affected transesterification for biodiesel production, similar to laboratory CaO. Ideal conditions were found at a 0.5:1 methanol to oil ratio, 5 wt.% catalyst loading, stirring speed 500 rpm, and a reaction temperature 65°C. Reusability consequences established that the arranged catalyst could be recycled for up to 11 cycles. The actual examination was performed utilizing a central composite design to assess the commitment and execution of the parameters on biodiesel quality. Chakraborty et al. (2011) obtained CaO from waste eggshells, which was considered as a viable catalyst for transesterification at 65°C, with an oil/alcohol proportion of 1:9, and catalyst stacking at 10 wt.%. Approximately 97% to 98%. FAME yield was achieved, and the catalyst could be reused up to 17 reaction cycles. Viriya-empikul et al. (2010) studied the transesterification reaction of palm olein oil for biodiesel production, where waste eggshell, golden apple, and *Meretrix venus* were used as a waste base for the solid heterogeneous catalyst. In their study, operating conditions were 60°C, the molecular ratio of alcohol to oil was 18:1, catalyst loading was 10 wt.%, and reaction time was 1 h. The study produced 97%, 83%, and 78% biodiesel yields, respectively. Effective waste administration and waste to vitality transformation can facilitate biodiesel generation utilizing eggshells. Du et al. (2004) studied the biodiesel production from soybean oil

where waste eggshells were used as a heterogeneous catalyst. Operating conditions were as follows: temperature was 70 °C, the molar ratio of alcohol to oil was 6.9:1, catalyst loading was 5 wt.%, and reaction time was 5 h. Approximately 97.73% biodiesel yield was achieved, and the catalyst could be reused up to 6 times. An alternate specialist, Nakatani et al. (2009) inspected the transesterification of soybean oil catalyzed by calcination shellfish shells.

2.6.3 Review on eggshell extracted catalyst

Eggshells are one of the vast by-products of food processing and manufacturing plants. Most of the waste eggshells are currently stockpiled on-site without any pretreatment (Danlin Zeng et al., 2015). The laboratory grade CaO catalytic performance can be compared with waste eggshell heterogeneous catalyst during transesterification reaction (Tan et al., 2015). Wei and Xu reported, 3 wt% eggshell extracted catalyst loading can produce 95% biodiesel yield from soybean oil when the calcined at 1000°C. Methanol to oil molar ratio 9:1, reaction temperature 65°C and reaction time 3 h was reported as reaction conditions. The CaO catalyst can be reused up to 13 times without any significant loss of activity. Chen et al. (2015) reported CaO–SiO_2 catalysts were successfully synthesized through a biomimetic silicification approach by using eggshell and Na_2SiO_3 as raw materials. More specifically, the powdered egg shells, where lysozyme (the inducer) was located, were dispersed into the Na_2SiO_3 aqueous solution to implement the biomimetic silicification under ambient conditions. The obtained eggshell SiO_2 composites were then calcined at 800°C under an oxygen atmosphere, thus acquiring the CaO–SiO_2 catalysts. These catalysts were detailed characterized by SEM, EDS, Si-NMR, FTIR, XRD, BET analysis, and Hammett indicator.

Joshi et al. (2015) observed the efficiency of the catalysts was highly influenced by the calcination temperature. ZnO–CaO (cesp) catalyst was found to be the most efficient catalyst among all. The maximum conversion for the transesterification of Jatropha and

Karanja oils were achieved using 5 wt% catalyst, 65°C temperature and 12:1 methanol/oil ratio. The catalyst could be reused effectively during four cycles. Use of the CaO (cesp) based mixed oxides made the process more eco-friendly and economical. Du et al. (2004) studied the biodiesel production from soybean oil where waste eggshells were used as a heterogeneous catalyst. Operating conditions were as follows: temperature was 70°C, the molar ratio of alcohol to oil was 6.9:1, catalyst loading was 5 wt.%, and reaction time was 5 h. Approximately 97.73% biodiesel yield was achieved, and the catalyst could be reused up to 6 times. An alternate specialist, Nakatani et al. (2009) inspected the transesterification of soybean oil catalyzed by calcination shellfish shells.

Niju et al. (2015) produced biodiesel from waste frying oil using calcium oxide derived from the calcination of egg shell as a heterogeneous base catalyst. The catalyst was characterized by X-ray diffraction, Fourier transform infrared (FTIR) spectroscopy, Brunauer–Emmett–Teller analysis, scanning electron microscopy, and energy-dispersive atomic X-ray spectrometry. The effects of reaction variables such as methanol/oil molar ratio, the amount of catalyst, reaction temperature, and reaction time on biodiesel yield were investigated. The activity of the eggshell derived CaO was compared with the commercial CaO. A high biodiesel yield of 95.05% and conversion of 96.11% were obtained at 3 wt. % catalyst (based on oil weight), methanol/oil molar ratio of 9:1, a reaction temperature of 65°C, and reaction time of 3 h. The structure of biodiesel has characterized by FTIR, and the biodiesel conversion has determined by “H” nuclear magnetic resonance spectroscopy.

Viriya-empikul et al. (2010) reported that the eggshell based catalyst has better catalytic activity in oil transesterification than mollusk shells. The author concluded that the main parameters which affect the egg shell-based catalyst's catalytic activity are catalyst surface area and calcium content. Due to the different calcium matrix organization, eggshell produces a more porous and higher surface in the case of calcium

oxide. Thus the catalytic activity of eggshell is better than a mollusk. He also reported the good performance of eggshells among the waste selection in transesterification as chicken egg shell contains the highest calcium and larger surface area as compared to golden apple snail and Meretrixvenus shell. Recently, Semwal et al. (2011) had produced the metal oxide $CaTiO_3$ using egg shell by calcination at 1050°C for 3.5 h which yielded over 95% methyl ester content. This showed that CaO solid catalyst could speed up the transesterification reaction. However, Tan et al. (2015) reported the composition that may present in chicken eggshell and the quail eggshells are reported in Table 2.5.

Table 2.5: Inorganic components of chicken and quail eggshells

Inorganic component	**Composition (wt.%)**	
	Chicken eggshell	Quail eggshell
Na_2O	0.1	0.1
MgO	0.5	1.0
Al_2O_3	Trace	-
SiO_2	-	-
P_2O_5	0.2	1.1
SO_3	0.1	0.4
K_2O	-	-
$CaCO_3$	99.0	97.3
SrO	-	-
Total	100.0	100.0

2.7 Engine performance, combustion and emission with biodiesel

The major parameter for engine performance along with emission behavior are discussed fueled with biodiesel and its blends for different operating condition.

2.7.1 Brake power and thermal efficiency

The final output power of the engine is known as brake power. This is the product of engine torque and angular speed. Some researchers reported that engine brake power is decreased while running with biodiesel (Aydin & Bayindir, 2010). The reasons are attributed to the lower calorific value and inefficient combustion of biodiesel compared to diesel fuel (Nettles-Anderson & Olsen, 2009). A few authors also reported controversial results which it is attributed to higher viscosity, density and bulk modulus of biodiesel compared to diesel. (Gürü et al., 2010). According to them, a higher density of biodiesel ensures increased the mass of fuel injection, while higher viscosity reduces fuel leakage (Gürü et al., 2010). However, the higher mass flow rate of biodiesel cannot sufficiently compensate about 12% lower heating value of biodiesel. Here in Table 2.6, the engine performance of palm and jatropha biodiesel will be shown regarding power, BTE and BSFC compared to diesel fuel as reported in the literature (Ndayishimiye & Tazerout, 2011; Ozsezen & Canakci, 2011).

Table 2.6: Engine performance biodiesel compared to diesel fuel

Engine Type	Test condition	Power	BTE	BSFC
6-Cyl., DI, WC, NA **CR: 1:15.9** **D: 991 cc** **RP: 81 kW** **RS: 2600 rpm**	Constant speed (1500 rpm) and full load	Decreased by 2.5%	Decreased by 0.48%	Increased by 7.5%
4-Cyl., IDI, WC, NA **CR: 1:21.47** **D: 449.77 cc** **RP: 38.8 kW** **RS: 4250 rpm**	Full load at different speeds and different blends (5%, 20%, 50% and 100%)	Decreased with biodiesel increment	_	Increased with biodiesel increment

Table 2.7: Continued….

Engine Type	Test condition	Power	BTE	BSFC
1-Cyl., DI, AC, NA CR: 1:18 D: 634 cc RP: 5.4 kW RS: 1800 rpm	Constant speed (1800 rpm) and variable loads	–	On average 1% lower for 50% blend and 2% lower for 100% blend	About 10% increased for 100% biodiesel and 20 to 35% increased for 50% blend
4-Cyl., IDI, NA, WC CR: 21.47:1 RP: 38.8 kW RS: 4250 rpm	Variable speeds, full load and multiple blends (10%, 30%, 40%, 60%, 80% and 100%)	No changes for 10% blend and a maximum of 7% reduction observed	On average 8% decreased	On average 11% increased
1-Cyl., DI, WC, NA CR: 16.5:1 RP: 3.5 kW RS: 1500 rpm	Constant speed	–	No changes	Almost same
1-Cyl., DI, NA, AC RP: 4.6 kW RS: 3500 rpm CR: 22:1 D: 347 cc	Variable loads, speeds and multiple blends (50% and 100%)	–	–	Increased
1-Cyl., DI, NA, WC CR: 17.5:1 RP:5.2 kW RS: 1500 rpm D: 662 cc	Constant speed (1500 rpm), variable loads and multiple blends (25%, 50%, 75% and 100%)	–	Decreased	Increased
1-Cyl., DI, WC, NA D:1.007 L CR:16.3:1 RP: 11.77 kW RS: 2200 RPM	Constant speed (2000 rpm) and variable loads (0%, 25, 50, 75 and 100%)	–	Almost same	On average 16% increased

Cyl. = Cylinder, DI = Direct Injection, IDI = Indirect Injection, NA = Naturally Aspirated, AC = Air Cooled, WC = Water Cooled, CR = Compression ratio, D = Displacement, RP = Rated Power, RS = Rated Speed

2.7.2 Engine emissions characteristics

Biodiesel showed lower CO emission compared to diesel fuel (Mustafa Canakci, 2007; Nabi et al., 2006; Öner & Altun, 2009). They reported 18%, 14% and 4% CO emission reductions, respectively while the engine was operated with 100% biodiesel. The higher oxygen content of biodiesel is attributed to lower CO emission. Moreover, lower C/H ratio of biodiesel compared to diesel fuel may also reduce CO emission. On average,

biodiesel contains 10% higher oxygen in their molecule than diesel fuel. The higher oxygen content of biodiesel results in a complete combustion of fuel inside engine cylinder which helps to convert CO to CO_2 (Nabi et al., 2006). For instance, jatropha and palm biodiesel emissions are reported in Table 2.8***:***. From the literature reviews (Huang et al., 2010; Takase et al., 2015).

Table 2.8: Engine emission of biodiesel compared to diesel fuel

Engine Type	Test condition	CO	HC	NO_X
6-Cyl., DI, WC, NA CR: 1:15.9 D: 991 cc RP: 81 kW RS: 2600 rpm	Full load and constant speed	About 86.89% decreased	About 14.29% decreased	About 22.13% increased
4-Cyl., NA, IDI CR: 1:21.47 D: 449.77 cc RP: 38.8 kW RS: 4250 rpm	Full load, variable speeds and multiple blends (5%, 20%, 50% and 100%)	Decreased	Decreased	Increased
4-Cyl., IDI, NA, WC CR: 21.47:1 RP: 38.8 kW RS: 4250 rpm	Variable speeds, full load and multiple blends (10%, 30%, 40%, 60%, 80% and 100%)	Maximum 60% decreased	About 35% decreased	About 70% increased
1-Cyl., DI, WC, NA CR: 16.5:1 RP: 3.5 kW RS: 1500 rpm	Constant speed	On average 30 to 45% reduced	–	On average 37 to 60% reduced
1-Cyl., DI, WC, NA D:1.007 L CR:16.3:1 RP: 11.77 kW RS: 2200 RPM	Constant speed (2000 rpm) and variable loads (0%, 25, 50, 75 and 100%)	About 10 to 15% reduced	About 35 to 46% reduced	Slightly decreased at full load
1-Cyl., WC, DI CR: 1:16.3 D: 1007 cc RP: 11.77 kW RS: 2200 rpm	Constant speed (2000 rpm) and variable loads (0%, 25%, 50%, 75% and 100%)	Average 15 to 25% decreased	Average about 30% decreased	Slightly reduced

Cyl. = Cylinder, DI = Direct Injection, IDI = Indirect Injection, NA = Naturally Aspirated, AC = Air Cooled, WC = Water Cooled, CR = Compression ratio, D = Displacement, RP = Rated Power, RS = Rated Speed

2.8 Summary

The most important conclusions of this chapter summarized as: Biodiesel fuels and their properties vary significantly on the raw material and production technology which requires more investigations. Low-quality feedstocks are involving with some pretreatment process and suitable catalyst selection is an important task for the process. Heterogeneous catalyst has an important role over the homogeneous catalyst in terms of reusability and recovery. Biodiesel, one of the renewable energy resources, have interesting impacts such as the reduction of external dependence regarding energy, their development and environmental benefits, and providing to the feed, food and raw material industries with raw materials in the world. From all the literature reviewed the concluding remark can be made. There is not enough literature which aimed to optimize production process of low-quality feedstock like *Aphanamixis polystachya* and to evaluate the combustion and emission on a single cylinder unmodified direct injection diesel engine in different engine operating condition.

CHAPTER 3: MATERIALS AND METHODOLOGY

3.1 Introduction

This chapter describes research methodology as well as a description of experimental set-up and experiment procedures for achieving the objectives of this particular work. These include catalyst extraction and development from waste eggshell, biodiesel production process optimization from non-edible *A. polystachya*, biodiesel characterization as well as engine testing approaches to evaluate combustion, performance and emission. All the equipment used for catalyst preparation, characterization and biodiesel production, characterization as well engine parameters are list down with the approaches taken. Also, different analytical tools and formulae also presented which have been utilized in the optimization process analysis, physicochemical properties analysis as well as the combustion, performance and emission analysis. The overview of this research can be represented by the Figure 3.1.

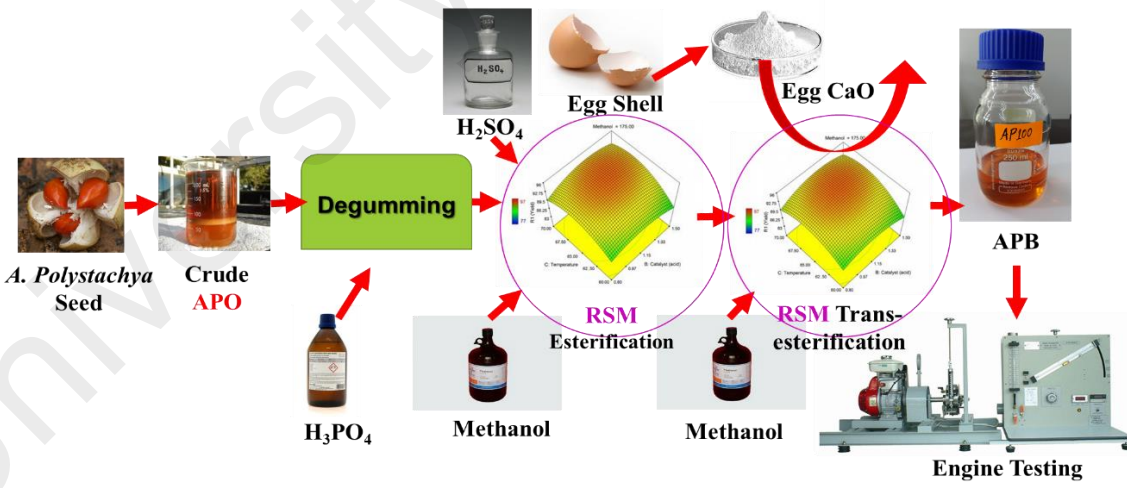

Figure 3.1: Overview of methodology

3.2 Catalyst preparation

Waste eggshell of chicken has been used as the raw material for the heterogeneous catalyst. Raw sources of catalyst i.e. waste eggshell are collected from the canteen of the University of Malaya at free of cost. Normally the eggshell is thrown as waste material

after using egg. Different steps related to the catalyst development from waste eggshell are presented in Figure 3.2.

Figure 3.2: Different steps of catalyst development

3.2.1 Cleaning and powder preparation

At first, the eggshell was cleaned in the warm water for cleaning the unexpected dust and mud from the upper surface and inner eggshell membrane. Then it was kept in sunlight for 2-3 hours for the drying. After drying, it was weighted in an electronic balance machine and then broken into a relatively smaller sized particle alike Figure 3.2(f). Eggshell was immured into 98% purity grade acetone for removing the moisture content from it. An ultrasonic (Figure 3.2 (d)) cleaner was used for 5 minutes to ensure

the proper cleaning of moisture, as well as other impurities, from the external surface. After cleaning, the dried smaller size eggshell was placed into a ceramics basin with mortar (Figure 3.2 (g)). With the help of the mortar, the small eggshell prepared into the microsized powder. This powdered mostly contains the $CaCO_3$ which have been used as a catalyst after calcination in the furnace (i.e. CaO).

3.2.2 Calcination at furnace

Calcination can be defined as the decomposition of calcium carbonate (limestone) to calcium oxide (lime) and carbon dioxide with the help of heat. An electrical furnace namely Nabertherm was used to calcine the prepared $CaCO_3$ powder. With this furnace, a constant temperature can be set within 30-3000 °C range as well as temperature rising rate can be controlled. The calcination temperature was chosen from the thermogravimetric analysis (TGA) of the $CaCO_3$ curve (Chapter 4, Section 4.2.1). The temperature was chosen greater than the final offset temperature. For this investigation, much higher temperature, for instance, 900 °C was chosen. The furnace was rising the temperature from 30 °C to 900 °C within 40 minutes and then 900 °C constant temperature was maintained for 4 hours (Jaggernauth-Ali et al., 2015). After that, the furnace was allowed for cooling down to its room temperature. During the calcination, an odder smell was coming from the furnace and the color of the powder is become whiter and converted into a fine grain. Figure 3.3 (a) and Figure 3.3 (b) shows the powder before and after calcination respectively.

(a) Before calcination (b) After calcination

Figure 3.3: Eggshell extracted catalyst (a) before and (b) after calcination at furnace

3.3 Catalyst characterization

Extracted and developed heterogeneous catalyst was undergoing through some characterization for confirming the presence of calcium oxide as well as the catalytic activity and inorganic component present. Major characterization like Fourier transform infrared (FTIR) spectroscopy analysis, scanning electron microscope (SEM), energy dispersive X-ray (EDX) spectroscopy and X-ray powder diffraction (XRD) were performed for confirming the presence of calcium oxide. The highly sophisticated equipment that were used for these characterizations are presented in Figure 3.4.

(a) FT-IR

(b) TGA

(c) SEM-EDX

(d) X-RD

Figure 3.4: Catalyst characterization equipment (a) FT-IR (b) TGA (c) SEM (d)XRD

FT-IR is frequently used to determine chemical bonds and functional groups of substances. Perkin Elmer (Model: Spectrum 400) combined with PerkinElmer spectrum

software was employed to analyze the sample. Before running the sample, the equipment was calibrated and background scanning was performed without sample.

SEM was performed to study the morphology and size of the catalysts using HITACHI TM3030 tabletop microscope. The powder sample was put on a doubled sided carbon tape and placed into a microscope with a non-conductive sample holder. The electron beam energy was fixed at 15 kV and the magnification was varied from 100× to 10000×. The high-quality images were obtained and processed using the VEGA3 software.

PANalytical X-ray diffraction system with Cu Kα radiation (λ = 1.54 Å) operated at 40 mA and 45 kV, has been used in the tests. The XRD was started from 5.0129 °2θ angle and stops at 79.9709 °2θ with a step size of 0.0260 °2θ angle. The experiment was performed at 25 °C and Cu was chosen as the anode material.

3.4 Biodiesel production from feedstock

Biodiesel production prom vegetable oil includes the feedstock, chemical and other material collection. It also consist the pretreatment process along with the step by step production process and the post treatment. Pretreatment process is necessary for undergoing through the production process. On the other hand, post treatment is required for eliminate the unnecessary impurities from the pure biodiesel like dissolve water, methanol, glycerol etc.

3.4.1 Materials and chemicals collection

The crude *Aphanamixis polystachya* oil (CAPO) and the crude *Millettia pinnata* oil (CMPO) were collected from local market from Naogaon, Bangladesh. Both the crude oil were extracted from seed by mechanical pressing after drying in the sun.

The obtained crude oil looks like dark brown in color and thick. Other chemicals and consumable items which are required in biodiesel production process and purification process were purchased from the local market of the Kuala Lumpur, Malaysia. Highly

pure grade analytical chemical such as 99.8% pure methanol (CH_3OH), 98% pure sulfuric acid (H_2SO_4) as acid catalyst, 85% pure phosphoric acid (H_3PO_4), and 99% pure sodium sulfate (Na_2SO_4) as anhydrase were chosen. Eggshell extracted and the developed catalyst was taken as the alkali catalyst for the transesterification stage. This biodiesel production was carried out at energy efficiency laboratory at the University of Malay through a double jacketed batch glass reactor which was 2100 ml in capacity. This biodiesel production includes the pretreatment of feedstocks, acid esterification stage and base transesterification and finally post-treatment process for obtaining the pure form of biodiesel.

3.4.2 Pre-treatment of feedstocks

Low-quality feedstock needs to do some pre-treatment before undergoing through the main chemical production process for achieving higher production yield. Pretreatment process consists of excess water content removal techniques, degumming process and acidity reduction techniques from crude oil.

The purpose of the degumming process is to expel contained gum in the crude oil as well as the phosphate, protein, carbohydrate, water residue and resin. This process is beneficial for not only impurities removal but also enhancing the oxidization stability of biodiesel. At first, both CAPO and CMPO were preheated for 30 minutes into a double jacket glass reactor with a constant stirring speed to remove the water contained from the feedstock. A 3% (v/v of oil) phosphoric acid (H_3PO_4, 85% concentration) was added to crude oil and maintained 60°C for 30 minutes. A mechanical stirrer was used for continuous stirring the oil-acid solution at 700 rpm. After 30 minutes of reaction time, gum and other impurities from oil were separated by gravity and gum was settling down due to the difference in density. After pretreatment 97.12% (v/v of oil) CAPO oil was obtained.

3.4.3 Acid-catalyzed esterification

As the crude *A. polystachya* and *M. pinnata* oil both contain the high acid value (more than 4 mgKOH/g), first acid esterification process was required to lower the free fatty acid (FFA) content of vegetable oil before going through the transesterification process. Acid-catalyzed esterification of vegetable oil is recommended before transesterification if the acid value equal or more than 4 mgKOH/g (Fattah et al., 2014). In this stage crude oils preheated to a certain temperature and then added the methanol-catalyst solution to the oil. Sulfuric acid (H_2SO_4) was used as an acid catalyst, IKA small electric motor was used to maintain stirrer speed (500 rpm) and 3 hours reaction time was maintained. The free fatty acids are converted to corresponding methyl ester thus lowered the acid value of the esterified oil. The basic esterification reaction of triglycerides is representing in Figure 3.5 where R represents a small alkyl group and R^1 fatty acid chains. After completing the reaction, the oil was poured into a separation funnel and kept it for 4 hours to form a separate layer. The lower layer was collected and washed properly with 60°C wormed water. Then IKA RV-10 rotary evaporator was used to evaporate the dissolved water as well as methanol.

Figure 3.5: Acid esterification reaction

3.4.4 Alkali-catalyzed transesterification process

In this process, the esterified oil was preheated at 60°C and eggshell extracted catalyst (i.e. CaO) was introduced as the base catalyst. The eggshell catalyst was mixed with methanol before adding with the esterified oil. Then a 900 rpm stirring speed was maintained for 2 h reaction period. After finishing the reaction, the reactants and products were poured into separation funnel for 12 hours to separate glycerol from biodiesels. This time upper layer holds desire products which is biodiesel (methyl ester) and lower layer

contains impurities and glycerol. An ordinary outline of the transesterification reaction for fatty acid methyl ester (FAME) is showed in Figure 3.6. Where R^1, R^2, R^3 represents fatty acid chains (Moradi et al., 2015).

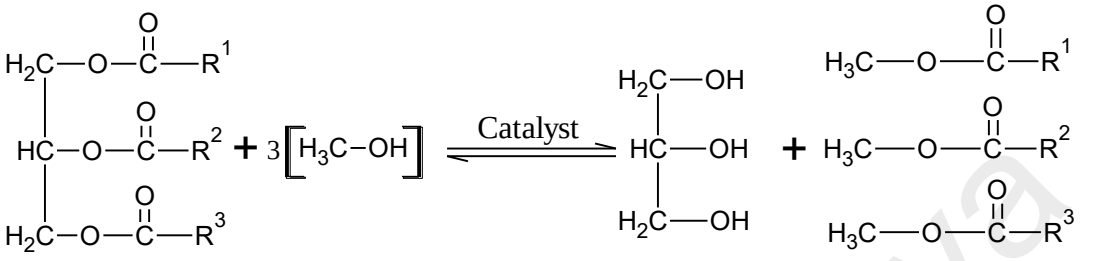

Figure 3.6: Basic alkali transesterification reaction

3.4.5 Post-treatment process

Post-treatment process is includes the washing, mechanical and chemical drying as well as the filtration process. The main purpose of these process is to get the pure biodiesel which will be soap, glycerol, dissolve methanol, dissolve water and other unwanted impurities free.

3.4.5.1 Washing

After draining out the lower layer from separation funnel, upper layer or biodiesel layer was washed with 60°C warm distilled water. The washing process was including sprays warm water in the upper surface of the biodiesel, the surface on separation funnel, shaking and stirred gently. The washing process was performed several times to properly remove the impurities from the produced methyl ester. This was confirmed by the crystal color of washed water during washing which is an indication of the absence of soap in biodiesel. Then the produced biodiesel was undergoing to the mechanical, chemical drying and finally filtration process.

3.4.5.2 Mechanical drying

Rotary evaporator IKA RV-10 was used for mechanical drying process (i.e. evaporation). In this process, the water bath temperature was maintained at 60°C, vacuum

pressure at 339 mbar for methanol removing stage and then 70°C temperature, 72 mbar vacuum pressure applied for water. The removal of water was confirmed by the automatic evaporator mode. It can also be confirmed by the visualisation of the bubble formation during evaporation inside the flask.

(a) Biodiesel reactor

(b) Washing & Separation

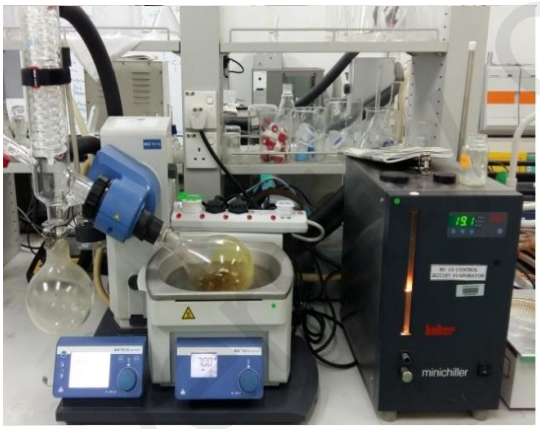

(c) Evaporation

(d) Pure Biodiesel

Figure 3.7: Biodiesel and production process equipment

3.4.5.3 Chemical drying and filtration

The sodium sulfate anhydrous (Na_2SO_4) powder was used for chemical drying. The insoluble excess amount of Na_2SO_4 was mixed with biodiesel and stirrer properly for absorbing further water or moisture content in biodiesel. Finally, the 180 mm of diameter qualitative filter paper was used for separating the anhydrous from the biodiesel. After filtration, the obtained clean methyl ester is the desired biodiesel and then yield was measured. From response surface methodology (RSM) designed table, each runs

experimental production yield was recorded and finally analyzed them to find out the best reaction condition for maximum conversion (Chapter 4).

3.5 Optimization of biodiesel production process

Response surface methodology (RSM) was employed to optimize the both chemical process namely esterification and transesterification. RSM explores the relationships between several explanatory variables and one or more response variables. It is an accumulation of scientific and factual systems for the exact model building. The goal is to improve a reaction (output variable) which is impacted by a few autonomous variables (input variables) with the help of cautious design of experiments. This method was first introduced by the G. E. P. Box and K. B. Wilson in the year of 1951. Central composite design (CCD) was chosen for this investigation. It is well suited for fitting a quadratic surface, which usually works well for process optimization.

3.5.1 Central composite design (CCD)

A two-level full factorial design (2^k) based on central composite design (CCD) was used to optimize the key parameters for the biodiesel production process. It delivers individual and combined effect of variables on the responses under consideration. It also improves the regression models with consequent optimization of the hypothesis process. Three independent key factors were chosen for both acid esterification and alkali transesterification process. The independent variables are methanol to oil ratio, catalyst loading and reaction temperature as well as percentage yield considered as responses. Input independent factors for esterification stage were presented by *A (*Methanol), *B* (Catalyst loading), *C* (Reaction temperature) and corresponding response *R* (Yield).

3.5.2 Experimental design

Based on the literature review and some initial research experiences, the range of the input factors was demarcated. The low level and high level for temperature were chosen

60°C and 70°C for both processes. The catalytic loading was chosen within 0.8 to 1.5% (v/v of oil) for acid esterification and 1% to 2% (w/w of oil) for alkali transesterification. Methanol to oil ratio was chosen 150 - 200% (v/v of pretreated oil) for esterification and 25-55% (v/v of esterified oil) for transesterification while reaction time and stirring speed were kept constant i.e. 3 hours for esterification, 2 hours for transesterification and 500 rpm for both. The low and high levels for independent variables were coded as (-1, +1) intervals, whereas (0, 0, ±α), (0, ±α, 0) and (±α, 0, 0) represented the axial points. Here, the distance between axial points with the center is denoted by "α." Also, trial runs were randomized to diminish the impacts of residual errors. At the center point, six experiments were conducted under identical conditions to calculate repeatability of the data. A coded variable with levels of the input factor parameters for both process presented in Table 3.1 and Table 3.2.

Table 3.1: Experimental design range and level for esterification process

Name of factors	Code	Units	Coded variable Level				
(k=3)			-α	-1	0	+1	+α
Methanol	A	v/v %	132.96	150	175	200	217.04
Catalyst (acid)	B	v/v %	0.56	0.8	1.15	1.5	1.74
Temperature	C	°C	56.59	60	65	70	73.41

Table 3.2: Experimental design range and level for transesterification process

Name of factors	Code	Units	Coded variable Level				
(k=3)			-α	-1	0	+1	+α
Methanol	A	v/v %	14.77	25	40	55	65.23
Catalyst (Eggshell)	B	w/w %	0.66	1	1.50	2.00	2.34
Temperature	C	°C	65.00	60	65	70.00	73.41

A total number of experiment for the CCD was twenty (2^k+2k+6), where "k" is the number of factors and in this study it equal to three. Here the alpha is considered is rotatable (i.e. α=1.68179). The complete and details experimental design matrix for both acid esterification and alkali transesterification are presented in Table 4.4 and Table 4.5 respectively (Chapter 4). This design matrix is composed of 8 factorial points, 6 axial

points, and 6 center points where the experiments are conducted under identical conditions to determine the residual error.

3.6 Blend preparation, characterizations and equipment

A high speed stirrer was use to blend the diesel-biodiesel fuel that are used for the engine testing Figure 3.8 (a). Diesel biodiesel blending was performed at 2000 rpm for 20 minutes. An electrical shaker Figure 3.8 (b) was used to blending the biodiesel with diesel which purpose was for fuel characterization. The shaker was set to a speed of 200 rpm for 30 minutes.

(a) Blender (b) Shaker

Figure 3.8: Diesel biodiesel blending by (a) Blender (b) Shaker

The physiochemical properties of the produced biodiesel and the prepared blends are characterized at the University of Malaya in the tribology and energy efficiency laboratory. The physiochemical properties are measured with the help of highly sophisticated equipment that is presented in Figure 3.9. The corresponding equipment was calibrated and the parameter was measured according to the ASTM standard.

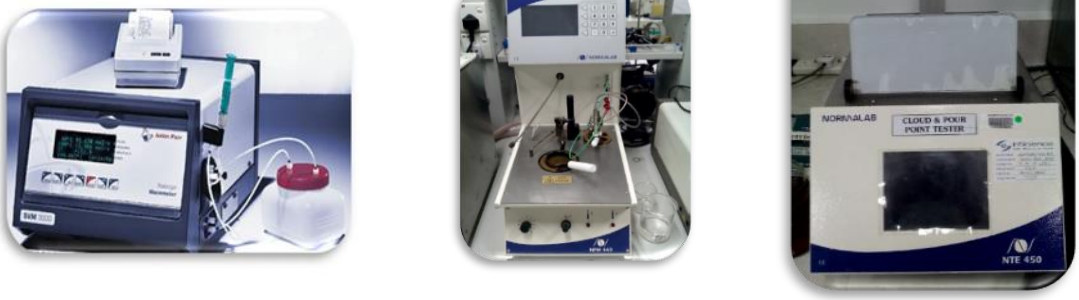

(a) Viscometer (b) Flash point tester (c) CP & PP tester

(d) CFPP tester (e) Acid value tester (f) Bomb calorimeter

(g) 873 Rancimat (h) Iodine Value tester (i) Gas Chromatography

Figure 3.9: Instruments used to biodiesel characterization

All the property measurement was repeated at least three times to ensure the correct results. The equipment name, manufacturers, model no. along with corresponding measuring ASTM standard and accuracy level is presented in Table 3.3. Fatty acid methyl ester (FAME) composition of the biodiesel sample was measured with the help of a GC (gas chromatographer). Agilent 7890 series, USA GC machine was used to measure the weight percentage of each FAME. Table 3.4 shows the GC operation condition for measuring the FAME composition.

Table 3.3: List of equipment used for measuring the physicochemical properties

Property	Equipment description	Manufacturer	Standard	Accuracy
Density	SVM 3000- automatic	Anton Paar, UK	ASTM D4052	± 0.1 kg/m^3
Kinematic viscosity	SVM 3000- automatic	Anton Paar, UK	ASTM D7042	± 0.35%
Dynamic viscosity	SVM 3000- automatic	Anton Paar, UK	ASTM D7042	
Viscosity index	SVM 3000- automatic	Anton Paar, UK	N/S	
Flash point	Pensky-martens flash point - automatic NPM 440	Normalab, France	ASTM D93	± 0.1°C
Cloud point	Automatic NTL Normalab NTE 450	Normalab, France	ASTM D2500	±0.1°C
Pour point	Automatic NTL Normalab NTE 450	Normalab, France	ASTM D97	
Cold filter plugging point	CFPP – automatic NTL 450	Normalab, France	ASTM D6371	N/S
Acid value	G-20 Rondolino automated titration system	Mettler Toledo, Switzerland	ASTM D664	±0.001 mgKOH/g
Calorific value	C2000 basic calorimeter – automatic	(IKA, UK)	ASTM D240	± 0.1% MJ/kg
Oxidation stability, 110°C	Metrohm 873 Rancimat	Metrohm, Switzerland	EN 14112 or ASTM D6751	± 0.01 hour

N/S: Not Specified

Table 3.4: Gas Chromatography (GC) operating condition

Parameter	Setting value/condition
Column	0.32 mm × 30 m, 0.25 μm
Injection volume	1 μL
Carrier gas	Helium, 83 kPa
Injector	Split/splitless 1177, full EFC control
Temperature	250°C
Linear velocity	24.4 cm/s
Split flow	100 mL min^{-1}
Column 2 flow	Helium at 1 mL min^{-1} constant flow
Oven	210°C isothermal
Column temperature	60°C for 2 min
	10°C min^{-1} to 200°C
	5°C min^{-1} to 240°C
	Hold 240°C for 7 min
	250°C, FID, full EFC control

3.6.1 Density and viscosity measurement

Density can be defined as the mass per unit volume of a substance at a given temperature and it can be expressed in units of a gram per liter (g/L) or kilogram per cubic meter (Kg/m^3). It has a great response to pressure and temperature variation thus this property significantly influences the efficiency of fuel atomization for combustion system

(Santos et al., 2008; Kaya et al., 2009; Uriarte, 2010) during engine combustion. Density is important because it gives an indication of the delay between the injection and combustion of the fuel in a diesel engine (ignition quality) and the energy per unit mass (specific energy).

Viscosity is the measure of its resistance to gradual deformation by shear stress or tensile stress. It is determined by measuring the amount of time taken for a given measure of oil to pass through an orifice of a specified size (Raj & Sahayaraj, 2010). The operation of fuel injection system is largely affected by viscosity particularly at low temperature because the fluidity reduces as viscosity increases (Demirbas, 2009; Fernando et al., 2007). In some cases, biodiesel can be more viscous or even solidified at low temperature. Viscosity can be classified as dynamic viscosity, kinematic viscosity, and bulk viscosity. Of them, kinematic viscosity is widely recognized as viscosity. According to ASTM standard, the maximum allowable limit of viscosity is in the range of 1.9-6.0 mm^2s^{-1} and 3.5-5.0 mm^2s^{-1} in EN ISO 3104 standard (Balat, 2011; Balat & Balat, 2010).

SVM 3000 automatic viscometer, manufactured by Anton Paar, UK was used for measuring the density, dynamic viscosity and kinematic viscosity. ISO 17025 / ISO Guide 34 viscosity and density reference standard have been used to check the calibration of the viscometer at a different temperature. Then both the density and viscosity were measured according to the ASTM D4052 and D7042 respectively at 40°C temperature.

3.6.2 Heating value measurement

Heating value is the amount of heat produced by a complete combustion of fuel per unit mass. It is measured as a unit of energy per unit mass or volume of a substance (e.g., kcal/kg, kJ/kg, J/mol and Btu/m^3). The heat of combustion of fuels is expressed by the higher heating value (HHV) or gross calorific value and lower heating value (LHV) or neat calorific value. The HHV was measured using a bomb calorimeter namely IKA C2000 basic and defined as the amount of heat released when fuel is combusted and

the products have returned to a temperature of 25°C. ASTM D240 measuring standard was followed by the measurement. For measuring HHV, 0.5 g of fuel sample weighted by a digital balance machine and placed in a crucible with a flammable string one side immersed. Another side of the string was coupled with the platinum registered filament which can supply the flame for fuel combustion. After placing the crucible into the bomb, chamber closed it tightly and then oxygen gas supplied in 30 bar pressure inside. At the same time, the water filled into the calorimeter which helps to cool down the bomb after combustion. Finally, it gives digital results with a graph of the measured fuel calorific value. Each experiment was repeated for three times and average was presented as a result. On the other hand, the LHV can be determined by subtracting the heat of vaporization of water vapor (generated by combustion of fuel) from the higher heating value according to the **Equation *3.1*** (Heywood, 1988). Where $\left(m_{H_2O}/m_f\right)$ is the ratio of the mass of H_2O produced to mass of fuel burned.

$$Q_{HHV=}Q_{LHV+}\left(\frac{m_{H_2O}}{m_f}\right)\times h_{fg\ H_2O} \qquad \textbf{3.1}$$

3.6.3 Flash point (FP) measurement

Flash point is the minimum temperature at which fuel can vaporize to form as an ignitable mixture in air. Flash point increases with the decreasing of any fuels volatility. The flash point of biodiesel is higher than the prescribed limit of diesel fossil fuel, which is safe for transport, handling and storage purpose (Atadashi et al., 2010). Usually, biodiesel has a flash point more than 150°C, while conventional diesel fuel has a flash point of 55-66°C (Sanford et al., 2009). Demirbas (2009) stated that the flash point values of fatty acid methyl esters are significantly lower than those of vegetable oils. The limit of flash point ranges in ASTM D93 is 93°C (Fernando et al., 2007). A Pensky-martens flash point tester (model NPM 440) was used to measure the flash point of the tested fuel. Flash point measuring interval is 20°C bellow and 80°C above to the set temperature. The flash point is measured by heating the fuel in a small enclosed copper cup until the vapor

ignites when a small flame is produced over the surface of the fuel. The cup is filled with 60 ml sample and closed using the lid. Then expected flash point temperature was set and the measurement procedure started. The sample was then stirred continuously and the temperature was raised automatically. 20 °C before the expected flash point, the equipment starts to produce a spark and continues to do so at 1 °C interval. When the flame produced a no sustained ignition which is detected by the equipment, detection is stopped automatically and the result is appeared on screen. ASTM D93 measuring standard was selected and all the experiment was repeated three times.

3.6.4 Oxidation stability (OS) measurement

The oxidation of biodiesel fuel is one of the major factors that helps assess the quality of biodiesel. Oxidation stability is an indication of the degree of oxidation, potential reactivity with air. Oxidation occurs due to the presence of unsaturated fatty acid chains and the double bond in the parent molecule, which immediately react with the oxygen as soon as it is being exposed to air (Atadashi et al., 2010; Sanford et al., 2009). A minimum IP (110°C) for 3 h is required for ASTM D6751, whereas a more stringent limit of 6 hours or greater is specified in EN 14214 (Moser & Vaughn, 2010).

The 873 Biodiesel Rancimat (Metrohm) instrument was used to measure the oxidation stability of the teste fuel as per EN14112 method specified by ASTM D6751. In order to measure the oxidation stability, the heating block is heated up to 110°C. The test tube shaped vessels and measuring vessels were filled with 7.5 g of fuel sample and 70 mL distilled water respectively. The closed vessels are then placed in the designated areas and tubing are connected. After that gas flow turned on by the measurement software and the START button was pressed to start the measurement. The gas flow rate of 10 L/h was passed through reaction vessel at 110°C and then through water in measuring vessel. A set of the electrode was inserted in the water and connected to a measuring and recording device. By continuously recording the conductivity and plotting them an ‘oxidation

curve' was obtained a whose point of inflection (tangential intersection point) is known as the Induction Period (IP). To determine the IP automatically, the second derivative of the obtained curve was executed.

3.6.5 Cloud point (CP) and pour point (PP) measurement

Cloud point in petroleum products and biodiesel fuels defined as the temperature of a liquid fuel when the smallest observable cluster of wax crystals first appears upon cooling under prescribed conditions. On the other hand, the lowest temperature at which movement of the test fuel is observed under prescribed conditions of the test. Normalab NTE 450 automatic cloud point and pour point tester was used to measure CP and PP of all test samples. To measure the CP and PP, samples are poured into the sample cup up to designated level (approximately 50 ml) and inserted into the groove of the head. Then start point of the testing is set using the software in the equipment. After finishing the test, the result is shown in the display and an audible alert is given automatically. Cloud and pour points are measured using ASTM D2500 and D97 procedures respectively. The behavior of biodiesel at low temperature is an important quality criterion. This is because of partial or fully solidification of the fuel may cause blockage of the fuel lines and filters, leading to fuel starvation, problems of starting, driving and engine damage due to inadequate lubrication.

3.6.6 Cold filter plugging point (CFPP) measurement

CFPP is defined as the lowest temperature where 20 mL of fuel passes safely through a 45 μm wire mesh filter under 200 mm H_2O (0.019 atm) vacuum within 60 s. This test gives an estimate of the lowest temperature that fuel will give trouble free flow in certain fuel systems. This is important as in cold temperate countries; a high cold filter plugging point will clog up vehicle engines more easily. An automatic measuring device, Normalab NTL 450, was used to measure the CFPP of all the samples according to the test method described in ASTM D6371 (Moser & Vaughn, 2010). In this equipment, the sample was

filled in the designated glass cup up to the marked level and placed inside the equipment. The head was then pulled down and placed above the cup. The starting point of the testing was set using the software in the equipment. After finishing the test, the result is shown in the display and an audible alert is given automatically.

3.6.7 Acid value (AV) measurement

Acid value (AV) or "neutralization number" is the mass of KOH in milligrams that is required to neutralize one gram of chemical substance. It also a measure of a number of carboxylic acid groups in a chemical compound, such as a fatty acid, or in a mixture of compounds (Raj & Sahayaraj, 2010). Free fatty acids (FFAs) are the saturated or unsaturated monocarboxylic acids that occur naturally in fats, oils or greases but are not attached to glycerol backbones. Fatty acids vary in carbon chain length and the number of unsaturated bonds (double bonds). The higher amount of free fatty acids leads to higher acid value. The acid value is expressed as mg KOH required for neutralizing 1 gm of FAME. Higher acid content can cause severe corrosion in fuel supply system of an engine. The acid value is determined using the ASTM D664 and EN 14104. Both standards approved a maximum acid value for biodiesel of 0.50 mg KOH/g (Agarwal, 2007; Sharma & Singh, 2009).

In ordered to measure the acid number the percentage free fatty acid (FFA), two step approached was taken. The first step was titration with the help of burette - conical flask and then an acid value tester apparatus namely “716 DMS Tirrino and 728 stirrer”.

Titration procedure: 0.5 g of oil sample was weighted in conical flask whereas 5 g sample size was taken for biodiesel and its blends. Excess iso-propanol (approximate 30 ml) added to it as solvent and 4-5 drop of P^H solution was added as an indicator. Then 0.1 N KOH solution was added to it drop by drop from the burette. The end point was detected by the color change and then AV was calculated from the Equation 3.2**,** and FFA% can be calculated from the corelation AV=1.99× FFA%.

$$AN = \frac{V_{KOH} \times W_{KOH} \times N_{KOH}}{W_{oil}} \quad \textbf{3.2}$$

Where, V_{KOH} = Voulme of KOH from burret,

W_{KOH} = Molar weight of KOH (56.11g),

N_{KOH} = Normality of KOH in tritation (0.1N),

W_{oil} = weight of Oil,

716 DMS Tirrino and 728 stirrer system: After turning on the machine, burette was filled with TAN solution in such was so that mo air bubble stuck or trapped inside tubes. Initially, blank TAN test was performed to check and calibrate the machine. A 125 ml of solvent was taken and sample added to it according to the sample size presented in Appendix C. The mixture was stirring continually with a magnetic stirrer. Then electrode and burette tip submerged into the container start the experiment. After finishing the test, the result was shown in the display and printing out with the connected printer.

3.6.8 Cetane number (CN) measurement

The cetane number (CN) is one of the most important parameters which are considered during the selection of biodiesel. It is the indication of ignition characteristics or the ability of fuel to auto-ignite quickly after being injected. Cetane number provides information about the ignition delay (ID) time of a diesel fuel upon injection into the combustion chamber. Better ignition quality of the fuel is always associated with higher CN value (Balat, 2011a). Biodiesel has higher CN than conventional diesel fuel, which results in higher combustion efficiency. The CN of diesel, specified by ASTM D613 is 47 min, and EN ISO 5165 is 51.0 min (Lapuerta et al., 2008). Pure biodiesels Iodine Value (IV), Saponification Number (SN) and Cetane Number (CN) were calculated from the percentage of fatty acid content (Chapter 4, Table X) using the Equation 3.3 to 3.5 (Krisnangkura, 1986).

$$\text{SN} = \sum \left(\frac{560 \times A_i}{MW_i} \right) \quad \textbf{3.3}$$

$$\text{IV} = \sum \left(\frac{254 \times D \times A_i}{MW_i} \right) \quad \textbf{3.4}$$

$$\text{CN} = \left(46.3 + \left(\frac{5458}{SN} \right) - (0.225 \times IV) \right) \quad \textbf{3.5}$$

Where, A_i is the weight percentage of each FAME component, MM_i is molecular mass of corresponding FAME and DB_i is the number of double bonds. The percentages of C, H, and O present in the biodiesel were also determined from the FAME structures.

Calculated cenatne index (CCI) was measured by Four Variable Equation for the diesel-biodiesel blends according to the ASTM D4737 standard. In this procedure 10%, 50% and 90% distillation recovery are needed according to ASTM D86. A distillation recovery result for AP20 as well as the sample calculation CCI for AP20 was presented in Appendix B.

3.6.9 Water content and sediment

Water can cause poor reactions & high soap content. Leads to poor conversions and difficulty washing the fuel. Water and sediment contamination are treated as housekeeping issues for biodiesel. Biodiesel can contain as much as 1500 ppm of dissolved water while diesel fuel usually only takes up about 50 ppm. Sediment may consist of suspended dust and dirt particles, or it may originate from the fuel as insoluble compounds formed during fuel oxidation (Li et al., 2010). Also, water in the fuel generally causes two problems. First, it can cause corrosion of vital fuel system components such as fuel pumps, injector pumps, fuel tubes, etc. The standard of water content and sediment for biodiesel in ASTM D2709 and EN ISO 12937 specifications is 0.05 (%v) max (Fernando et al., 2007; Sanford et al., 2009). Recommended limit for oil is below 3000 ppm (0.3% By Volume) and 500 ppm (0.05%) for biodiesel. Among 1500 ppm (0.15%) scale and 15000 ppm (1.5%) scale test procedure the 15000 ppm scale was

chosen in this study considered the high water content in crude oil as well as biodiesel. For this test, 4 ml of oil/biodiesel sample and 16 ml of reagent "B" were measured using 10 ml and 30 ml capacity syringe respectively and injected into the oil-reagent "B" chamber. After preparing a packet of reagent "A," it placed into chamber A in such way so that powder not spilled to oil-reagent "B" chamber and vice-versa. Sacked 3 times for 20 seconds each after screw cap on and ensured scale does not exceed 14 psi. Shacked again up to 15 to 20 minutes in 1 minute interval. Multiply gauge reading by 1000 to get water content in ppm.

3.6.10 Sulfur content

Combustion of fuel containing sulfur causes emissions of sulfur oxides. Most of the vegetable oils and animal fat-based biodiesel have very low levels of sulfur content. However, specifying this parameter is important for engine operability (Singh & Singh, 2010). ASTM D5453 standard procedure was followed to measure sulfur content.

3.6.11 Carbon residue

Carbon residue test is used to indicate the extent of deposits resulting from the combustion of fuel. Carbon residue which is formed by decomposition and subsequent pyrolysis of the fuel components can clog the fuel injectors. Carnations carbon residue for biodiesel is more important than that in diesel fuel because it shows a high correlation with the presence of free fatty acids, glycerides, soaps, polymers, higher unsaturated fatty acids and inorganic impurities. Although this residue is not solely composed of carbon, the term carbon residue is found in all standards because it has long been commonly used. The range of limit standard ASTM D4530 is Max 0.050% (m/m) and EN ISO10370 is Max. 0.30% (m/m) (Fernando et al., 2007; A. Murugesan et al., 2009).

3.7 Engine testing, instrumentations and analysis

Engine testing was accomplished in the heat engine laboratory of the University of Malaya. A single cylinder YANMAR (model no. TF 120M) engine test bed have been used for evaluating the fuel quality in the context of performance, combustion and emission characteristics. A 7.5 kW AC synchronous dynamometer (model no. ST-7.5) was used to apply the load for the engine. Details engine technical specification are presented in Table 3.5 and Figure 3.10 (a) presents a simple schematic diagram of the engine test bed with major components.

Table 3.5: Engine technical specification

Engine type	**4 Stroke DI engine**
Number of cylinders	One
Aspiration	Natural aspiration
Cylinder bore × stroke (mm)	92×96
Displacement (L)	0.638
Compression ratio	17.7
Maximum engine speed (rpm)	2400
Maximum power (kW) @ 2200 rpm	7.7
Maximum torque @ 2400 rpm	30.6 N.m
Injection timing (deg.)	15° before TDC
Injection pressure (kg/cm^2)	700
Power take-off position	Flywheel side
Cooling system	Water cooling
Connecting rod length (mm)	149.5
Fuel System	Common rail injection system

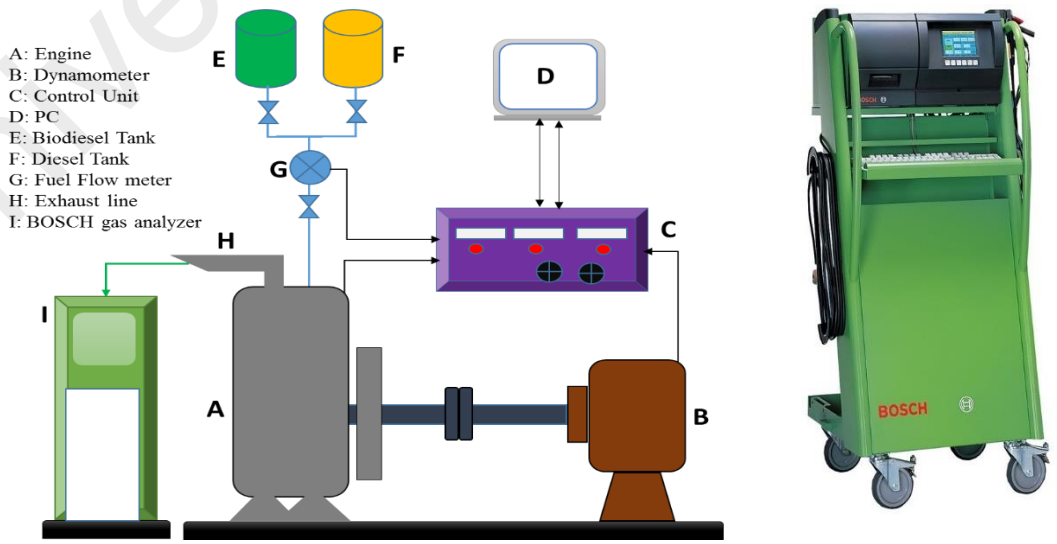

(a) Engine test bed (b) BOSCH BEA-350

Figure 3.10: (a) Schematic of engine test bed and (b) BOSCH gas analyzer

The dynamometer and exhaust gas analyzer was properly calibrated before running the test. At first, the engine was run by base fuel for few minutes to warm up. All the data were taken only once the engine reached the stable condition. Each time the engine was flushed out by the base fuel before running with other the tested fuel like biodiesel blends. All the experiments were repeated for 3 times to obtain a more accurate result and the average data presented as the final result. However, the engine testing was performed in three different operating conditions. They are:-

(a) Constant 17 N.m torque, variable engine speed (1200, 1500 and 1800 rpm)

(b) Constant 1800 rpm speed, variable torque (10 N.m 17 N.m and 25 N.m)

(c) Constant 1800 rpm speed, variable injection timing (10°, 15° and 20° bTDC)

3.7.1 Fuel system

A common-rail direct injection injector was used which was solenoid-actuated and working with 12-volt battery voltage, thus boost voltage is not required (Sealand Turbo-Diesel Asia Pte Ltd., 2016). This common rail injector was selected for its fast-acting response to close-coupled injection command. A 2.2 kW electric motor was used to increase the fuel pressure inside the rail and a solenoid valve was used to operate the opening. Figure 3.11 illustrated the schematic of fuel injector system.

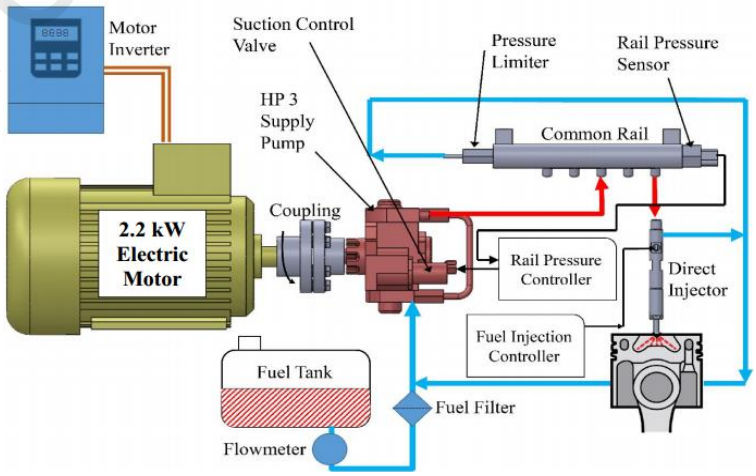

Figure 3.11: Fuel injection system

3.7.2 Combustion analysis

Kistler 6125B type pressure sensor was used to measure the in-cylinder pressure (ICP) of the engine. A PCB model 422E53 in-line charge converter was used to convert the charge signal out of the pressure sensor to a low-impedance voltage signal. An encoder with 0.125°CA resolution (X4 encoding) was used to identify the TDC position and corresponding crank angle (°CA) for each engine rotation. All related microcontroller boards were connected to the central computer via a serial USB for data acquisition. The data acquisition system is responsible for collecting signal, rectifying, filtering and converting the signal to the data to be read. The user can monitor, control and analyze the data using a LabVIEW based graphical user interface (GUI) program. All data could be logged simultaneously by clicking the record button and at the rate of 5 Hz. The ICP signal, injector current signal and encoder signals are connected with a high speed (14-bit resolution, 2MS/s sampling rate, 4 analog input channels) sampling data acquisition card namely ADLINK DAQ-2010. This card was integrated with the MATLAB® data acquisition toolbox 2.15 software with the help of a PC. This MATLAB® R2009b interface was used for direct control of the DAQ card. Also, the acquired data were further processed and analyzed with MATLAB software. To eliminate cycle-to-cycle variation in each test, 100 consecutive combustion cycles of pressure data were collected and an averaged was calculated. To reduce noise effects, smooth data using SPAN as the number of points used to compute each element was applied to the sampled cylinder pressure data.

The heat release rate (HRR) at each crank angle was obtained from the first law of thermodynamics as shown in Equation 3.6 without considering the heat losses through the cylinder wall.

$$\frac{dQ}{d\theta} = \frac{\gamma}{\gamma - 1} \times \frac{P.dV}{d\theta} + \frac{\gamma}{\gamma - 1} \times \frac{V.dP}{d\theta} \qquad \textbf{3.6}$$

Where $\frac{dQ}{d\theta}$ = rate of heat release (J/°CA), V=instantaneous cylinder volume (m^3), θ = crank angle (°CA), P = instantaneous cylinder pressure (Pa), γ = specific heat ratio which is considered constant at 1.35 (Shukla et al., 2015). In-cylinder pressure and cylinder volume with respect to crank angle considered as the input value. The volume (V) and the volume changes ($dV/d\theta$) with respect to every crank angle are represented by Equation 3.7 and Equation 3.8, respectively.

$$V = V_c + A.r\left[1 - Cos\left(\frac{\pi\theta}{180}\right)\right] + \frac{1}{\lambda}\left\{1 - \sqrt{1 - \lambda^2 Sin^2\left(\frac{\pi\theta}{180}\right)}\right\} \quad \textbf{3.7}$$

$$\frac{dV}{d\theta} = \left(\frac{\pi\theta}{180}\right) \times r\left\{Sin\left(\frac{\pi\theta}{180}\right) + \frac{\lambda^2 Sin^2\left(\frac{\pi\theta}{180}\right)}{2 \times \sqrt{1 - \lambda^2 Sin^2\left(\frac{\pi\theta}{180}\right)}}\right\} \quad \textbf{3.8}$$

Here, $\lambda = \frac{l}{r}$ and $A = \frac{\pi D^2}{4}$, where l is the connecting rod length, r is the crank radius= $0.5 \times stroke$, D is the cylinder bore and $V_c$is the clearance volume.

A function used to present the mass fraction burned versus crank angle curve which well known as Weibe function like as Equation 3.9.

$$x_b = 1 - exp\left[-a\left(\frac{\theta - \theta_{soc}}{\Delta\,\theta}\right)^{m+1}\right] \quad \textbf{3.9}$$

Where $\theta = Crank\ angle$, $\theta_{soc} = Start\ of\ combustion$,$\Delta\,\theta = Combustion\ duration$, a and m are adjustable parameter and considered $a = 5, m = 2$ (Heywood et al., 1979).

3.7.3 Performance analysis

The performance of an engine is measured by power output, fuel economy and durability. The power output which is refers to the brake power (BP) i.e. the power available at the crankshaft. The torque and engine speed was obtained from the PC through data accusation system and BP was calculated by the Equation 3.10. Brake specific fuel consumption (BSFC) defines as fuel flow rate (consumption) per unit BP output for a specific fuel. Kobold positive displacement gear wheel flow meter (Model: DOM-A05H) was used for measuring the fuel flow rate and BSFC was obtained from the Equation 3.11. An air flow meter turbine with 2 to 70 liters per second measuring range

was employed to measure the intake air flow rate. Also, a "K" type thermocouple was used to monitor the exhaust gas temperature. Brake Thermal Efficiency (BTE) is defined as break power of a heat engine as a function of the thermal input from the fuel. It is used to evaluate how well an engine converts the heat from a fuel to mechanical energy. BTE was obtained from the Equation 3.13.

$$BP = \frac{2\pi N \times T}{60 \times 1000}\ kW \quad \textbf{3.10}$$

$$BSFC = \frac{Specific\ fuel\ consumption}{BP} = \frac{\dot{m}_f}{BP}\ \text{Kg/kWh} \quad \textbf{3.11}$$

$$\text{Fuel mass flow rate, } \dot{m}_f = \frac{v\ (L) \times 10^{-3} \times \rho\ (\frac{Kg}{m^3})}{T\ (h)}\ \text{Kg/h} \quad \textbf{3.12}$$

$$BTE = \frac{Heat\ equivalent\ to\ one\ kW\ hour}{Heat\ in\ fuel\ per\ BP} = \frac{3600}{\frac{\dot{m}_f \times CV}{BP}} = \frac{3600}{BSFC \times CV} \quad \textbf{3.13}$$

Where, $N =$ Engine speed in rev/min (rpm) and $T =$ Torque in $N.m$, $BP = Brake\ Power\ in\ kW$, $m_f = fuel\ consumption\ in \frac{Kg}{h}$, $CV = Calorific\ Value\ in \frac{kJ}{Kg}$

3.7.4 Emission analysis

BOSCH BEA-350 exhaust gas analyzer was connected to the engine exhaust outlet to measure the major exhaust gas like nitric oxide (NO), carbon dioxide (CO_2), carbon monoxide (CO) and unburned hydrocarbon (UHC). The used analyzers gas measuring method with their measuring range, measuring accuracy and experimental percentage uncertainty were listed in Table 3.6. The measured emission was converted to globally acceptable unit g/kWh according to the SAE J177 (Society of Automotive Engineers, 2002). The equations are given bellow:-

$$CO\ \left(\frac{g}{kWh}\right) = \frac{5.79 \times 10^{-2} \times CO\ (ppm) \times \dot{m}_{exhaust}(kg/min)}{BP\ (kW)} \quad \textbf{3.14}$$

$$CO_2\ \left(\frac{g}{kWh}\right) = \frac{9.09 \times 10^{-2} \times CO_2\ (ppm) \times \dot{m}_{exhaust}(kg/min)}{BP\ (kW)} \quad \textbf{3.15}$$

$$HC\ \left(\frac{g}{kWh}\right) = \frac{2.87 \times 10^{-2} \times HC\ (ppm) \times \dot{m}_{exhaust}(kg/min)}{BP\ (kW)} \quad \textbf{3.16}$$

$$NO\ \left(\frac{g}{kWh}\right) = \frac{6.20 \times 10^{-2} \times NO\ (ppm) \times \dot{m}_{exhaust}(kg/min)}{BP\ (kW)} \quad \textbf{3.17}$$

Table 3.6: Gas analysers specification

Model	Method	Item	Measuring range	Accuracy	% Uncertainty
BOSCH BEA 350	Non-dispersive infrared	CO	0-10% vol.	±0.001% vol.	±1.00%
	Non-dispersive infrared	CO_2	0-18% vol.	0.01% vol.	±1.50%
	Flame ionization detector	HC	0-9999 ppm	±1 ppm	±1.00%
	Electrochemical detector	NO	0-5000 ppm	±1 ppm	±1.30%

3.7.5 Error and uncertainty analysis

Instrumental accuracy and measuring uncertainty are kinds of error during measuring data. Accuracy is the resolution of a measuring instrument which was provided by the manufacturer for a specific instrument. It indicates that how precisely the instrument can measure the value. Errors and uncertainties may arise during the experiment from various sources, such as calibration, observation, reading, ambient condition, test planning, data input, test assembly, etc (Shahabuddin et al., 2012). Therefore, uncertainty analysis is a significant technique to validate the experimental results. A sample calculation for uncertainty analysis of brake power (BP) and other relevant measuring parameters uncertainty for diesel was presented at Appendix B. Error analysis was presented by the error bar for the performance and emission parameters. A sample error calculation is shown in Appendix B. In this study, percentage relative uncertainty was determined by the linearized approximation method of uncertainty. After calculating the individual uncertainty of measuring instrument, overall experimental uncertainty was computed by the Equation 3.18 (How et al., 2014). It was observed that the overall experimental uncertainty was less than 5% (95% confidence level), which was within the acceptable range.

$$\text{Overall uncertainty} = \sqrt{\sum (Uncertainty\ of\ each\ parameter)^2} \quad \textbf{3.18}$$

Overall uncertainty = Square root of [(uncertainty of fuel flow rate)^2 + (uncertainty of BP)^2 + (uncertainty of BSFC)^2 + (uncertainty of BTE)^2 + (uncertainty of CO)^2 + (uncertainty of CO_2)^2 + (uncertainty of NO)^2 + (uncertainty of UHC)^2 + (uncertainty of UHC)^2 + (uncertainty of pressure sensor)^2 + (uncertainty of Crank angle encoder)^2]

$$= \sqrt{(\pm 2)^2 + (\pm 1.75)^2 + (\pm 1.95)^2 + (\pm 1.74)^2 + (\pm 1)^2 + (\pm 1.5)^2 + (\pm 1.3)^2 + (\pm 1)^2 + (\pm 1)^2 + (\pm 0.03)^2}$$

$= \pm 4.56\%$

3.8 Summary

Selection of appropriate strategy is an essential factor for accomplishing the experiment as well as the objectives. This chapter clarifies how the investigation was directed from the earliest starting point till the end to get a clear picture of the study to readers. It was started with the catalyst extraction from waste eggshell, its characterization procedure and followed by the biodiesel production process parameter optimization, fuel characterization and engine testing procedure.

CHAPTER 4: RESULTS AND DISCUSSIONS

4.1 Introduction

The results, as well as the findings of all analysis for this investigation are reported and discussed in this chapter. This chapter starts with the discussion with eggshell extracted catalyst and followed by the biodiesel production process optimization as well as engine testing. In the catalyst characterization, properties and element of eggshell extracted catalyst reported and compared with commercially available CaO. Then the design matrix as well as the experimental results are discussed for the biodiesel production process parameter optimization in both esterification and transesterification stage for crude *Aphanamixis polystachya* oil (CAPO). Response surface methodology (RSM) design justified and discussed with ANOVA analysis as well as previous study. Then physicochemical properties of the produced biodiesels (*A. polystachya* and *M. pinnata*) and their blends with diesel and are measured and discussed. Finally, combustion, performance and emission results of 20% and 30% blends in a light duty diesel engine are presented, compared with ordinary diesel (OD) as well as discussed with the previous study.

4.2 Eggshell catalyst characterization

4.2.1 Thermogravimetric analysis (TGA)

TGA method has been used to study the thermo-oxidative behavior of waste eggshell extracted $CaCO_3$, developed Egg CaO and commercial Pure CaO. This technique is based on the principle of variation of sample mass as a function either of time or temperature. The most important parameters of TGA are onset temperature (T_{on}) and offset temperatures (T_{off}) which can be seen from Figure 4.1. An T_{on} is used to indicate the resistance of the material to thermal degradation (Nik et al., 2005). This is determined by extrapolating the horizontal baseline at 1% degradation.

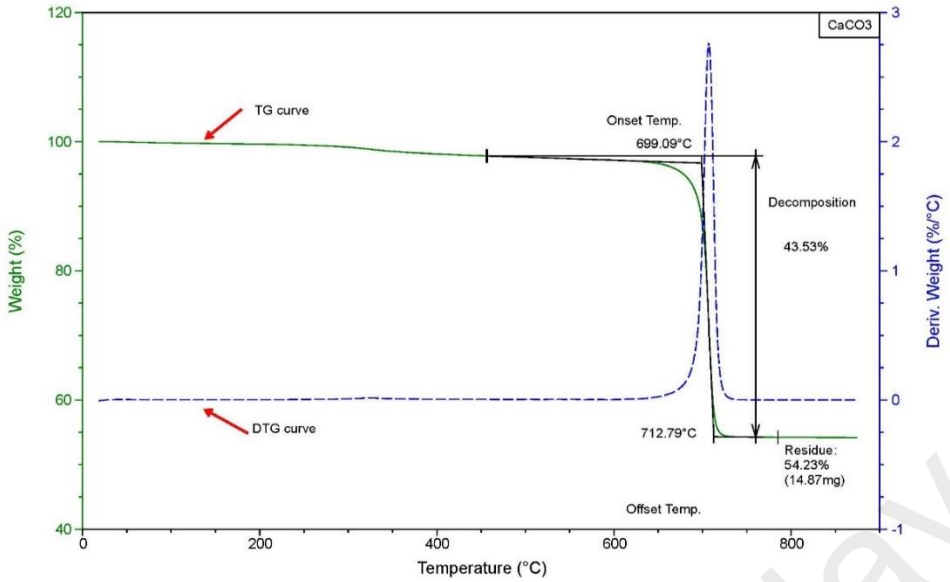

(a) TGA of eggshell extracted power (i.e. $CaCO_3$)

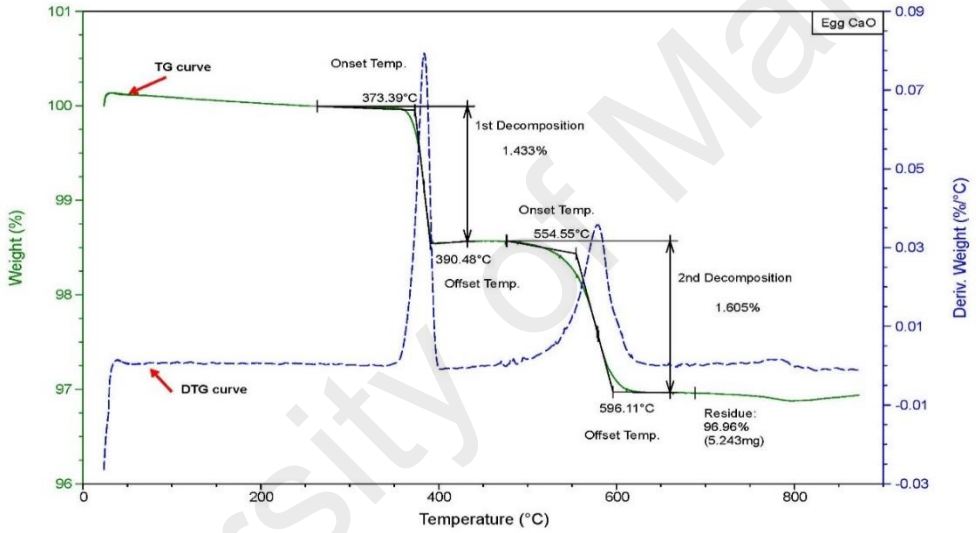

(b) TGA of calcined powder (i.e. Egg CaO)

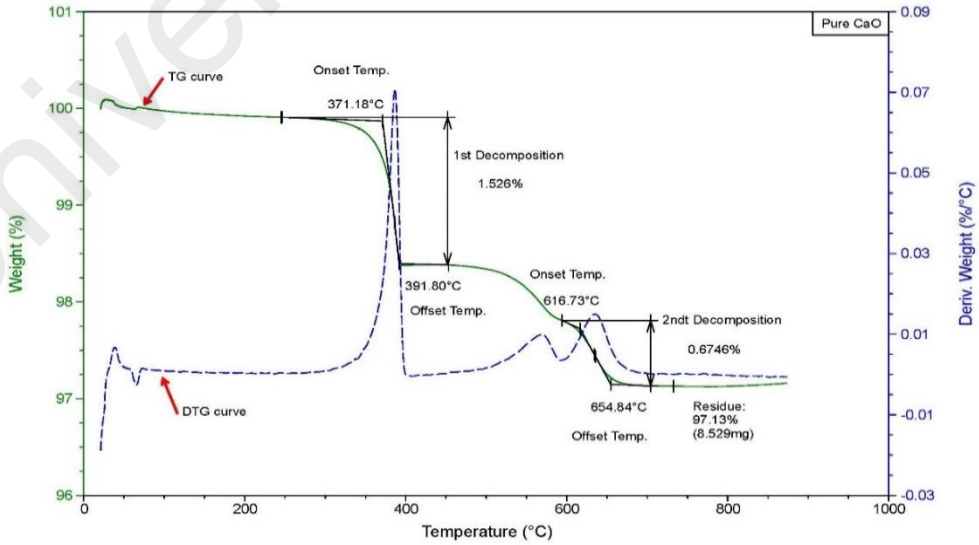

(c) TGA of commercial CaO (i.e. Pure CaO)

Figure 4.1: TGA of (a) $CaCO_3$ (b) Egg CaO and (c) Pure CaO

The intercept of this line with the tangent to the downward portion of the weight curve is defined as the T_{on}. At last, when the sample is completely burnt and TGA curve become almost flat then, the intercept of the extrapolation on the same line and the tangent to the downward portion is called as T_{off}. The derivative thermogravimetric (DTG) curve is defined as the differentiated curve from TGA. Figure 4.1 (a) illustrated the TGA results of powder that extracted from the eggshell i.e. $CaCO_3$. The Experimental work has shown that first decomposition starts at 699.09 °C which indicates the conversion starting temperature form $CaCO_3$ to CaO. The total conversion ends at 712.79°C which is the offset temperature or end of the decomposition temperature. Total decomposition amount by weight was 43.53% of the sample and the residue was 54.23%. Theoretically, it should be 44% and residue should be 46% (Jaggernauth-Ali et al., 2015). Here, the residue is the amount of the required developed catalyst. With the help of the electrical furnace the eggshell powdered was calcined at 900 °C for the 4 hours which is much higher to the required temperature. After calcination, the produced Egg CaO also placed to do TGA to find the result and to compare the properties to the commercial Pure CaO. Figure 4.1 (b) shown the TGA and DTG curve for the calcined $CaCO_3$ (i.e. Egg CaO) and Figure 4.1(c) shown the commercial Pure CaO TG and DTG curve pointing all the onset and offset temperature including the percentage decomposition and the residue. From the graphical representation, it was clear that the for both Egg CaO and Pure CaO there are two decompositions but the percentage decomposition is very less compared to $CaCO_3$. This results can be attributed to the adsorbed moisture content into the CaO during storage as CaO anhydrous in nature (Frei et al., 2008). The summary of all points including the percentage decomposition and residue in each stage is listed in Table 4.1.

Table 4.1: TAG result of $CaCO_3$, Egg CaO and Pure CaO

Item	1st Onset Temp. (°C)	1st Offset Temp. (°C)	1st decomposition (wt.%)	2nd Onset Temp. (°C)	2nd Offset Temp. (°C)	2nd decomposition (wt.%)	Residue (wt.%)
$CaCO_3$	699.09	712.79	43.53	-	-	-	54.23
Egg CaO	373.39	390.48	1.433	554.55	596.11	1.605	96.96
Pure CaO	371.18	391.80	1.526	616.73	654.84	0.6746	97.13

4.2.2 Fourier transform infrared spectroscopy (FTIR)

FTIR spectroscopy has proved to be a powerful analytical tool for the identification of basic compositional group presence in the sample. FTIR spectra, in transmittance mode, of raw waste eggshell power (before calcination) i.e. $CaCO_3$, and Egg CaO (after calcination) in the wavenumbers measured in 4000-400 cm^{-1} range and shown in Figure 4.2. Spectra were identified by using a tolerance of ±10 cm^{-1} to the obtained values (Yan et al., 2009). The most noteworthy peak intensity of eggshell particle at 1412 cm^{-1}, strongly associated with the presence of carbonate minerals within the eggshell matrix (Tsai et al., 2006). There are also two observable peaks at about 872 $cm^{-1}$and 710 cm^{-1}, respectively, which should be associated with the out-plane deformation and in-plane deformation modes respectively, in the presence of carbonate ions (CO_3^{2-}). Stretching vibrations of surface hydroxyl groups (Ca–OH) and physisorbed moisture were noticed. The surface carbonate and hydroxyl species existed due to the catalyst exposure to the air for some time while performing the FTIR analysis. The FTIR result clearly demonstrates the tendency of CaO to react with moisture and CO_2 in the air. There is an increase in the intensity of Egg CaO at the 2351 cm^{-1} band which is due to the combined –OH group and a decrease in the 1412 cm^{-1} bands for which are due to O–Ca–O group (Yan et al., 2009). This suggests the increase of Bronsted base concentration and a decrease of Lewis base concentration. Furthermore, the bands related to free water were the peak intensities at 2351, 1412 cm^{-1} and 872 cm^{-1} decreased, reflecting the reduction of the amount of the combined –OH group and O–Ca–O group on the catalyst surface. The band at

1048 cm^{-1} in the spectrum of Egg CaO catalyst was assigned to molecular CO_2 adsorbed by the basic hydroxyl groups in the catalyst (Tsai et al., 2006). Since, the major sharp transmittance peaks of FTIR spectra are an alkane, which indicates biodiesel are saturated the metal oxides thus potential to be used as alkali catalyst.

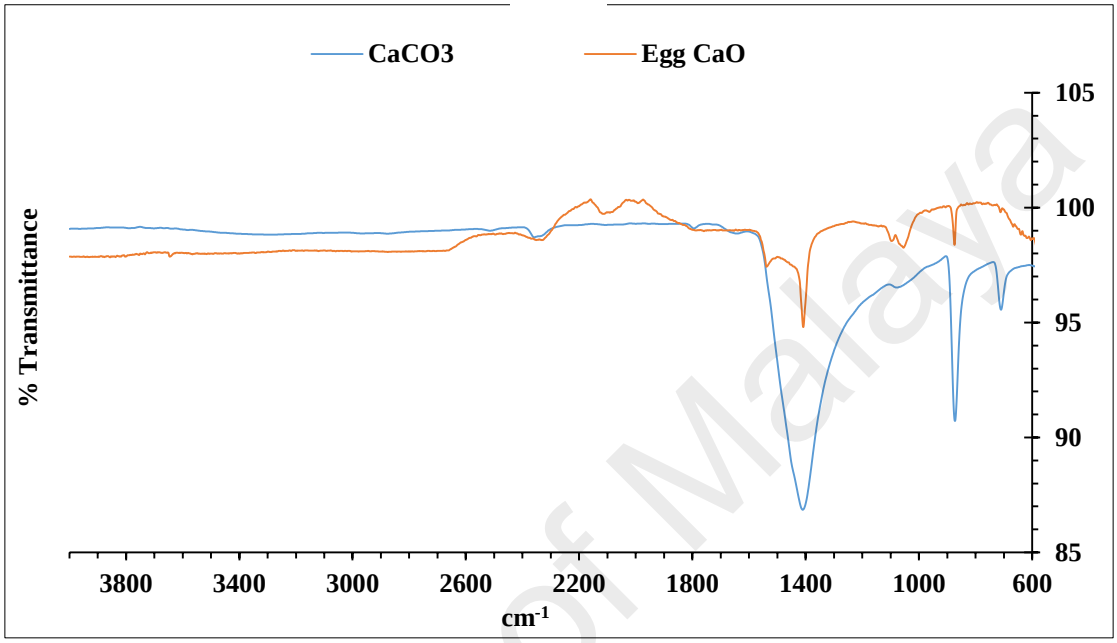

Figure 4.2: FTIR result of before and after calcination of powder

4.2.3 Scanning electron microscope (SEM)

Figure 4.3 illustrated the SEM image of (a) uncalcined $CaCO_3$ powder (b) calcined Egg CaO and (c) commercial Pure CaO. It was observed that the particles of the catalyst have a spherical structure and are agglomerated into lumps. This is because the sample was in the oxide form. The isolated particles were reasonably isotropic. It was seen from the image that the size of calcined Egg CaO (6.34 µm) and Pure CaO (4.48 µm) are smaller than uncalcined $CaCO_3$ (8 µm). It is also noticeable that the edges shape of Egg CaO becomes rounded after calcination in an electric furnace at 900°C. The smaller size and the spherical shape occupies relatively higher surface area during reaction medium thus provides superior catalytic activity (Danlin Zeng et al., 2015).

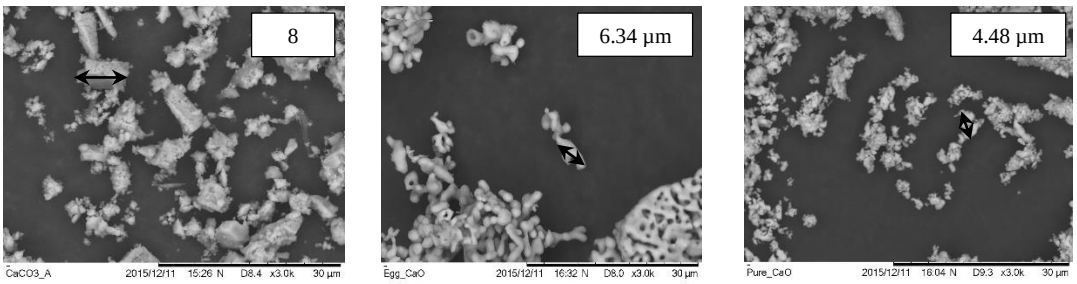

(a) $CaCO_3$, @3K magnification (b) Egg CaO, 3K magnification (c) Pure CaO, 3K magnification

(a) $CaCO_3$ @ 5K magnification (b) Egg CaO, 5K magnification (c) Pure CaO, 5K magnification

(a) $CaCO_3$ @7K magnification (b) Egg CaO, 7K magnification (c) Pure CaO, 7K magnification

Figure 4.3: SEM image of (a) $CaCO_3$, (b) Egg CaO and (c) Pure CaO at different magnification

4.2.4 Energy dispersive X-ray spectroscopy (EDX)

EDX is the technique by which atomic or weight percentage of each element can be determined. It is a way to know about the elements that are presented in the specimens. EDX also did by the same table top HITACHI TM3030 machine. After taking SEM image, the EDX has performed at least 6 points for each sample. The average of the 6 points taken and presents as results in Table 4.2. It can be seen that wt.% of calcium (Ca) molecule increases after calcination and decreases carbon (C) and oxygen (O_2) molecule. This result can be attributed to the weight loss during calcination.

Table 4.2: Elementary analysis of $CaCO_3$, Egg CaO and Pure CaO

Element	$CaCO_3$		Egg CaO		Pure CaO	
	Wt%	Atom. %	Wt%	Atom. %	Wt%	Atom. %
Ca	28.78	12.80	38.76	18.03	29.24	12.06
O	47.72	52.98	28.98	33.44	29.09	29.89
C	23.00	33.91	31.91	48.19	42.70	58.43
Mg	0.25	0.19	0.39	0.29	0.26	0.17
Na	0.18	0.14	0.06	0.04	-	-
Al	0.13	0.09	-	-	0.08	0.05
Si	-	-	-	-	0.06	0.04

4.2.5 X-ray powder diffraction (XRD)

The crystalline phases and extracted (a) $CaCO_3$, (b) Egg CaO and (c) commercial Pure CaO.

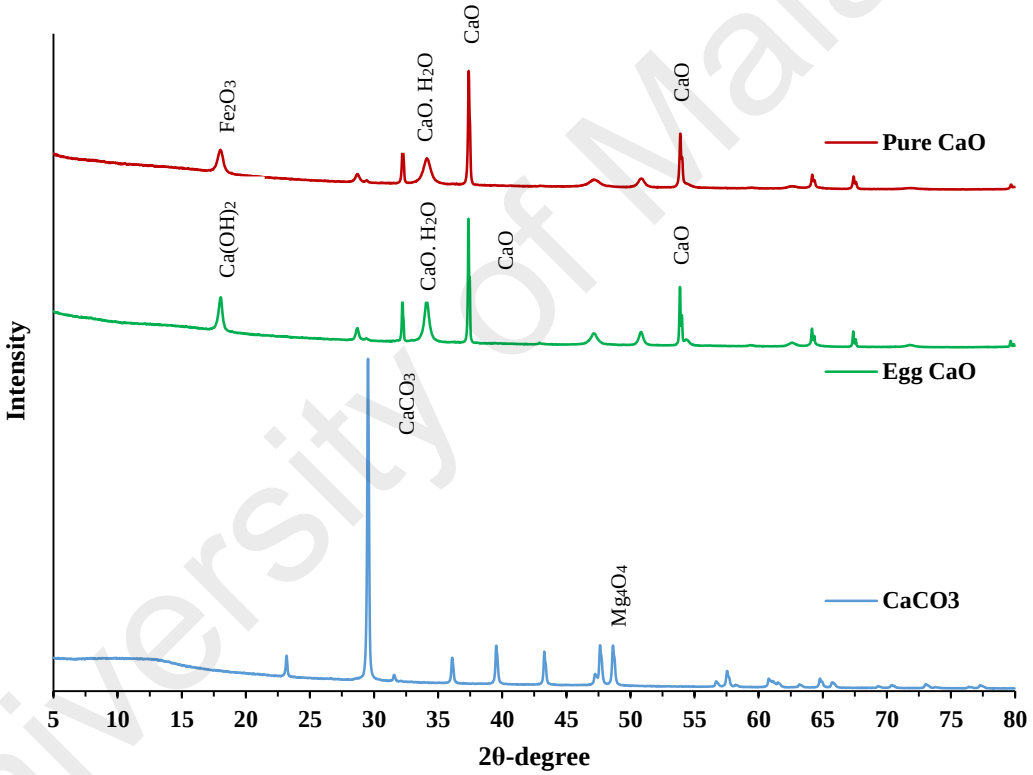

Figure 4.4: XRD peaks of $CaCO_3$, Egg CaO and Pure CaO

It can be seen from the illustration that the major peaks are found at 29 °2θ for uncalcined $CaCO_3$ (b) 37 °2θ for both Egg CaO and commercial Pure CaO. The diffraction peaks at 29.40, 29.45, 29.55 °2θ in the eggshell spectrum are ascribed to $CaCO_3$ and 29.39 °2θ presents calcite (calcium carbonate mineral). Also, some other components in oxide form found in 23.09 °2θ (Cristobalite, a high-temperature polymorph of silica), 47.47 °2θ (Periclase, a cubic form of magnesium oxide) were

noticed at the extracted uncalcined eggshell powder. While in the spectrum of Egg CaO catalyst, the characteristic peaks found near to 37 °2θ and 54 °2θ which are attributed to the presence of CaO derived from $CaCO_3$ in the eggshell by calcination (Witoon, 2011). Other peaks and the corresponding compound along with their chemical formulae are listed in Table 4.3. Some unexpected compound can found near to the major peaks those can arise from the crystal of Cu-α and Fe. Further revealing of an incident of the reaction between KF and $CaCO_3$ during the calcination process (Gao et al., 2010; Liu et al., 2012).

Table 4.3: Compound name with chemical formulae of XRD angle

Sample Type	2θ-degree	Chemical Formulae	Compound Name
$CaCO_3$	23.09	Si_8O_{16}	Cristobalite
	29.39	$Ca_6C_6O_{18}$	Calcite
	29.40, 29.45, 29.55 (Max. Peak)	**$CaCO_3$**	**Calcium Carbonate**
	36.06	Mn_4S_4	Alabandite
	39.45,39.50,39.52	W	Tungsten
	43.27, 43.31, 43.32	BN	Boron Nitride
	47.47	Mg_4O_4	Periclase
	48.63, 48.73	Ca_4F_4	Fluorite
Egg CaO	18.05	$Ca(OH)_2$	Calcium Hydroxide
	28.69	$Mg_{0.64}Ca_{0.94}(CO_3)$	Magnesium Calcium Carbonate
	31.92	$CaMg(CO_3)_2$	Calcium Magnesium Carbonate
	34.06, 47.15	$CaO.H_2O$	Calcium Oxide Hydrate
	37.25	Ca_4O_4	Lime
	37.36 (Max. peak), 53.86	**CaO**	**Calcium Oxide**
	50.79	Fe_2	Iron
	67.31	Al_2O_3	Aluminum Oxide
Pure CaO	18.3	Fe_2O_3	Iron Oxide
	28.71	$B(CeO_3)$	Barium Cerium Oxide
	28.72, 28.73	SiO_2	Silicon Dioxide
	28.8	Ca_2	Calcium-gamma
	32.23	$Sr(RuO_3)$	Strontium Ruthenium Oxide
	32.33	Ag_4O_4	AgO
	34.10, 34.11	$Ca(OH)_2$	Calcium Hydroxide
	34.19	$CaO.H_2O$	Calcium Oxide Hydrate
	37.18, 37.34	Ca_4O_4	Lime
	37.36 (Max. peak), 54.23	**CaO**	**Calcium Oxide**
	46.98	CoS	Cobalt Sulfite
	50.90	Fe_2	Iron
	67.31	Al_2O_3	Aluminum Oxide

4.2.6 Catalytic activity test

Hammett indicator titration approaches have been taken for measuring the basic strength of the catalyst. The used Hammett indicators are phenolphthalein (pKa=9.8), indigo carmine (pKa=12.2) and 2, 4-dinitroaniline (pKa=15). Approximately 25 mg of sample was weighted and shaken with 4 ml of a solution of Hammett indicator diluted in methanol. The mixture was left for 2 h to equilibrate and the color noted. The basic strength of the catalyst was taken to be higher than the weakest indicator that underwent a color change and lower than the strongest indicator that underwent no color change. (Niju et al., 2014). The basic strength of the calcined eggshell extracted catalyst i.e. Egg CaO (9.8<H_<10.1) was found slightly lower than commercial Pure CaO (10.1<H_<12.2). This activity level comparable to other extracted CaO from different sources like marlstones red (6.8 to 7.2), marlstones white (10.1 to 15.0), quail eggshell (7.2-9.8) whereas commercially available CaO lied between 10.1 to 015 (Jaggernauth-Ali et al., 2015; Tan et al., 2015).The extracted Egg CaO catalyst activity can be further improved up to 15<H_<18 level by impregnation of 1% to 5% Li loading (Boro et al., 2014).

4.3 Optimization of production process through RSM

The optimization approached done by the RSM tools and the designed models acceptability were verified by the different statistical point of view.

4.3.1 Mathematical model development and interpretation of regression

Stat-Ease Design Expert v7.0.0 software was used to carry out the statistical analysis. According to CCD design, twenty run experiment was performed for both esterification and transesterification step. Table 4.4 and Table 4.5 represented the complete experimental matrix for acid esterification and alkali transesterification respectively, which are composed of 8 factorial points, 6 axial and 6 center points where 20 run experiments were conducted under identical conditions to determine the residual error and other statistical analysis. After conducting the experiment, response variable was fitted with the second order model for both R_1 (esterified oil yield) and R_2 (biodiesel yield). In order to find the best model, different models were checked in which general model can be explained by Equation 4.1.

$$R = \beta_o + \sum_{i=1}^{k} \beta_i X_i + \sum_{i=1}^{k} \beta_{ii} X_i^2 + \sum_{i=1}^{k-1} \sum_{j=i+1}^{k} \beta_{ij} X_i X_j + \varepsilon \qquad \textbf{4.1}$$

Where, R is the response factor (yield), X_i and X_j is the independent design variable, β_o is the constant co-efficient intercept, β_i is the first order or linear coefficient of the model, β_{ii} is the quadratic co-efficient of i factor, β_{ij} is the interaction co-efficient between i and j factors, k is the number of factors considered for optimization in the experiment and ε is the experimental error attributed to R.

Table 4.4: Experimental design (actual) matrix for acid esterification of pre-treated *A. polystachya* oil

Std	Run	Point type	Level (Coded Factors)			Reaction variables (Actual factors)			Response
						Methanol, A (v/v % of Oil)	Catalyst (acid), B (v/v % of Oil)	Temperature, C (°C)	Yield, R_1 (v/v % of Oil)
1	6	Factorial	-1	-1	-1	150.00	0.80	60.00	97.0
2	14	Factorial	+1	-1	-1	200.00	0.80	60.00	77.0
3	8	Factorial	-1	+1	-1	150.00	1.50	60.00	85.0
4	11	Factorial	+1	+1	-1	200.00	1.50	60.00	84.0
5	9	Factorial	-1	-1	+1	150.00	0.80	70.00	96.5
6	5	Factorial	+1	-1	+1	200.00	0.80	70.00	78.0
7	18	Factorial	-1	+1	+1	150.00	1.50	70.00	84.5
8	7	Factorial	+1	+1	+1	200.00	1.50	70.00	96.5
9	4	Axial	-1.68179	0	0	132.96	1.15	65.00	97.0
10	19	Axial	+1.68179	0	0	217.04	1.15	65.00	93.0
11	12	Axial	0	-1.68179	0	175.00	0.56	65.00	88.0
12	13	Axial	0	+1.68179	0	175.00	1.74	65.00	92.0
13	16	Axial	0	0	-1.68179	175.00	1.15	56.59	83.0
14	10	Axial	0	0	+1.68179	175.00	1.15	73.41	89.0
15	1	Center	0	0	0	175.00	1.15	65.00	95.0
16	20	Center	0	0	0	175.00	1.15	65.00	96.0
17	3	Center	0	0	0	175.00	1.15	65.00	95.5
18	17	Center	0	0	0	175.00	1.15	65.00	94.0
19	2	Center	0	0	0	175.00	1.15	65.00	94.5
20	15	Center	0	0	0	175.00	1.15	65.00	95.5

Table 4.5: Experimental design (actual) matrix for alkali transesterification of the esterified *A. polystachya* oil

Std	Run	Point type	Level (Coded Factors)			Reaction variables (Actual factors)			Response
						Methanol, A (v/v % of Oil)	Catalyst (Eggshell), B (w/w % of Oil)	Temperature, C (°C)	Yield, R_2 (v/v % of Oil)
1	14	Factorial	-1	-1	-1	25.00	1.00	60.00	96.00
2	17	Factorial	+1	-1	-1	55.00	1.00	60.00	91.80
3	9	Factorial	-1	+1	-1	25.00	2.00	60.00	91.00
4	20	Factorial	+1	+1	-1	55.00	2.00	60.00	87.20
5	13	Factorial	-1	-1	+1	25.00	1.00	70.00	91.30
6	15	Factorial	+1	-1	+1	55.00	1.00	70.00	90.40
7	10	Factorial	-1	+1	+1	25.00	2.00	70.00	95.00
8	18	Factorial	+1	+1	+1	55.00	2.00	70.00	92.50
9	6	Axial	-1.68179	0	0	14.77	1.50	65.00	93.20
10	12	Axial	+1.68179	0	0	65.23	1.50	65.00	89.50
11	7	Axial	0	-1.68179	0	40.00	0.66	65.00	92.00
12	4	Axial	0	+1.68179	0	40.00	2.34	65.00	91.00
13	16	Axial	0	0	-1.68179	40.00	1.50	56.59	94.00
14	8	Axial	0	0	+1.68179	40.00	1.50	73.41	95.00
15	2	Center	0	0	0	40.00	1.50	65.00	97.60
16	1	Center	0	0	0	40.00	1.50	65.00	97.00
17	19	Center	0	0	0	40.00	1.50	65.00	96.60
18	11	Center	0	0	0	40.00	1.50	65.00	98.00
19	5	Center	0	0	0	40.00	1.50	65.00	96.60
20	3	Center	0	0	0	40.00	1.50	65.00	97.90

4.3.2 Model Fitting

After completing the 20 run experiments for both individual esterification and transesterification stage, fit summary for all possibilities of sequential models sum of squares are presented in Table 4.6. It was observed from sequential models that quadratic model was suggested for both esterification percentage yield *(R_1)* and transesterification percentage yield *(R_2)*. The best model should have an insignificant probability value, or P-value>0.10 ("Stat-Ease Handbook for Experimentesrs,"). It can be seen from the table that P-value is greater than the required level for the both steps. The cubic model was aliased for the both responses thus relatively higher order quadratic model showed as the suggested. Furthermore, ANOVA analysis was performed to justify the models lack of fit and adequacy by the quadratic model for both yields.

Table 4.6: Sequential models sum of squares

Responses	Source	Sum of squares (SS)	df	Mean square	F-value	P-value (Prob>F)	Comments
Yield (R_1) for Esterification stage	Linear	573.79	11	52.16	41.18	0.0003	
	2FI	244.44	8	30.56	24.12	0.0014	
	Quadratic	**16.16**	**5**	**3.23**	**2.55**	**0.1636**	**Suggested**
	Cubic	6.40	1	6.40	5.05	0.0745	Aliased
	Pure Error	6.33	5	1.27			
Yield (R_2) for Transesterification stage	Linear	158.42	11	14.40	35.85	0.0005	
	2FI	125.95	8	15.74	39.20	0.0004	
	Quadratic	**1.20**	**5**	**0.24**	**0.60**	**0.7071**	**Suggested**
	Cubic	0.21	1	0.21	0.52	0.5014	Aliased
	Pure Error	2.01	5	0.40	35.85	0.0005	

4.3.3 ANOVA analysis and lack of fit

Analysis of variance (ANOVA) is a popular tool in statics to recheck the model fit summary and can be justified the model lack of fit with the analysis of consequent F-value and p-value (Prob>F). The level of significance for all independent variable can be explained. Higher F-value indicates the more variance can be explained and lower F-value is an indication of the more variance due to the noise thus higher F-value is expected. Smallest P-value value indicates (less than 0.05) the higher level of significance for related variable and individual parameters in the model ("Stat-Ease Handbook for

Experimentesrs,"). P-value also signifies the interaction intensity among all other parameters. Thus higher F-value with lower p-value fits the model best. Table 4.7 and Table 4.8 Presented the ANOVA analysis and fittest summary for esterified percentage yield (R_1) and transesterified percentage yield (R_2) of the *A. polystachya*.

Table 4.7: ANOVA analysis and lack of fit test for percentage yield response (R_1) of esterified *A. polystachya*

Source	Sum of squares	df	Mean square	F value	P value (Prob>F)	Comments
Model	677.25	9	75.25	33.46	< 0.0001	**significant**
A- Methanol	77.77	1	77.77	34.58	0.0002	
B-Acid catalyst loading	1.09	1	1.09	0.49	0.5016	
C-Reaction temperature	40.75	1	40.75	18.12	0.0017	
AB	294.03	1	294.03	130.73	< 0.0001	
AC	30.03	1	30.03	13.35	0.0044	
BC	5.28	1	5.28	2.35	0.1564	
A^2	5.07	1	5.07	2.26	0.1640	
B^2	80.34	1	80.34	35.72	0.0001	
C^2	168.74	1	168.74	75.02	< 0.0001	
Residual	22.49	10	2.25			
Lack of Fit	16.16	5	3.23	2.55	0.1636	**not significant**
Pure error	6.33	5	1.27			
Cor Total	699.74	19				

Table 4.8: ANOVA analysis and lack of fit test for percentage yield response (R_2) of *A. polystachya* biodiesel

Source	Sum of squares	df	Mean square	F value	P value (Prob>F)	Comments
Model	183.90	9	20.43	63.69	< 0.0001	**significant**
A- Methanol	22.74	1	22.74	70.87	< 0.0001	
B-Catalyst loading (Eggshell)	2.20	1	2.20	6.86	0.0257	
C-Reaction temperature	1.75	1	1.75	5.44	0.0419	
AB	0.18	1	0.18	0.56	0.4711	
AC	2.65	1	2.65	8.24	0.0166	
BC	29.65	1	29.65	92.39	< 0.0001	
A^2	66.74	1	66.74	208.00	< 0.0001	
B^2	63.49	1	63.49	197.87	< 0.0001	
C^2	15.53	1	15.53	48.42	< 0.0001	
Residual	3.21	10	0.32			
Lack of Fit	1.20	5	0.24	0.60	0.7071	**not significant**
Pure error	2.01	5	0.40			
Cor Total	187.11	19				

The appropriateness of the model demonstrated by F-value, P-value, Coefficient of variance (COV) along with the determination coefficient (R^2), adjusted R-squared(R^2_{adj}),

predicted R^2 and predicted residual error sum of squares (PRESS). R^2 is a measure of the amount of variation around the mean explained by the model. It can also be used as the precision and accuracy measurement tools of the proposed model. R^2_{adj}, which is obtained after adjusting for the number of terms in the model relative to the number of design point, represents the amount of variation that can be explained by the model. R^2_{adj} decreases as the number of terms in the model increases if those additional terms do not add value to the model (Lee et al., 2011). Predicted R^2 is a measure of the amount of variation in new data explained by the model. The predicted R^2 and the R^2_{adj} should be within 0.20 of each other. Otherwise there may be a problem with either the data or the model (Lee et al., 2011; Yücel, 2012). Co-efficient of variance (COV) or the relative standard deviation (RSD) indicates the extent of error of any model which is measured as the percentage of standard deviation over mean value. COV of a model within the 10% is an indication of the reproducible of the model. All the statistical equations that used for this analysis are given in Equation 4.2 to Equation and the model summary statistics for both percentage yield is presented in Table 4.9.

$$F - value = \frac{mean\ of\ square\ regression}{mean\ of\ square\ residual} = \frac{MnS_{RG}}{MnS_{RD}} \quad \textbf{4.2}$$

$$COV = \frac{Standerd\ Deviation}{mean} \times 100 = \frac{\sigma}{\bar{X}} \times 100 \quad \textbf{4.3}$$

$$R^2 = 1 - \frac{SS_{residual}}{SS_{residual} + SS_{model}} \quad \textbf{4.4}$$

$$R^2_{adj} = 1 - \left(\frac{SS_{error}/_{DF_{error}}}{(SS_{model} + SS_{error})/(DF_{model} + DF_{error})} \right) \quad \textbf{4.5}$$

$$Pred.R^2 = 1 - \frac{PRESS}{SS_{total} - SS_{block}} \quad \textbf{4.6}$$

Table 4.9: Model summary statistics for percentage yield (R_1 and R_2)

Response	Standard Deviation	Mean	COV (%)	PRESS	R^2	Adjusted R^2	Predicted R^2	Adequate precision
Yield (R_1)	1.50	90.53	1.66	139.85	0.9679	0.9389	0.8001	19.588
Yield (R_2)	0.57	93.68	0.60	12.78	0.9829	0.9674	0.9317	24.938

It can be seen that the Predicted R^2 value in reasonable agreement with the R^2_{adj} value for both steps. Also the adequate precision which is the measure of the signal to noise ratio found 19.588 for esterification and 24.938 for transesterification step which is a clear indication of adequate signal whereas greater than 4 is desirable. This is a clear confirmation that these model can be used to navigate the design space. Subscuquient second order final coded equation obtained by the application of least squares method and muttiple regression study on the obtained data and given the esterification yield in Equation 4.7 and transesterification yield in Equation 4.8.

$$R_1 = +94.88 - (2.39 \times A) + (0.28 \times B) + (1.73 \times C) + (6.06 \times A \times B) + (1.94 \times A \times C) + (0.81 \times B \times C) - (0.59 \times A^2) - (2.36 \times B^2) - (3.42 \times C^2) \quad \textbf{4.7}$$

$$R_2 = +97.29 - (1.29 \times A) - (0.40 \times B) + (0.36 \times C) - (0.15 \times A \times B) + (0.58 \times A \times C) + (1.93 \times B \times C) - (2.15 \times A^2) - (2.10 \times B^2) - (1.04 \times C^2) \quad \textbf{4.8}$$

Where R_1 is the esterification percentage yield of esterified oil and R_2 is the transesterification percentage yield of biodiesel. Whereas A (methanol), B (catalyst) and C (Temperature) are the coded form of independent variables of the model.

4.3.4 Indicative statistics for model acceptability

It is fundamental to validate first whether the fitted model gives a sufficient estimation of the actual values or not. Although the model clarifies an adequate fit, a further continuation of the investigation and enhancement of the coordinated reaction surface has a tendency to avoid lacking or deceiving comes (Khan et al., 2014). A few analytical strategies are available which can evaluate the adequacy of the model as well as the process parameters (Karim et al., 2014). The aptness of the models was appraised by the influence plots and the residuals. Residuals refer to the dissimilarity difference between predicted estimation value and actual value (experimental value). Residuals are also a reflection of the components of variations, inaccurately fitted to the model and it is successively anticipated that they act according to the normal distribution (Ates & Erginel, 2016). Figure 4.5 illustrated the normal probability to the internally studentized

residuals which refer to a graphical representation of contemplation of the proper method. Wheather they lying reasonably close on a straight line and reveal no deviation of the variance and thus the normal distribution of data can be affirmed. The Shapiro-Wilks test for normality is not available in this graph because the test is dependent on the assumption of independence. There is autocorrelation between the residuals, which invalidates the Shapiro-Wilks test thus visual inspection of the graph is sufficient (Myers et al., 2016).

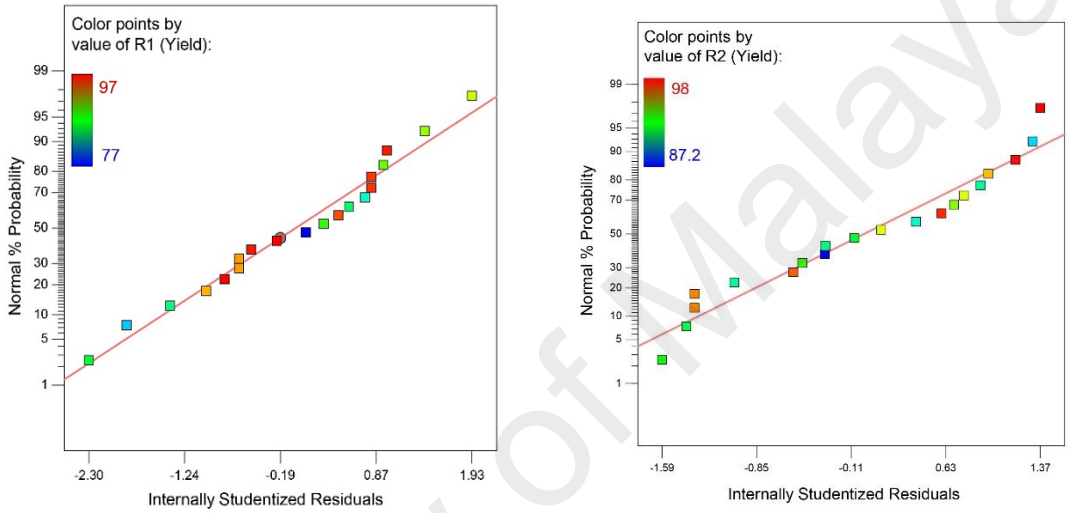

(a) Esterification (b) Transesterification

Figure 4.5: Normal probability plot vs residuals for yield (a) esterification and (b) transesterification step

Residuals versus the ascending predicted response values test the assumption of constant variance and this plot should be a random scatter (constant range of residuals across the graph). Expanding variance in this plot indicates the need for a transformation (Montgomery, 2008). Figure 4.6 illustrated the residuals and predicted yield responses for (a) esterification and (b) transesterification of the esterified product in the batch production. It can be seen that the plot is scattered indiscriminately which refers to the variance of the actual finding is constant for both responses. This is also an indication of the deficiency of the largely biased errors in the experiment (Karim et al., 2014). Both the Table 4.7 and Table 4.8 also a reflection of this statement.

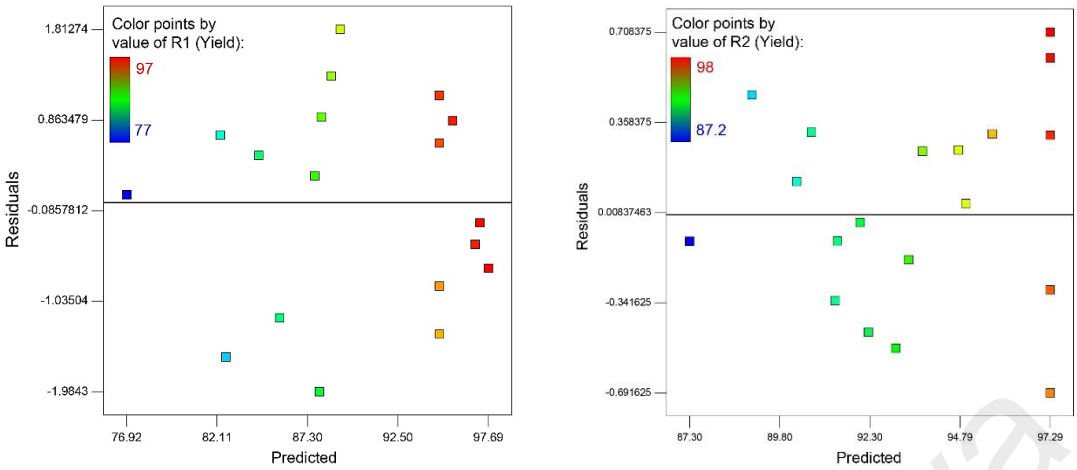

(a) Esterification (b) Transesterification

Figure 4.6: Residuals and predicted response to yield (a) esterification and (b) transesterification step

Table 4.12 illustrated the internally studentized residuals versus the experimental run order plot which checks for lurking variables that may have influenced the response during the experiment. A randomly scatter plots (no specific trends or patterns) can be seen as the both step which is desirable for good model. Specific trends or patterns indicates a time-related variable lurking in the background. Blocking and randomization provide protection against trend running.

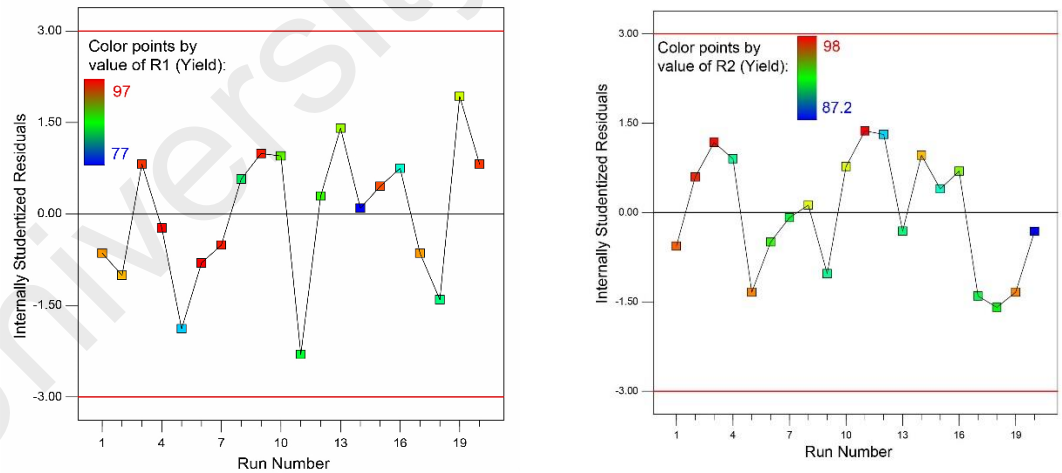

(a) Esterification (b) Transesterification

Figure 4.7: Internally studentized residuals vs. run number of yield for (a) esterification and (b) transesterification stage

Externally studentized residual (Outlier t, R-Student) is a measure of how many standard deviations of the actual value deviates from the value predicted after deleting the point in question. Outliers should be investigated to find out if a special cause can be

assigned to them. If a cause is found, it may be acceptable to analyze the data without that point. If no special cause is identified, then the point probably should remain in the data set. Figure 4.8 illustrated the outlier t plot for this design model and all the runs found to be within the expected range for both responses i.e. ±3.50. Thus all the data set were being considered for analysis and special issues are not needed to take into account.

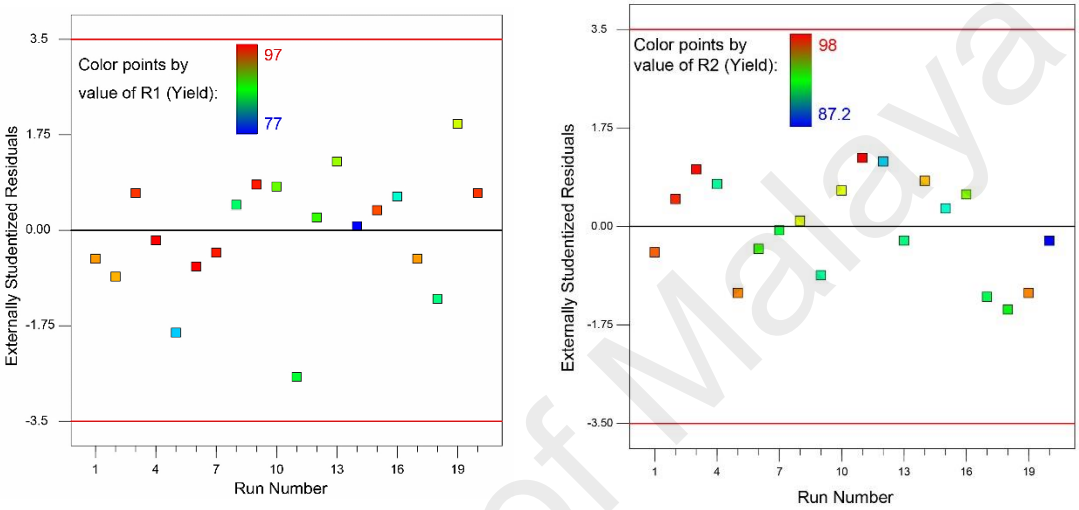

(a) Esterification (b) Transesterification

Figure 4.8: Externally studentized residual vs run number for (a) esterification and (b) transesterification stage

The regression model was utilized to figure out the predicted estimates of the percentage yield and acid value as well as contrasted with the experimental result. A model delivered great impact on products if the predicted estimate and experimental result are adjacent to each other (Khan et al., 2014). Figure 4.9 illustrated the actual (experimental) versus predicted (mathematically calculated) yield percentage for (a) esterification (b) transesterification step. An appropriate correlation among the predicted estimation and the actual result was found which was conveyed nearly neighboring the straight line. This spectacle demonstration verifies the regression equation used for fitting the relevant data. Also, the CCD model aggregates in the experimental design which is competently convenient for converting product i.e. percentage yield.

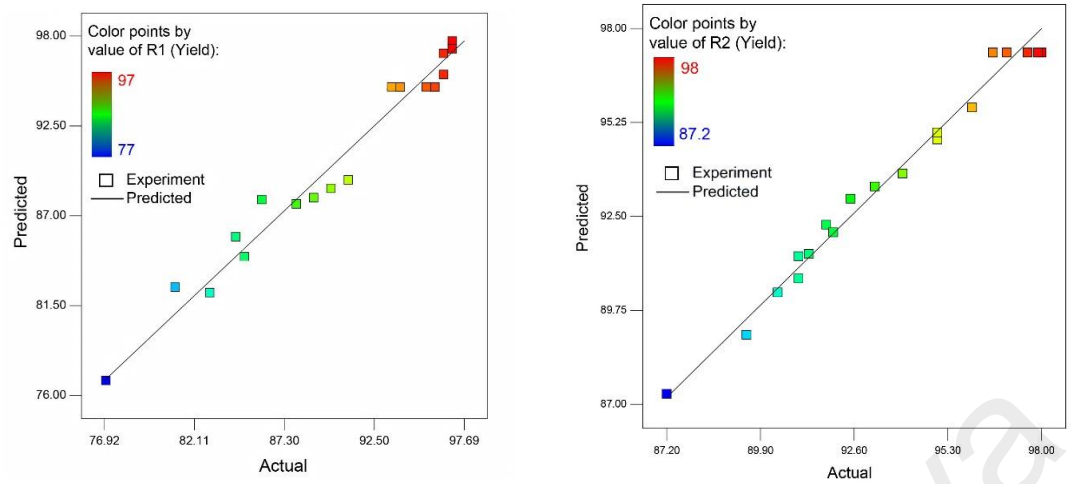

(a) Esterification

(b) Transesterification

Figure 4.9: Actual vs Predicted yield for (a) esterification and (b) transesterification step

The perturbation plot which helps to compare the effect of all the parameters within a similar design space. The impact of one parameter is assessed and plotted against the yield while different parameters are kept consistent (Kafuku et al., 2010). Figure 4.10 illustrated each variable and constant parameter with coded value for (a) esterification percentage yield and (b) transesterification percentage yield. Methanol (A) has a relatively greater influence on yields. Both catalyst loading (B) and reaction temperature (C) have an influence on yield to a certain level. Compare to the catalyst loading; the temperature has much more impact on yield. However, for transesterification yield, both catalyst and temperature show the same influences. This is also revealed from the results presented in Table 4.7 and Table 4.8 that methanol has large F-value indicating the sturdiest effect on the yield followed by catalyst loading and reaction temperature.

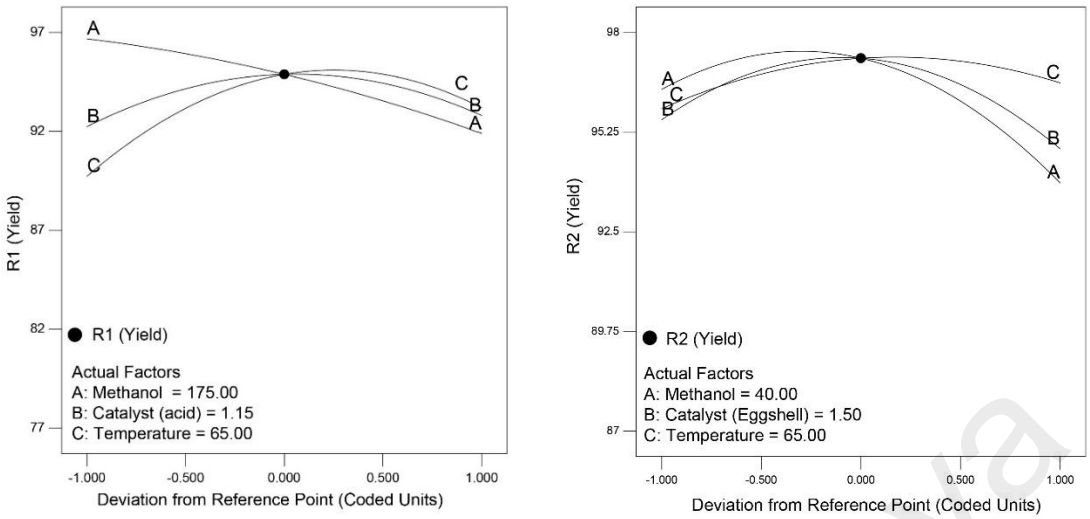

(a) Esterification (b) Transesterification

Figure 4.10: Deviation graph of process parameter for (a) esterification and (b) transesterification stage

4.3.5 3D response surface and yield

Figure 4.11 represented the 3D response surface analysis for the combined effects of factors (a) methanol-catalyst (b) methanol-temperature (c) temperature-catalyst for esterification yield and Figure 4.12 for transesterification. This 3D response surface was plotted for graphical representation of the conversion rate (yield) as well as an affected level by the others variable. It also helps to analyze the interaction within independents process parameters to obtain the combined influence of linking two independent factors efficiently. The highest point of the surfaces presented the optimum responses which is percentage yield in this instance.

It can be observed from the graphical representation that (a) increase of catalyst loading along with methanol reduce yield because higher amount catalyst caused the soap formation during washing. Also, methanol enhances the yield up to a certain level after that it also reduces the yield because the produced ester again dilutes with excess methanol which did not take part in the chemical reaction. From (b), reaction temperature also enhances the yield up to a certain level this can be attributed to the boiling point of the methanol thus in high temperature it escape out from the reaction chamber. In (c) not

much significant interaction found between catalytic loading and the reaction temperature. The P-value also confirms this from both Table 4.7 and Table 4.8.

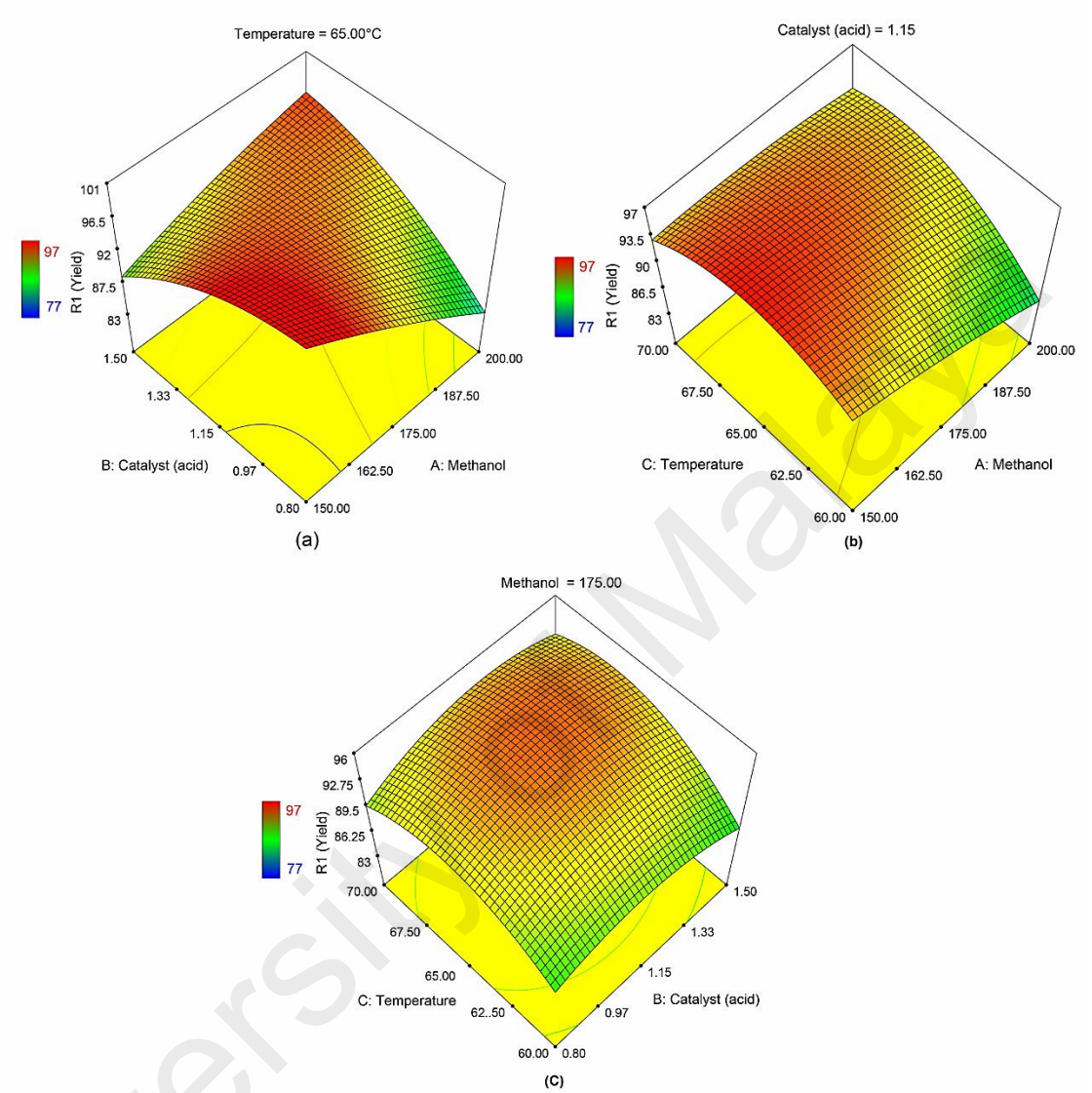

Figure 4.11: Combined effect of factors (a) methanol-catalyst (b) methanol-temperature (c) temperature-catalyst for esterification yield

However, 8 optimum points were suggested for esterification step by the predicted model in the case of maximizing yield, minimizing methanol, catalyst and temperature. Three of them repeated (experiment) to recheck the model desirability and the COV of the predicted result and the experimental result. From Table 4.10, on an average yield was found to be 96.53% at the optimal condition with desirability level of 0.965 and COV < 1% which is acceptable up to 10% (Mason et al., 2003). The desirability and COV of

the predicted and experimental results prove the model accuracy, acceptability and repeatability.

Table 4.10: Optimization and validation of process parameter for esterification stage

Selected solution	Methanol	Catalyst	Temp.	Desirability	Percentage yield (R_1)		
	(v/v %)	(v/v %)	(°C)		Predicted by Model	Experimental	COV (%)
1	151.87	0.80	60.00	0.969	96.9996	96.5	0.37
4	152.79	0.80	60.29	0.965	96.9999	96.0	0.73
8	155.46	0.83	60.00	0.952	95.5913	94.5	0.81

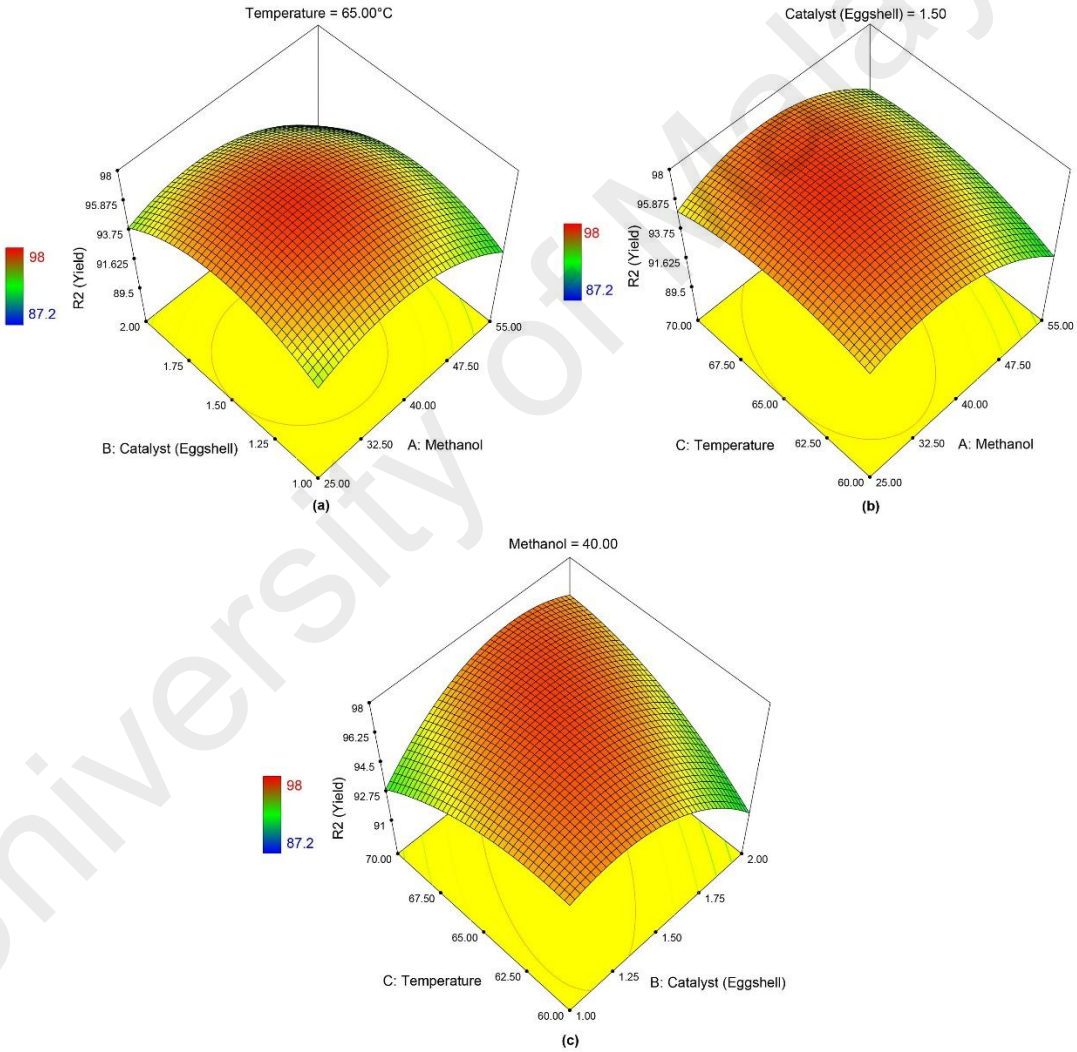

Figure 4.12: Combined effect of factors (a) methanol-catalyst (b) methanol-temperature (c) temperature-catalyst for transesterification yield

On the other hand, only one optimal point was found by maximizing the production yield at transesterification step. Maximum 97.5% biodiesel production yield was obtained at 35.59 % (v/v) methanol, 1.46% (w/w) eggshell catalyst loading and 65.10 °C reaction

temperature for 2 hours reaction time. After repeating the experiment on the optimal operating condition the yield obtained with 0.41% error. The optimal condition for transesterification reaction step is reported in Table 4.12.

Table 4.11: Optimization and validation of process parameter for transesterification

Selected solution	Methanol	Catalyst (Eggshell)	Temp.	Desirability	Percentage yield (R_2)		
	(v/v %)	(w/w %)	(°C)		Predicted by model	Experimental	error (%)
1	35.59	1.46	65.10	0.954	97.5005	97.1	0.41

The overall yield from the CAPO can be calculated by multiplying the yield at degumming stage, esterification step and transesterification step. At degumming stage, degummed CAPO yield was found 97.12%, the yields in optimal points in esterification and transesterification step were found about 96.53% and 97.5% respectively. Thus the overall yield from crude *Aphanamixis polystachya* oil can be reported 91.4%.

4.4 Physicochemical properties analysis

The major physicochemical property of crude A. polystachya and M. pinnata oil were presented in Table 4.12. It was found that the acid value for both feedstocks were higher than 4 mgKOH/g thus both the production was undergoes with two-step production process. *M. pinnata* has relatively higher acid value (39.67 mgKOH/g) than *A. polystachya* (18.79 mgKOH/g) but slightly lower density (918.5 kg/m^3) and higher viscosity (46.683 mm^2/s) at 40°C.

Table 4.12: Physicochemical properties of crude oil

Property	Unit	Test Method (ASTM)	CAPO	CMPO
Density	Kg/m^3	D4052	919.1	918.5
Kinematic viscosity @40°C	mm^2/s	D7042	40.443	46.683
Dynamic viscosity @40°C	mPa.S	D7042	37.160	42.878
Acid value	mg KOH/g	D664	18.79	39.67
Free Fatty Acid	%	-	9.44	19.94
Flash point	°C	D93	212.5	215.0

The quality of a biodiesel depends on its fatty acid structure, production, handling, and storage processes. FAME compositions affect some of the physicochemical properties of biodiesels (Puhan et al., 2010). The compositions may vary depending on the source of a

particular biodiesel. The amount of each fatty acid, the carbon chain length, and the number of double bonds are the determinant factors of biodiesel physicochemical properties.

Table 4.13 represented the fatty acid methyl ester (FAME) composition of the A. polystachya and M. pinna*ta* biodiesel in weight percentage. It was found that methyl palmitate (C16:0), a saturated FAME, was found to be 1.6% higher in APME compared to MPME but 3.6% lower for methyl stearate (C18:0). Methyl oleate (C18:1), monounsaturated FAME, was found 12.1% lower, whereas polyunsaturated methyl linoleate (C18:2) and methyl linoleate (C18:3) found about 5.7% and 9.8% higher respectively, in APME compared to MPME. Among the two biodiesels, APME showed 4% lower saturation level (26.83%), whereas MPME showed the higher (30.43%). Accruing the higher degree of saturation level, MPME possesses a high cetane index (i.e., 57.99) and vice versa to other biodiesel (i.e. 52.59 for APME). The cetane index of each biodiesel was calculated from their corresponding FAME composition and other diesel-biodiesel blends calculated with the help of Four Variable Equation. The percentages of C, H, and O present in the biodiesel were also determined from the FAME structures. However, the CN of the biodiesels increased with the increase of carbon chain length and saturation level, whereas the IV and SN decreased with the increase of saturation level (Bala et al., 2015). A higher degree of saturation in FAME indicates a lower chance of oxidation or a lesser scope of oxygen addition. Thus, the higher the saturated structure is, the higher the oxygen stability and the lower the HHV become. All major physicochemical properties of the two biodiesels and their corresponding 20% and 30% blends with diesel were measured by following the ASTM standard and are listed in Table 4.14.

Table 4.13: Fatty acid methyl ester composition of *A. polystachya* and *M. pinnata* biodiesel

FAME	Structure	Formula	Molecular weight	Composition APME (wt. %)	Composition MPME (wt. %)
Methyl hexanoate	C6:0	$CH_3(CH_2)_4COOCH_3$	130.185	<0.1	<0.1
Methyl octanoate	C8:0	$CH_3(CH_2)_6COOCH_3$	158.238	< 0.1	< 0.1
Methyl decanoate	C10:0	$CH_3(CH_2)_8COOCH_3$	186.291	< 0.1	< 0.1
Methyl laurate	C12:0	$CH_3(CH_2)_{10}COOCH_3$	214.344	< 0.1	< 0.1
Methyl myristate	C14:0	$CH_3(CH_2)_{12}COOCH_3$	242.398	< 0.1	< 0.1
Methyl palmitate	C16:0	$CH_3(CH_2)_{14}COOCH_3$	270.450	14.4	12.8
Methyl palmitoleate	C16:1	$CH_3(CH_2)_5CH=CH(CH_2)_7COOCH_3$	268.435	0.1	0.1
Methyl stearate	C18:0	$CH_3(CH_2)_{16}COOCH_3$	298.504	9.5	13.1
Methyl Oleate	C18:1	$CH_3(CH_2)_7CH=CH(CH_2)_7COOCH_3$	296.488	33.1	45.8
Methyl Linoleate	C18:2	$CH_3(CH_2)_4CH=CHCH_2CH=CH(CH_2)_7COOCH_3$	294.472	24.7	19.0
Methyl Linolenate	C18:3	$CH_3CH_2CH=CHCH_2CH=CHCH_2CH=CH(CH_2)_7COOCH_3$	292.456	11.8	2.0
Methyl arachidate	C20:0	$CH_3(CH_2)_{18}COOCH_3$	326.557	1.0	1.7
Methyl eiosenoate	C20:1	$CH_3(CH_2)_7CH=CH(CH_2)_9COOCH_3$	324.541	0.5	0.5
Methyl Behenate	C22:0	$CH_3(CH_2)_{20}COOH$	354.610	1.4	2.1
Methyl erucate	C22:1	$CH_3(CH_2)_7CH=CH(CH_2)_{11}COOCH_3$	352.594	0.3	0.4
Methyl Lignocerate	C24:0	$CH_3(CH_2)_{22}COOH$	382.663	0.5	0.7
Unknown	-	-	-	2.7	1.8
			Saturation	26.83%	30.43%
			Mono-unsaturated	33.98%	46.78%
			Poly-unsaturated	36.48%	20.99%
			Unsaturated	70.47%	67.77%

Table 4.14: Physicochemical properties of *A. polystachya* and *M. pinnata* biodiesel and their blends

Property	Unit	Test Method	Diesel	*A. polystachya* and *M. pinnata* blend					
		ASTM	OD	AP	AP20	AP30	MP30	MP20	MP
Density @40°C	kg/m^3	D4052	831.0	871.6	840.3	843.6	843.4	840.2	869.6
Kinematic viscosity@40°C	mm^2/s	D7042	3.2947	4.8119	3.5987	3.6914	3.7600	3.6288	5.0410
Dynamic viscosity@40°C	mPa.S	D7042	2.7379	4.1941	3.0240	3.1140	3.1721	3.0488	4.3837
Acid value	mgKOH/g	D664	0.205	1.233	0.335	0.336	0.447	0.391	1.119
Iodine value	g I_2 /100g	EN14111	-	106.7	28.4	36.1	30.6	25.1	80.1
Flash point	°C	D93	74.5	202.5	75.0	78.0	77.0	75.0	204.5
Cold filter plugging point	°C	EN 116	-	7	7	7	7	7	11
Higher heating value	kJ/kg	D240	43936.1	38742.5	43837.7	43310.7	43015.4	43628.5	38158.0
Oxidation stability 110 °C	h	EN14112	39.61	1.95	19.32	10.97	15.44	26.96	5.47
Cetane Index	-	D4737	[a]47.51	[b]52.59	[a]50.48	[a]51.13	[a]51.30	[a]50.60	[b]57.99
Phosphorus content	ppm	D4951	n. d.	< 1	< 1	< 1	< 1	< 1	< 1
Sulfur content	mg/kg	D5453	n. d.	265	214	238	286	278	290
Ash Content	%(m/m)	D482	n. d.	<0.001	< 0.001	< 0.001	< 0.001	< 0.001	<0.001
Carbone Residue	% mass	D4530	n. d.	0.17	0.02	0.05	0.04	0.04	0.32
Carbon	wt%		87	76.00	n. d.	n. d.	n. d.	n. d.	76.10
Hydrogen	wt%		13	12.34	n. d.	n. d.	n. d.	n. d.	11.4
Oxygen	wt%		0	11.65	n. d.	n. d.	n. d.	n. d.	12.5

[a] Calculated Cetane Index by ASTM D4737 method, [b] Calculated from FAME, n. a.= Not Applicable, n. d. Not Determined

4.5 Engine testing and analysis

Engine combustion, performance and emission characteristics were investigated with the 20% (v/v) and 30% (v/v) biodiesel blends and compared the results with ordinary diesel (OD). *Aphanamixis polystachya* (AP) and *Millettia pinnata* (MP) biodiesel blends namely AP20, AP30, MP20 and MP30 were tested at (a) Constant 17 N.m torque, variable engine speed (b) Constant 1800 rpm engine speed and variable torque and (c) Constant 1800 rpm speed, variable injection timing engine operating condition.

4.5.1 Engine performance analysis

Brake specific fuel consumption (BSFC) and brake thermal efficiency (BTE) is the key parameters to evaluate the performance. Because engine fuel consumption per unit power output as well the thermal efficiency were strongly governed by the physical and chemical properties of the fuel used.

4.5.1.1 Brake specific fuel consumption (BSFC)

BSFC is defined as the fuel consumption to produce unit BP for a specific fuel. Fuel properties such as density, viscosity and heating value have significant influences on engine BSFC for a certain condition (Murillo et al., 2007). The consumption rate may vary to the engine operating conditions for a specific fuel. Figure 4.13 illustrated the BSFC in g/kWh with variation of (a) engine speed (b) torque and (c) injection timing for all the tested fuels. The figure shows that BSFC of biodiesel blends is slightly higher than that of ordinary diesel in all the experimental condition as well as the operating points. This may be attributed to higher density, viscosity and lower HHV (higher heating value) of biodiesel blends compared to OD (Arbab et al., 2014). Combined effect of this properties creates high injection in premixed region, poor fuel spray formation, incomplete combustion and high global fuel-air ratio equivalence ratio for lowering the BP of biodiesel blends than petrodiesel (Chen et al., 2014). However, the higher density

and lower HHV can provide more mass flow for same amount power output. It can be seen from the illustration that the BSFC for all fuels increases with (a) increasing of engine speed at constant 17 N.m torque. Decreased volumetric efficiency and increased frictional loss at higher speed might be the reason for this increase. It also found that the BSFC increases with increasing blend ratio of biodiesel (Fattah et al., 2014). Higher density and viscosity of biodiesel blends leads to the higher mass flow rate in fuel injection system as fuel is injected volumetrically affecting the fuel atomization in a bad way (Payri et al., 2015). Also, highest BSFC was attained due to the consolidated impact of poor fuel atomization time and elevated piston-cylinder frictional force at this speed (Imtenan et al., 2015). In higher speed and torque engine towards the lean combustion thus the amount of injected fuel subjected to atomize greater quantity compared to the lower speed and Torque. Thus atomization ratio increasesThe minimum BSFC for OD, AP20, AP30, MP20 and MP30 were recorded 295.25, 297.37, 301.70, 296.15 and 300.05 g/kWh at 1200 rpm and maximum were 316.64, 315.46, 321.18, 317.52 and 320.58 g/kWh at 1800 rpm respectively for constant 17 N.m torque condition. Which was 0.58%, 1.76%, 0.14% and 1.40 % higher for AP20, AP30, MP20 and MP30 respectively, compared to OD.

For (b) constant 1800 rpm engine speed and increased torque, the fuel consumption of all the fuels comparatively decreases due to increase in atomization ratio subsequently, the air-fuel equivalence ratio, which influences air and fuel mixing (Habibullah et al., 2015; Ozsezen et al., 2008). In higher speed and torque engine towards the lean combustion thus the amount of injected fuel subjected to atomize greater in quantity compared to the lower speed and torque results increased atomization ratio. Which also results decrease in BSFC with the increasing of the engine torque. The minimum BSFC for OD, AP20, AP30, MP20 and MP30 were recorded 285.96, 291.16, 297.83, 286.15 and 288.29 g/kWh when torque was 25 N.m and maximum were found 377.10, 382.17,

389.69, 382.22 and 387.40 g/kWh respectively, when torque was 10 N.m for constant 1800 rpm engine speed. Which was 1.06%, 3.13%, 0.70% and 1.78 % higher for AP20, AP30, MP20 and MP30 respectively, compared to OD.

BSFC slightly increased for (c) the constant 1800 rpm speed with advancing the injection timing (e.g. 20° bTDC). The engine needs to raise the injection pressure earlier thus sprays more volumetric mass flow during injection. Thus the fuel consumption increased with the advancement of the injection timing at constant 1800 rpm engine speed. The minimum BSFC for OD, AP20, AP30, MP20 and MP30 were recorded 308.58, 312.59, 313.34, 313.45 and 313.76 g/kWh at 10° bTDC whereas maximum was found 317.42, 322.53, 323.31, 324.48 and 321.61 g/kWh respectively, at 20° bTDC when operating condition was constant 1800 rpm engine speed. The AP20 showed 1.61% higher consumption at 5 °CA advanced injection and 1.30% higher consumption for 5 °CA retarded injection whereas at 15° bTDC it provided only 0.52% higher consumption compared to OD. This outcome may be attributed to the combined effect of the density and viscosity that diminish the inner spillage in the pump (Buyukkaya et al., 2013) and flash point that affects atomization or sprays formation of fuel during combustion. Another reason could be the combined effect of additional oxygen content in biodiesels (Can, 2014) and improvements of CN of combined blends.

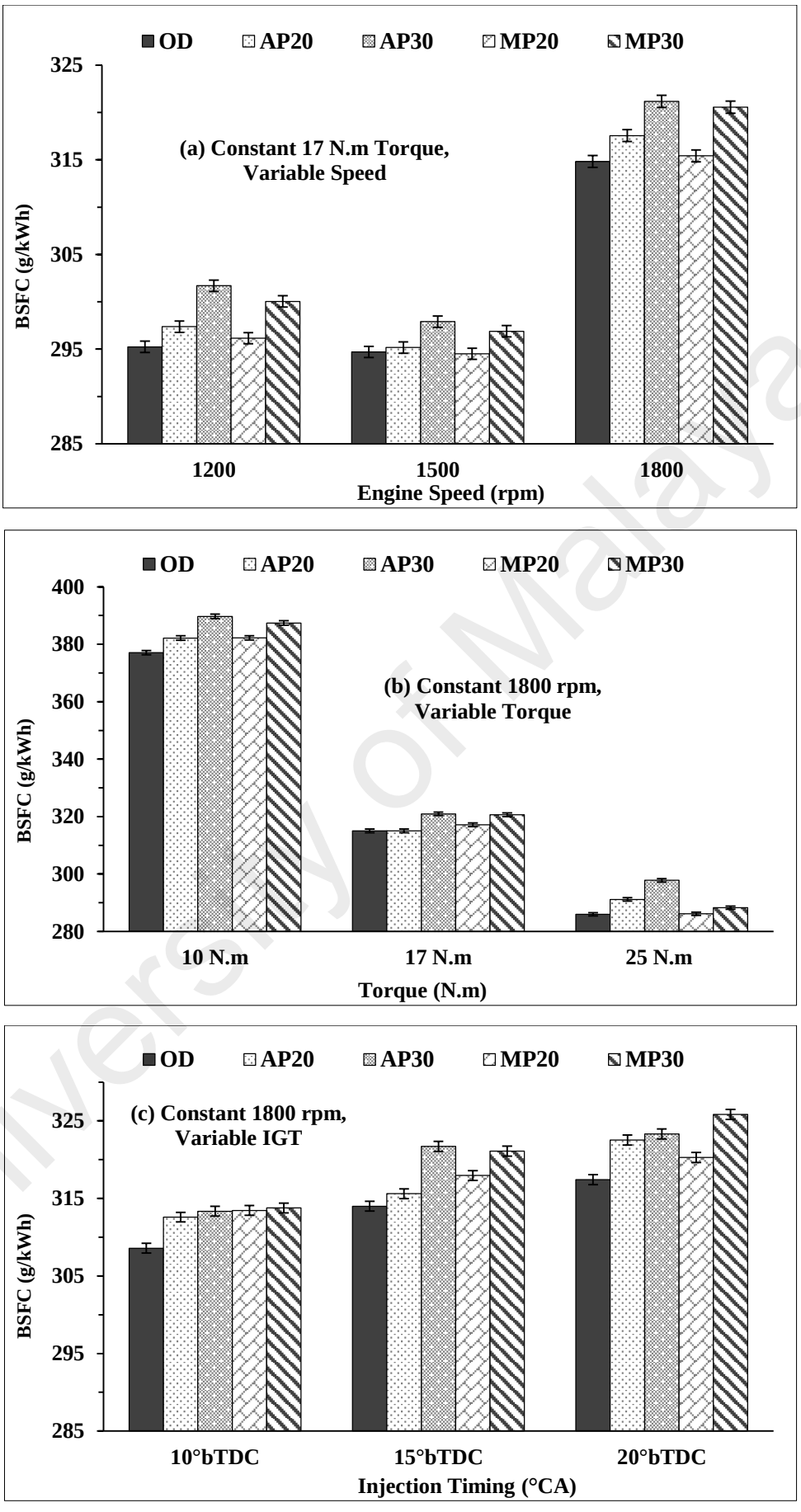

Figure 4.13: BSFC at different operating conditions

4.5.1.2 Brake thermal efficiency (BTE)

Brake thermal efficiency (BTE) is defined as for break power of heat engine as a function of the heat input by the fuel. Figure 4.14 represented the BTE with variation of (a) engine speed (b) torque and (c) injection timing for all the tested fuels. It can be seen from the demonstration that BTE slightly varies for biodiesel blends compared to OD, depending on the fuel consumption and the HHV of that particular fuel. The lower the BSFC and HHV the higher the BTE according to the Equation 3.13. BTE level of biodiesel based fuels is same or higher for few fuels because of their better energy conversion rates (Kinoshita et al., 2007). The fuel consumption is directly related to the density, viscosity fuel atomization and volatility of fuel in a particular engine operating condition. For (a) constant 17 N.m torque BTE eventually decreased along with increased engine speed for each of the investigated fuels. This results attributed to the higher fuel consumption for the increased engine speed. The maximum BTE for OD, AP20, AP30, MP20 and MP30 were recorded 27.75, 27.62, 27.55, 27.86 and 27.89 % at 1200 rpm, whereas minimum was found 25.88, 26.03, 25.88, 25.99 and 26.11 % respectively, at 1800 rpm engine speed when torque was constant at 17 N.m. On an average, AP was provided 0.33% lower BTE compared to OD. On the other hand, MP20 and MP30 showed superior BTE at all the engine speed and showed 0.65% higher compared to OD. This changes due to the significant fuel variation. BTE changed with the variety in BSFC and HHV of the biodiesel. Individual MP20 possesses higher density and CN but lower HHV and viscosity compared to AP20. Thus it showed slightly higher BTE than AP20. The addition of higher percentage of biodiesel in diesel increases BTE and thus 30% blends of AP and MP provided slightly improved BTE among all other tested fuel.

For (b) constant 1800 rpm engine speed, BTE gradually increased with the increasing of torque. According to the equation *3.10* BP will increase with the increasing of the torque for a constant speed. Also, increased BP provides a lower BSFC in terms of g/kWh.

Thus it can be considered as the opposite relation to BTE and BSFC. This results can be explained by the proper combustion and fuel atomization at the higher torque condition. At lower torque, the power output is low thus BSFC is high which results in lower BET whereas at higher torque it behaves vice-versa. The maximum BTE for OD, AP20, AP30, MP20 and MP30 were recorded 28.65, 28.20, 27.91, 28.84 and 29.03 % at 25 N.m torque whereas minimum were found 21.73, 21.49, 21.33, 21.59 and 21.60 % respectively, at 10 N.m torque when engine speed was maintained at 1800 rpm.

BTE for (c) constant 1800 rpm with variable injection timing not much fluctuated. The BTE lay between 25%-27% for all tested fuel. This phenomenon can explain to the combustion phasing additional impacts the energy conversion of heat energy to work. A quick injection of biodiesel together with high CN results in the early start of combustion (SOC) (Imtenan et al., 2015). Early SOC, raises pumping function and endorses heat decrease in the cycle (Can, 2014; Payri et al., 2015). This trend, collectively along with low heating value and higher density, viscosity, negatively impacts engine performance (Devan & Mahalakshmi, 2009; Park et al., 2012).

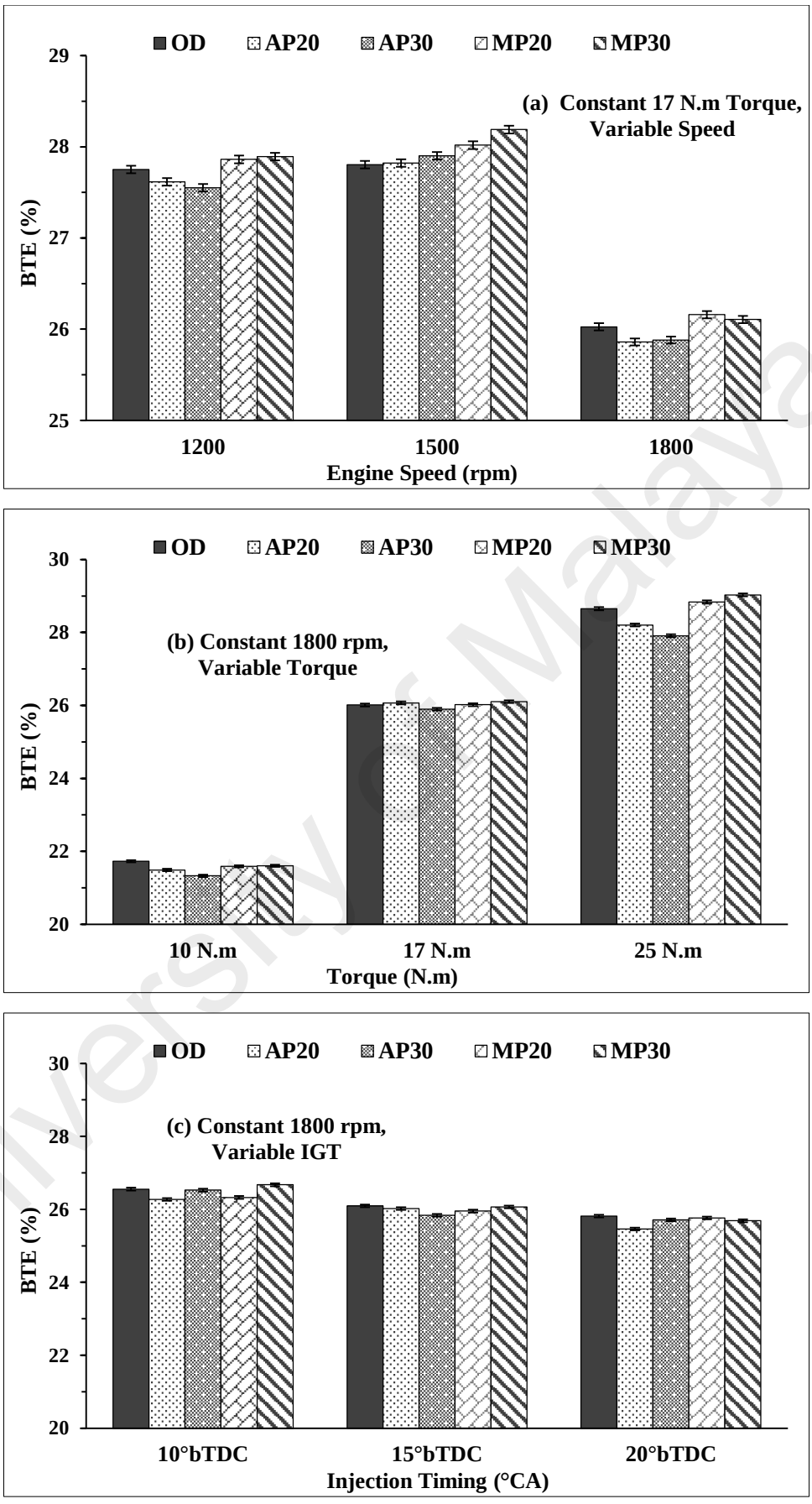

Figure 4.14: BTE at different operating conditions

4.5.1.3 Exhaust gas temperature (EGT)

Figure 4.15 illustrated the exhaust gas temperature (EGT) for tested fuel at (a) variable engine speed (b) variable torque and (c) variable injection timing. It can be seen from the illustration that the variation in exhaust temperature with the variation in both engine speed and torque for biodiesel blends were increased. Such phenomena are the result of variations in the relative importance of heat transfer in the cylinder and heat transfer to the exhaust valve and port. The amount of fuel combusted in the combustion chamber within a unit time increases; consequently, the heat energy produced increases as the engine speed as well as torque increases (Ong et al., 2014). It was observed that biodiesel blends provide relatively higher EGT compare to the OD. This can be attributed to the 11.46% higher oxygen content than OD, the higher in-cylinder pressure but lower HRR of fuel which influences to increase the premixed of biodiesel (Teoh et al., 2013) and bulk-gas-averaged temperature (Benjumea et al., 2010). It is seen that, on an average 23-29% higher EGT was risen for variable torque condition compared to speed condition. However, all biodiesels exhibit higher exhaust temperatures than diesel, for example, 2.53% at constant torque and 1.05% at a constant speed on average. Such differences are due to physical delay because proper atomization is retarded by high density and viscosity (Usta, 2005). This characteristic of biodiesel leads to initial slower burning and finally burning with sufficient oxygen. It is found that, on an average AP20 and MP20 provided 3.20% and 2.85% higher EGT among all operating conditions, compare to the OD depending on their fuel consumption (due to high density) and lower energy conversion rate (lower HRR) and shorter combustion duration.

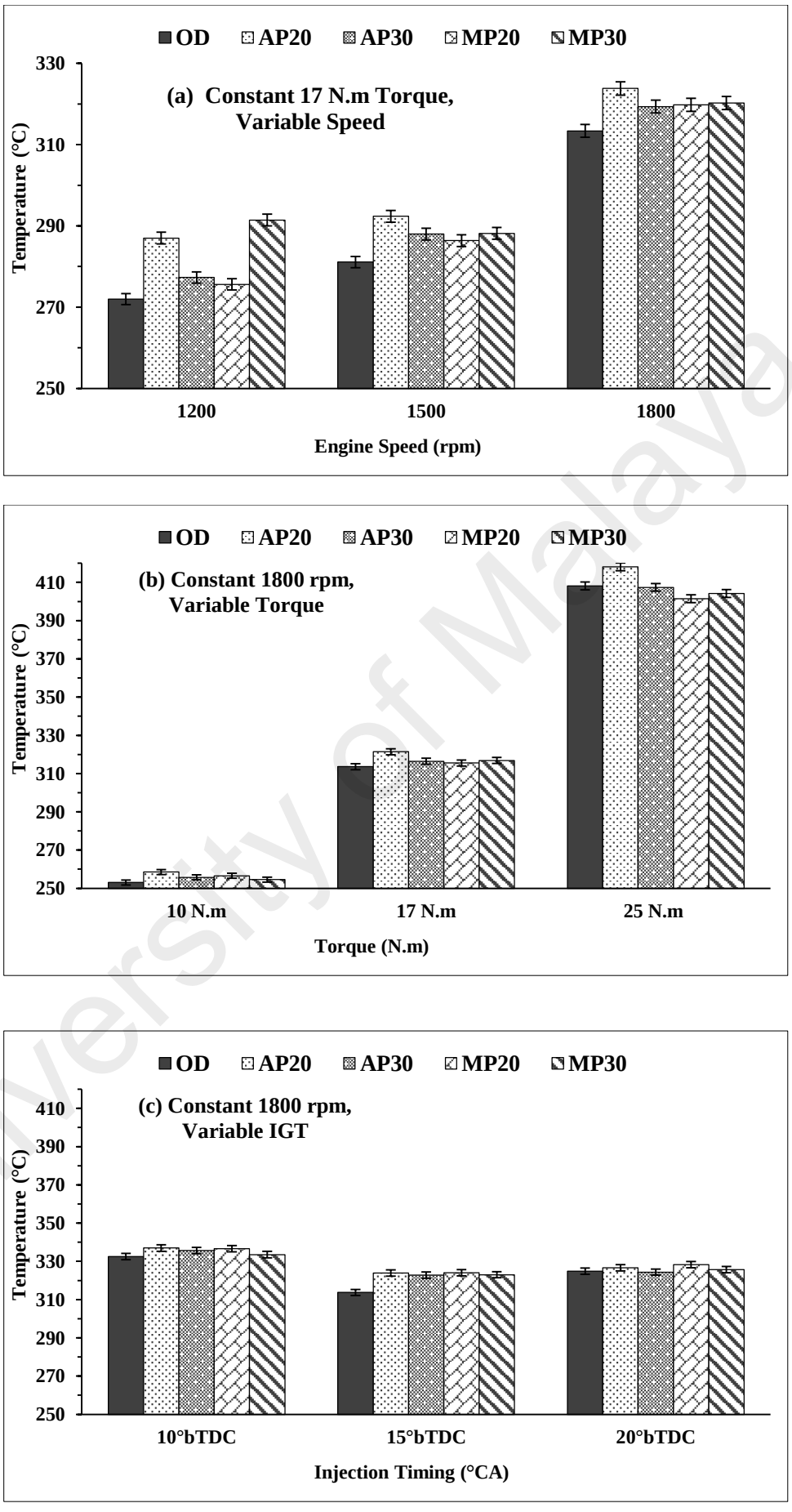

Figure 4.15: Exhaust gas temperature at different operating conditions

4.5.2 Engine combustion analysis

Combustion parameter like in-cylinder pressure (ICP), heat release rate (HRR), mass fraction burned (MFB) and start of combustion (SOC), ignition delay (ID) and combustion duration have been taken into account for evaluating the combustion quality of all tested fuel. In this study full load variable load (1200 rpm, 1500 rpm and 1800 rpm) engine speed and constant 1800 rpm engine speed with variable load (100%, 75% and 50%) condition have been carried out. 1800 rpm engine speed with 100% loading condition was presented here for combustion evaluation as this point is common for both the load test and speed test condition. The constant 700 bar fuel injection pressure were maintained for all three and the start of injection at 15° bTDC (before top dead center) for both (a) and (b) operating conditions.

4.5.2.1 In-cylinder pressure (ICP) and heat release rate (HRR)

In-cylinder pressure (ICP) of the combustion cycle was directly obtained from the pressure signal. In-cylinder pressure characteristics of fuels can be explained in a better way conjoining the HRR analysis. Figure 4.16 illustrated the ICP pressure and corresponding HHR of a combustion cycle with respect to crank angle for (a) constant 17 N.m torque with variable 1200, 1500 and 1800 rpm speed (b) constant 1800 rpm speed with variable 10, 17 and 25 N.m torque, and (c) constant 1800 rpm speed with 10°, 15° and 20° bTDC injection timing variation for all the tested fuel including OD.

From (a) it can be seen that the peak pressure rises in the cylinder after top dead center (aTDC) within a range of 2.125-5.25 °CA and HHR bTDC within a range of 6.75-3.875 °CA for variable speed at 17 N.m constant torque. Peak ICP for OD, AP20, AP30, MP20 and MP30 were found 73.88, 73.96, 73.77, 73.78, and 74.09 bar respectively and corresponding peak HRR found 40.10, 40.86, 40.73, 40.16 and 39.58 J/°CA at 1800 rpm. The ICP peak pressure decreases a bit with increasing engine speed from 1200 to 1800 and the peak shifts from TDC. It can be explained by the higher BSFC at lower speed to

produce the constant 17 N.m torque. This provides relatively poor fuel burning and unburned fuel into combustion chamber during combustion which might cause higher ICP in lower speed. This ICP pressure is not converted into energy thus relatively lower BP, higher NO, HC and CO emission were found. HRR is directly obtained from ICP according to equation and also depends on the fuel properties i.e. how easily fuel can burn or transfer the chemical energy into heat energy. Desire HHR pick should be just before the TDC which can be achieved by proper ignition as well as combustion phenomenon. As higher speed provides the superior burning quantity thus HRR at higher speed occurs later (i.e. much closer to TDC). Also, earlier HRR can be explained by the piston reaching before to the TDC. Lower EGT also responsible for this poor combustion and early HHR at constant torque with lower engine speed.

From (b) it can be seen that the peak pressure rises in the cylinder after top dead center (aTDC) within a range of 3.50-7.625 °CA and HHR bTDC within a range of 4.5-3.875 °CA for variation of torque in constant 1800 rpm engine speed. Peak ICP for OD, AP20, AP30, MP20 and MP30 were found 76.73, 76.67, 76.51, 76.67 and 76.93 bars respectively and corresponding peak HRR found 40.01, 40.51, 39.20, 38.68 and 38.24 J/°CA at 25 N.m. The ICP peak pressure increases and shifts from TDC with the increasing torque from 10 N.m to 25 N.m. This result can be ascribed as the better combustion phenomenon as lower BSFC; higher BTE obtained at 25 N.m. Lower HC, CO NO and higher CO_2 emission also can explain this better combustion. HRR found to very close and as EGT found thus NO also found less.

From (c) it can be seen that the peak pressure rises in the cylinder after top dead center (aTDC) within a range of 2.375-9.375 °CA and HHR bTDC within a range of 8-0 °CA for variation of injection timing in constant 1800 rpm engine speed. Peak ICP for OD, AP20, AP30, MP20 and MP30 were found 80.09, 81.34, 81.26, 81.48 and 81.64 bars respectively and corresponding peak HRR found 53.75, 54.63, 55.21, 53.61 and 53.02 at

20 °CA. The ICP was increased with advancement of Injection timing and decreases with retardation.

Significant different was not found cylinder pick pressure within biodiesel blends and diesel for a certain operating point. This is a clear indication of chemical energy conversion of fuel into mechanical energy as efficient for 20% biodiesel blends as for the diesel (Imtenan et al., 2015). It also observed that in-cylinder peak pressure slightly decreased with the increasing of engine speed at (a) constant 17 N.m condition and (b) increased with the increasing of engine load at constant 18000 rpm. The peak pressure slightly shifted to the right with increasing the torque at (b) constant speed and shifted to left with decreasing the speed at (a) constant torque. At (c) constant speed with advancing injection time, the peak pressure slightly increased and shifted to left. Advancement of the injection timing builds up a rapid combustion pressure in the compression stock thus beginning to oppose the upward movement of the piston and causing deterioration of the BSFC (Teoh et al., 2013). Due to the lower neat heating value of biodiesel blends, more fuel is required for the same power output for a certain condition causes longer fuel injection process as well BSFC. The higher initial HHR, rapidly emitted after ignition is probably because of the greater amount of combustible fuel-air mixture which formed in the longer ignition delay thus peak of HHR directly proportional to ignition delay. Note that the end of combustion almost same for the tested fuels (Kinoshita et al., 2007).

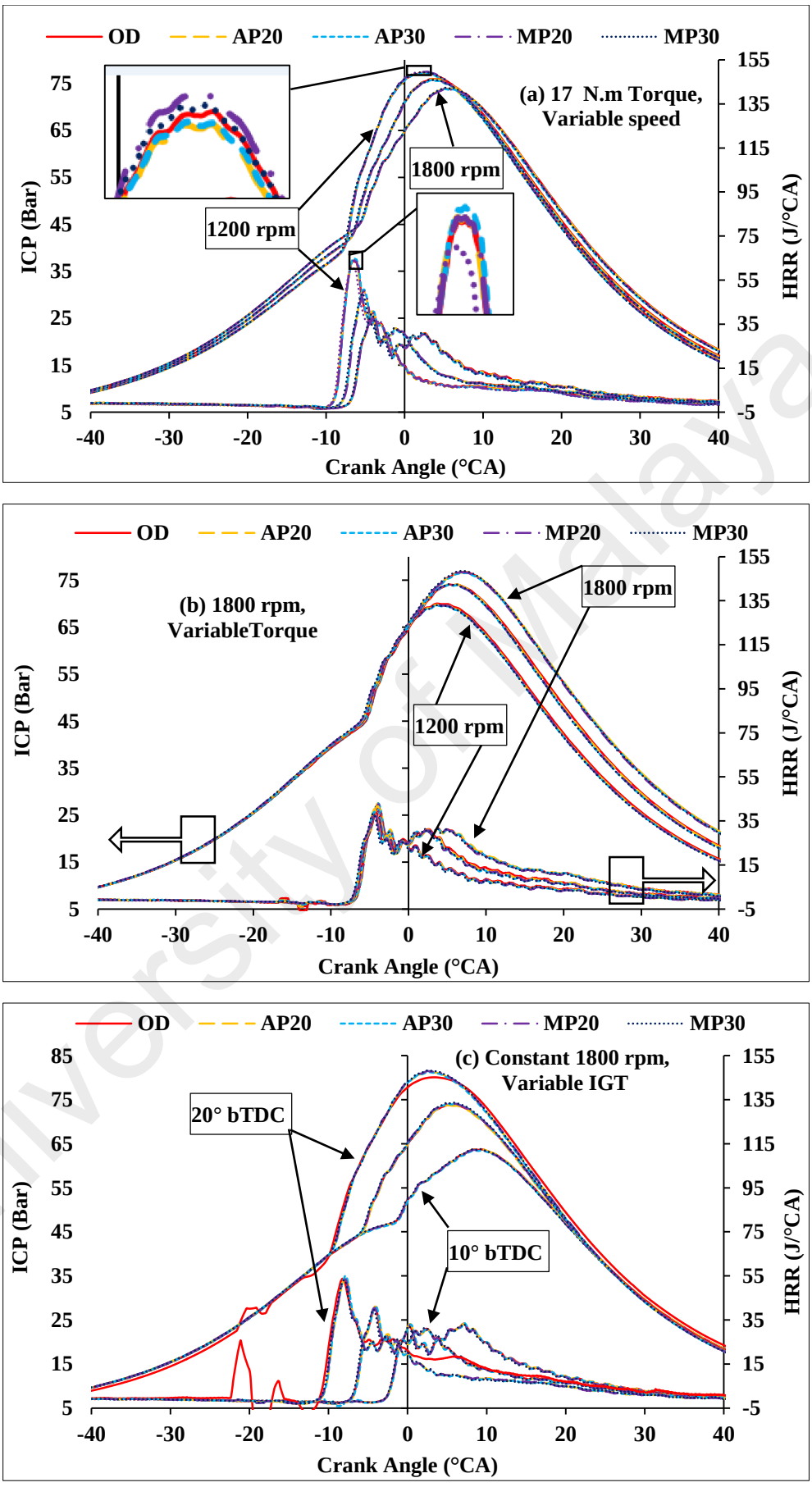

Figure 4.16: In-cylinder pressure (ICP) and heat release rate (HRR) with °CA

The average of 100 successive combustion cycles peak ICP and peak HHR for each tested fuel with each operating point are presented in Figure 4.17.

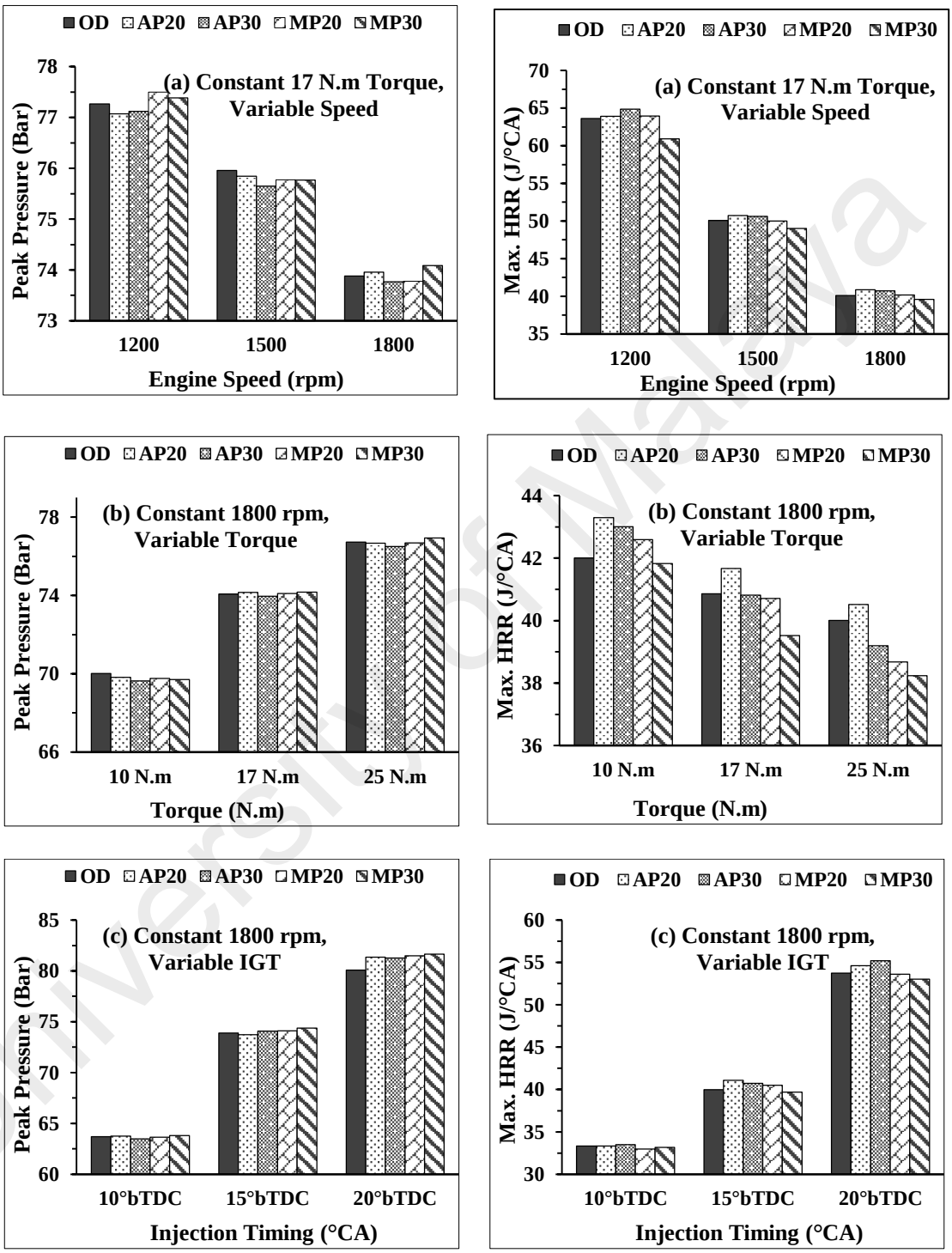

Figure 4.17: Peak ICP and peak HRR

4.5.2.2 Ignition delay

The time between the start of injection (SOI) and the start of detectable heat release is known as ignition delay. SOI was set at 15 °bTDC for (a) constant torque (b) constant speed condition and fuel injection pressure were kept constant at 700 bar for all operating point. The start of combustion (SOC) and ignition delay can be an important phenomenon to evaluate the combustion characteristics with a specific fuel. Ignition delay was obtained from the difference between the SOC and SOI. Injector lag which refers to milliseconds level delay happened due to the mechanical function (the difference between theoretical and actual injection timing) of injector valve opening was not taken into account for this study. SOC timing can be simply identified by the difference in combustion rates from the HRR versus crank angle diagram. Theoretically, during the compression stroke as the piston comes near to the TDC, fuel vaporization caused a negative heat release and with the start of combustion, heat release momentarily becomes positive at a point (Allen et al., 2011). This point described by SOC. Ignition delay was varied with the range of 4 °CA to 12.25 °CA depending on the operating condition as well as the tested fuel properties. All the Ignition delay for each tested fuel with their operating points are listed in Table 4.15.

Table 4.15: Ignition delay of all tested fuel

(a) Constant 17 N.m Torque, Variable Speed					
rpm	**OD**	**AP20**	**AP30**	**MP20**	**MP30**
1200	5.875	5.875	5.875	5.875	5.75
1500	7	7	7	7	6.875
1800	8	8	8	8	8
(b) Constant 1800 rpm & Variable Torque					
N.m	**OD**	**AP20**	**AP30**	**MP20**	**MP30**
10 N.m	8.125	8.25	8.25	8.325	8
17 N.m	8	8.125	8	8	7.875
25 N.m	7.75	7.75	7.75	7.75	7.625
(c) Constant 1800 rpm Variable Injection Timing					
bTDC	**OD**	**AP20**	**AP30**	**MP20**	**MP30**
10°	12.25	12.38	12.63	12.25	12.25
15°	8	8	8.625	7.875	7.875
20°	4.5	4.125	4.125	4	4

The ignition delay was ignition delay mostly depends on fuel spray development affecting factors (injection timing, quantity, velocity rate drop size and spray formed type) and the air charge state (e.g. pressure temperature and velocity) for a specific operating condition (Heywood, 1988). Ignitability order can be matched with the order of cetane number. Although the ignitability not only depends on the FAME (cetane number) but also the residual impurities like glycerine, methanol and water content which may affect combustion negatively (Kinoshita et al., 2007). Also, effects on ignition delay can be minimized by only increasing the fuel injection pressure for the same engine (Lyn & Valdmanis, 1968; Shahabuddin et al., 2013). However, AP20 showed slightly inferior ignition delay compared to MP20 having inferior cetane number and combined effect of viscosity and calorific value but very close to OD.

4.5.2.3 Mass fraction burned (MFB) and combustion duration

Mass fraction burned (MFB) or fraction of fuel energy release profile is a function of crank angle in each combustion cycle. It contains flame development angle which is considered as 10% and rapid burning angle which is considered as 90% of the total energy release of fuel. This rapid burning duration or maximum fuel burning rate which lie down in between 10% MFB to 90% MFB is termed as combustion duration. In this study, SOCs were acquired from the HHR versus crank angle diagram. It was found that the combustion duration for diesel was slightly longer compared to biodiesel blends due to the higher HHV of OD. Longer combustion duration helps to lessen the combustion efficiency. Figure 4.18 illustrated the MFB with crank angle at constant 1800 rpm, 17 N.m torque and 15 °bTDC injection °CA. Biodiesel blends possess higher cetane number hence the SOC is earlier as ignition delay is less compared to diesel. From the illustration, it is clear that biodiesel blends started to burn earlier and takes less time to deliver heat (i.e. shorter combustion duration). This results can be attributed to the higher cetane number and oxygen content of biodiesel compare to the diesel. However, combustion

duration for OD was found about 23.5 °CA which ranging 5.5-19° aTDC and for other tested blends the range varies between 4.9-26° aTDC (about 21.1 °CA). Among the biodiesel blends, AP20 and AP30 provide very close combustion duration to OD.

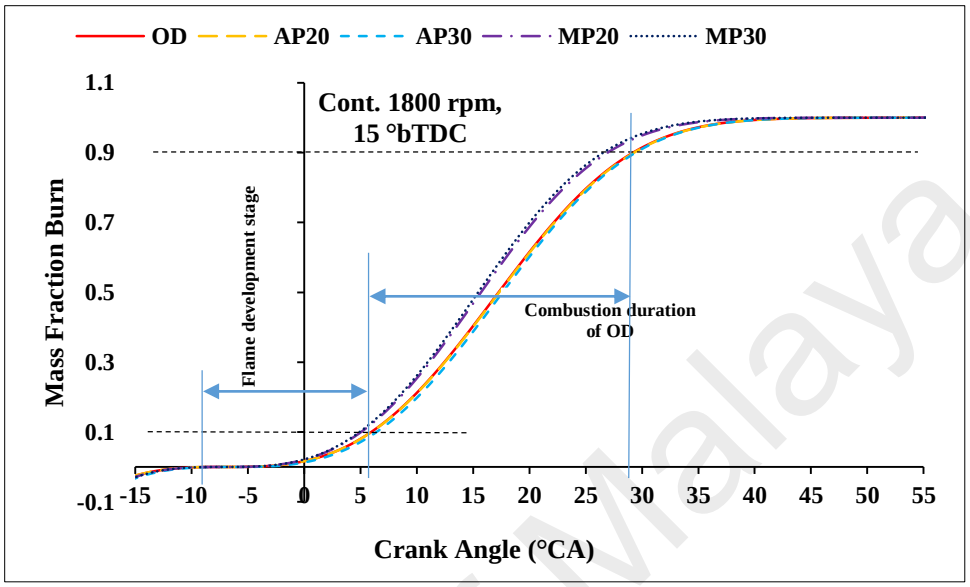

Figure 4.18: Mass fraction burned at constant 1800 rpm speed

4.5.3 Engine emission analysis

Major emission parameter such as nitric oxide (NO), carbon dioxide (CO_2), carbon monoxide (CO), and unburned hydrocarbon (HC) was investigated in this study. The emissions are presented in terms of globally acceptable unit i.e. per unit power output.

4.5.3.1 Nitric oxide emission (NO)

Atmospheric tripled bonded nitrogen behaves as an inert gas, but in high combustion temperature it splits up and undergoes a series of reaction with oxygen and creates NO_2. NO_X emission mainly includes nitric oxide (NO) and nitrogen dioxide (NO_2) emission to the environment. During combustion, atmospheric nitrogen (about 78.09% by volume) come into the reaction and become the main source for NO_X emission for the internal combustion engine; this is treated as the thermal NO_X. This NO_X formation mechanism is known as Zeldovich mechanism. NO_X forms in prompt (Fenimore) mechanism because of the generation of hydrocarbon radicals via molecular unsaturation (Benjumea et al.,

2010; Sharon et al., 2012). It can be said that NO is the prevalent oxide delivered inside the engine cylinder. However, these hazardous emissions should be stringently controlled because it can affect human health such as damage to lung tissue and reduction in lung function (Omidvarborna et al., 2015).

Figure 4.19 demonstrated the NO emission for a different operating condition such as (a) constant speed, variable speed (b) constant speed, variable load and (c) constant speed, variable injection timing condition. NO formation through the biodiesel blend is quite high due to 12-13 % higher oxygen content in biodiesel, which provides a high in-cylinder temperature for both premixed and diffusion combustion condition rather than OD (Kannan et al., 2012). Together with higher CN, air surplus coefficient, residence time and higher bulk modulus of elasticity can be ascribed as the reason for higher NO formation (Imtenan et al., 2014). The bulk modulus of elasticity causes the early nozzle opening and advancement of the ignition, which increases global fuel-air equivalence (Boehman et al., 2004). Higher CN provides shorter ignition delay and higher oxygen content in biodiesel results higher combustion temperature. Because of the higher in-cylinder temperature during combustion MP30 gives slightly higher and AP20 provides relatively lower NO emission owing lower CN among the tested biodiesel blends. Because of the higher in-cylinder temperature during combustion MP30 gives slightly higher and AP20 provides relatively lower NO emission among the tested biodiesel blends. This can be attributed to the combined effect of higher CN and the higher percentage of the saturated methyl ester composition present in the MP Biodiesel (about 4%).

It can be seen that brake specific NO was gradually decreasing with increasing engine speed at (a) constant load and (b) increasing torque at a constant speed hence combustion temperature increase. For (a) advancement of injection timing i.e. at 20° bTDC, the NO emission also found higher. This behavior can be attributed to the higher NO_2 formation

tendency hence amount of NO decreased at a higher temperature according to Zeldovich mechanism. The lowest NO emission was observed at were observed amount all the tested fuel at constant 1800 rpm and 25 N.m torque. On an average 7.14% higher NO emission was found for biodiesel blends compared to OD whereas individually AP provides 4.83%.

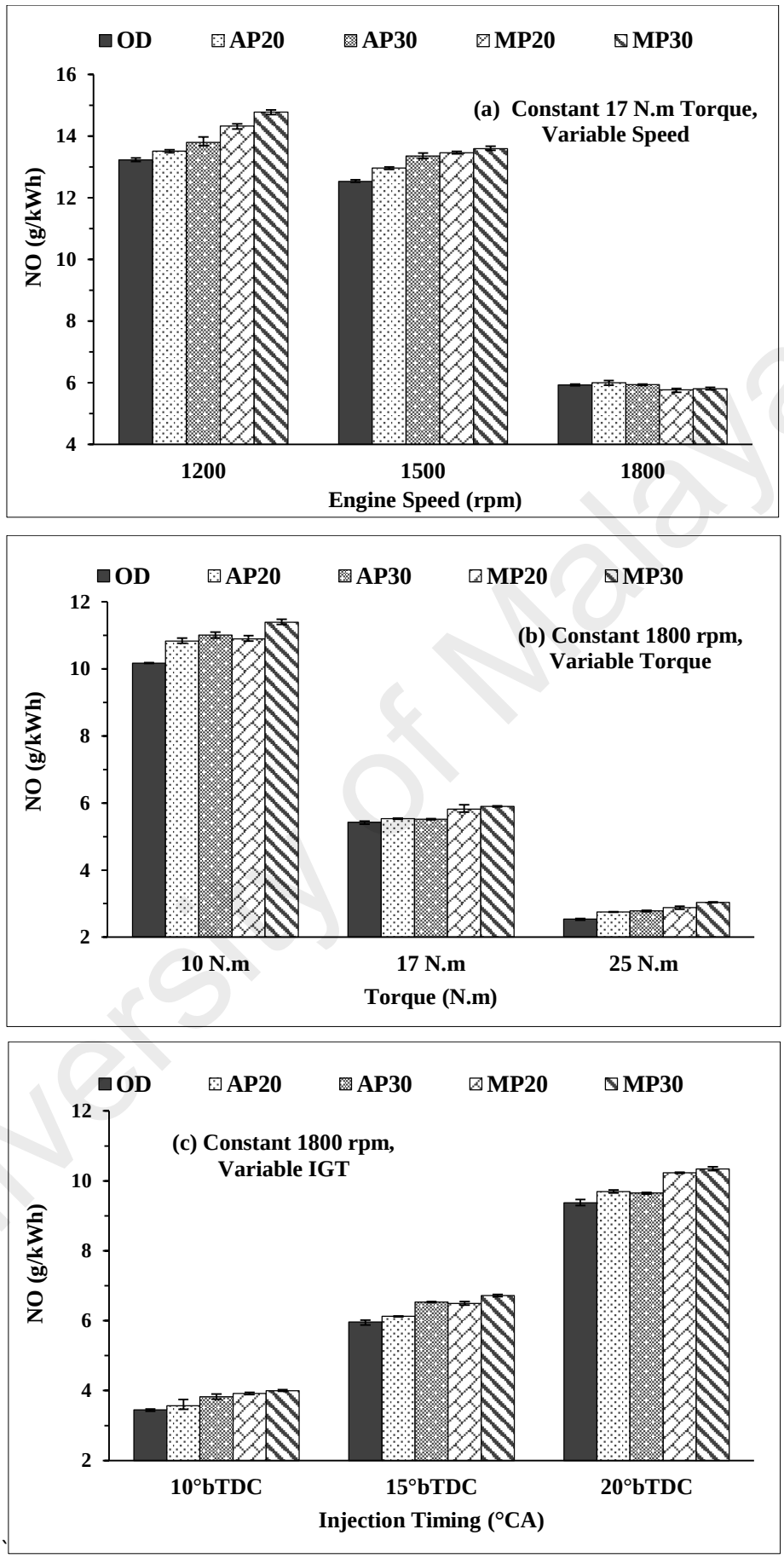

Figure 4.19: NO emission at different operating condition

4.5.3.2 Carbon monoxides emission (CO)

The existence of a higher CO content in exhaust emissions cause of partial combustion which caused by insufficient oxygen supply during combustion (Abedin et al., 2016). All this happens because of air-fuel equivalence ratio, fuel pressure, fuel type and injection timing. Among them, ignition mixture because of lower air-fuel equivalence ratio can be considered as the main cause of CO emissions. Figure 4.20 illustrated CO variation for (a) variable engine speeds at constant torque (b) variable torque at constant engine speed and (c) variable injection timing at constant engine speed. Reduction of CO observed for all biodiesel-diesel blends in all the operating points. This can be ascribed as higher in borne oxygen content and higher CN of biodiesel, which shorting the ignition delay, thus provides better combustion and prevents less over-lean zones (Kinoshita et al., 2007; Sanjid et al., 2014).

It can be seen that CO emission decreases with (a) increasing the engine speed and (b) increasing the engine load but (c) increases with advancing the injection timing. This can be attributed to the higher air-fuel equivalence ratio, higher cylinder temperature and pressure was introduced during combustion, which ensures relatively better combustion and thus reduced the CO emission (Can, 2014; Sayin, 2010). The variation in CO between diesel-biodiesel blends found inversely proportional to the higher volatility (lower flash point) and oxygen content. Minimum CO emission for diesel, AP20, AP30, MP20 and MP30 were recorded at 25 N.m. torque at constant 1800 rpm engine speed. On average biodiesel blends provides 10.70-12.43% reduction in CO emission compared to OD whereas individually AP biodiesel blends provide 13.90-14.80% reduction.

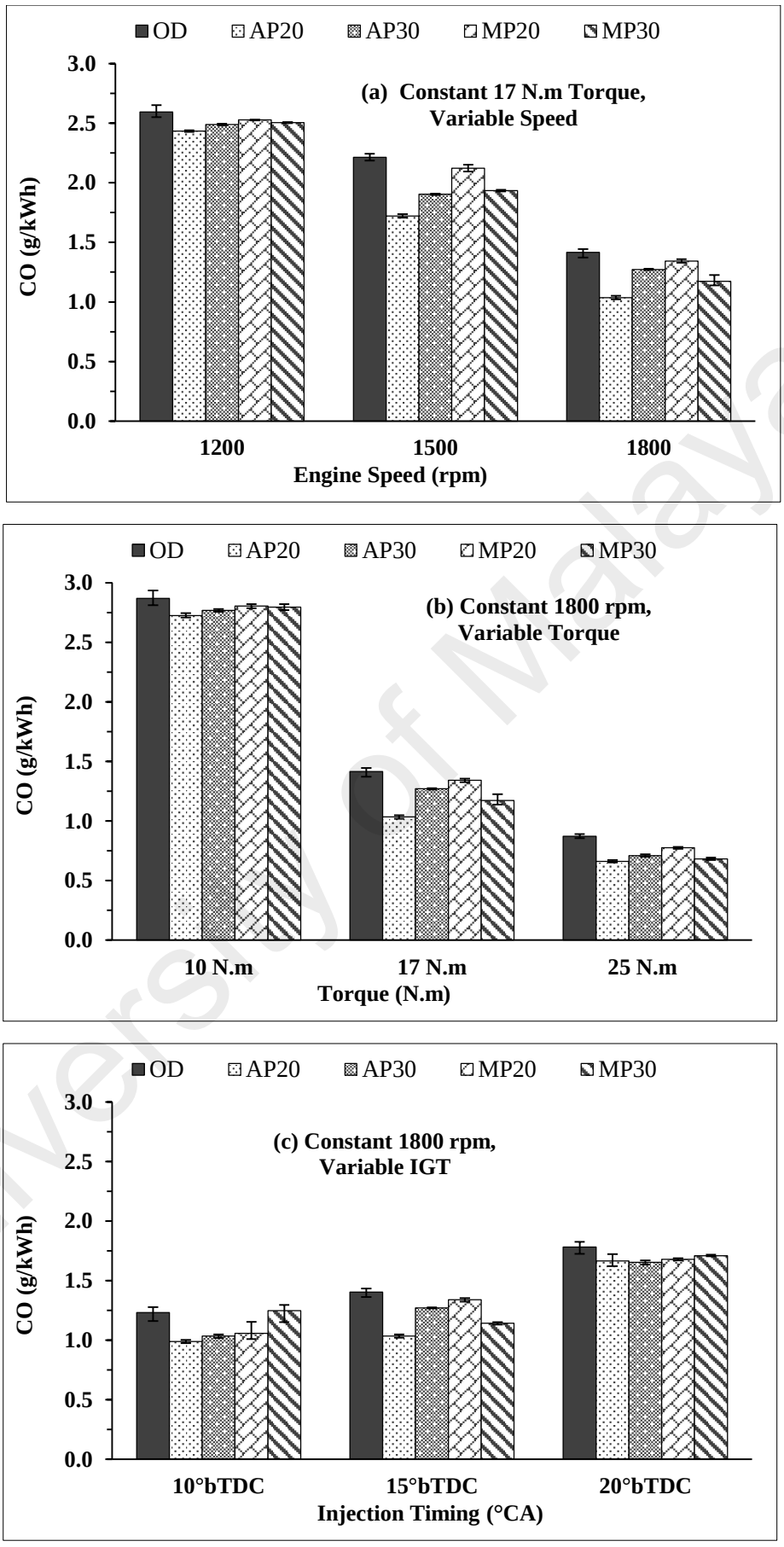

Figure 4.20: CO emission at different operating condition

4.5.3.3 Carbon dioxide (CO_2)

Fuel combustion inside the combustion chamber results in CO_2 emission in the exhaust. The higher the complete combustion of fuel is, the higher the CO_2 emission gets. The variation of CO_2 happens because of engine speed, air-fuel ratio, fuel pressure, fuel type and injection timing. Figure 4.21 illustrated that CO_2 emission variation for (a) variable engine speeds at constant torque (b) variable torque at constant engine speed and (c) variable injection timing at constant engine speed. It can be found that CO_2 increases with the increase of biodiesel percentage in the blend. This increase can be attributed to the higher oxygen content in the biodiesel, which helps achieve a complete combustion (Gumus et al., 2012). Diesel-biodiesel blends showed relatively higher CO_2 emissions compared to OD in all the operating point due to slightly higher BSFC, improved combustion as it contained in borne oxygen content which helps to burnt fuel properly.

CO_2 emission increased with the increasing of (a) engine speed at constant torque (b) engine torque at a constant speed and (c) at the advancement of injection timing. It can be seen from the illustration that CO_2 emission increases gradually at higher load and speed hence comparatively complete combustion occurs compared with lower engine speed and load. With increasing of engine speed, and torque, higher air-fuel ratio, higher cylinder temperature and the pressure was introduced during combustion, which ensures relatively better combustion and thus increased the CO_2 emission (Can, 2014; Sayin, 2010). In reiterating the injection timing, lower CO_2 emission attributed to the ICP, poor atomization due to density, viscosity and flash point, shorter combustion duration and prevents less over-lean zones (Sanjid et al., 2014).

Maximum CO_2 emission for diesel, AP20, AP30, MP20 and MP30 were recorded at 25 N.m. torque at constant 1800 rpm engine speed. On average biodiesel blends provides 7.24-10.64% increase in CO_2 emission compared to OD whereas individually AP biodiesel blends provide 13% increased CO_2 emission. CO_2 emission from the

combustion of fossil fuels causes various environmental problems, such as the accumulation of CO_2 in the atmosphere. Although there are CO_2 emissions from biofuel combustion, the absorption of this emission by biofuel crops helps maintain CO_2 levels. Therefore, biodiesel combustion can be considered a source of lower neat CO_2 emission than diesel fuel.

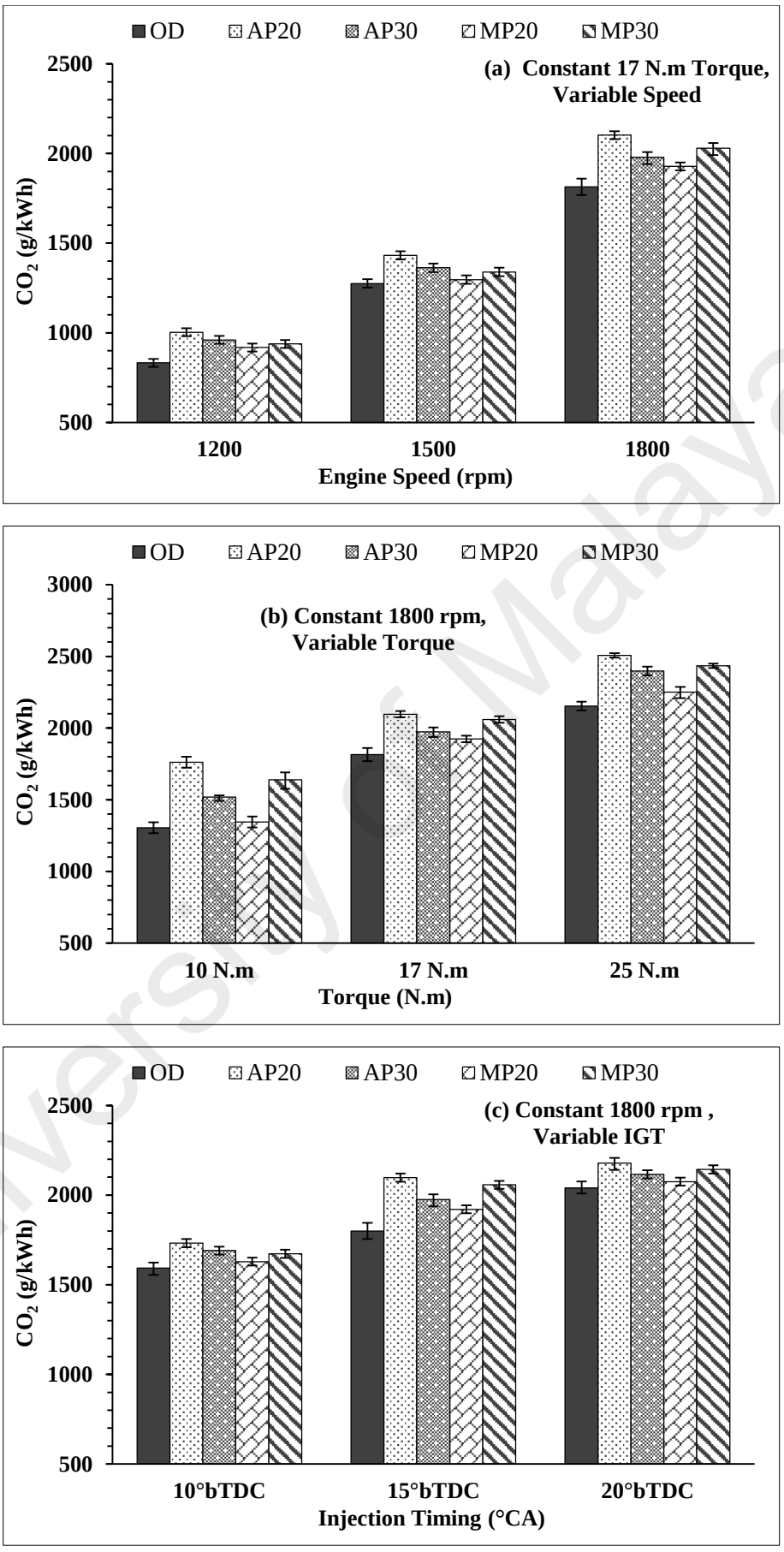

Figure 4.21: CO_2 emission at different operating condition

4.5.3.4 Unburned hydrocarbon emission (HC)

The reasonable factors that creates the HC emission for petrodiesel are fuel trapping in the crevice volume of combustion (Imtenan et al., 2015), low temperature bulk quenching of oxidation reaction , locally over-lean or over-rich mixture, liquid wall filaments for excessive spray impingement and incomplete fuel evaporation (Heywood, 1988). The Figure 4.22 illustrated that HC emission variation for (a) variable engine speeds at constant torque (b) variable torque at constant engine speed and (c) variable injection timing at constant engine speed. This emission can be seen similar CO emission reduction. HC emission for diesel-biodiesel blends found to be lower in all the operating point compared to OD. Reduction of HC for biodiesel blends probably due to the presence of inborn oxygen the reduction of incomplete combustion. Shorter ignition delay of the ester fuels may also have an effect on reduction of HC (Kinoshita et al., 2007). HC emission gradually decreases with (a) increasing engine speed and (b) torque. This results also can be attributed to high in-cylinder temperature due to the high in cylinder pressure, hence better combustion (Shancita et al., 2016). Maximum HC emission for diesel, AP20, AP30, MP20 and MP30 were recorded at 10 N.m. torque at constant 1800 rpm engine speed. On average biodiesel blends provide, 4.46-10.56% reduced HC emission compared to OD whereas individually AP biodiesel blends provide 7.45%.

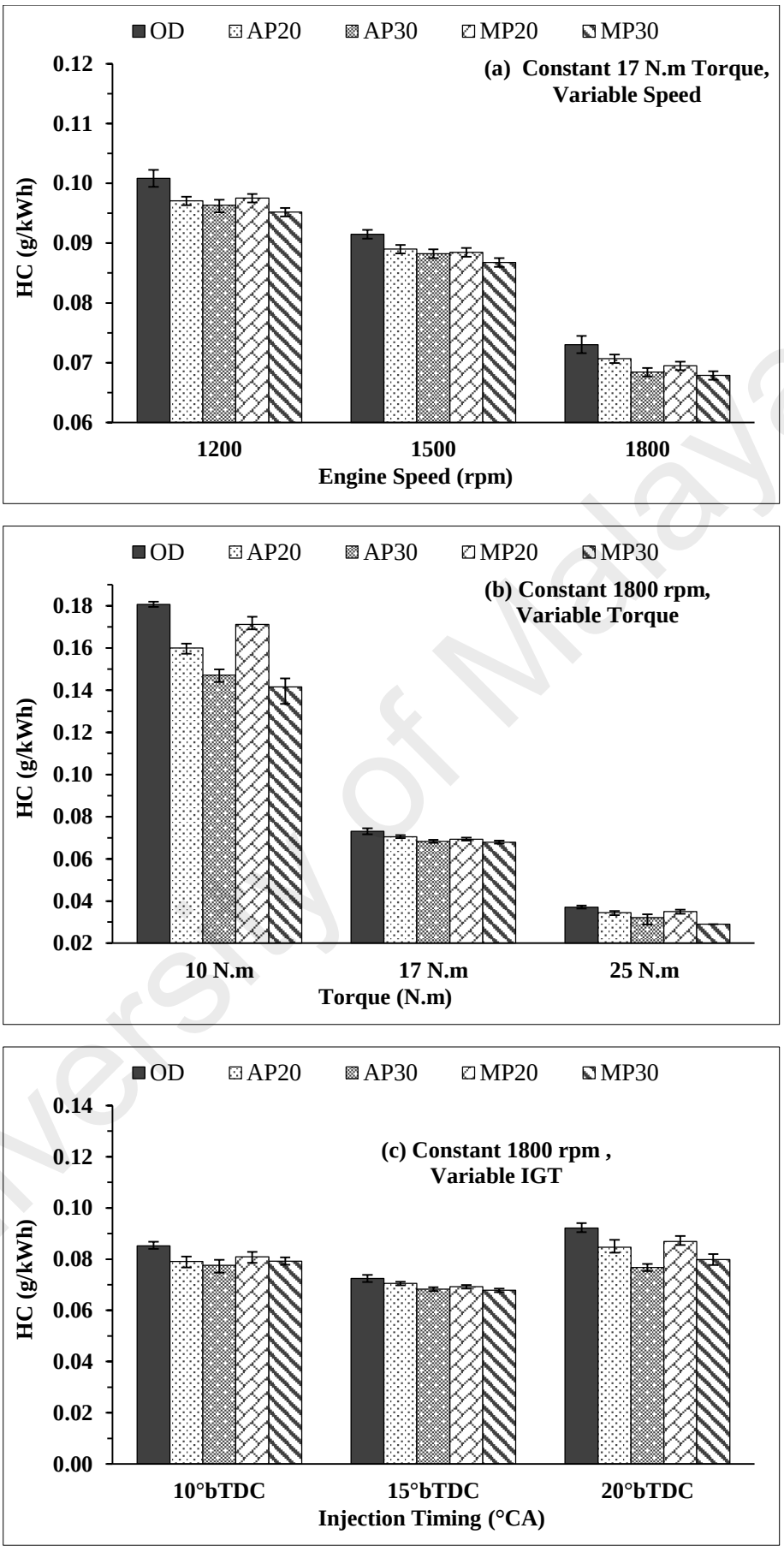

Figure 4.22: HC emission at different operating condition

4.6 Summary

This chapter discussed the characterization of the developed heterogeneous catalyst as well as the biodiesel production process optimization employing that heterogeneous catalyst by response surface methodology. The catalytic property of the eggshell extracted heterogeneous catalyst was confirmed by the TGA, FTIR, EDX, and X-RD characterization. The developed catalyst was utilized in the transesterification stage. The biodiesel production process was optimized with RSM and then justified the model with ANOVA analysis. Then major physical and chemical properties of the optimized biodiesel as well as other tested fuel (diesel-biodiesel blend) are discussed. Engine performance, combustion and emission characteristics of biodiesel blends are also investigated and reported. It can be seen that 20% diesel-biodiesel blends are provided very close performance, combustion behavior to OD and acceptable emission range with an automotive application. Thus this 20% *A. polystachya* can substitute the conventional diesel fuel.

CHAPTER 5: CONCLUSIONS

5.1 Introduction

In this study, a heterogeneous catalyst namely Egg CaO produced from the waste eggshell. Characterization of the produced catalyst has been done through FTIR, TGA, SEM, EDX and XRD analysis to confirm the catalytic activity very near to the commercially available Pure CaO. This developed catalyst was employed in the transesterification step of biodiesel production process from the low-quality vegetable oil namely *A. polystachya.* Central composite design (CCD) based response surface methodology (RSM) was employed to optimize both the acid esterification and alkali transesterification. Various important physicochemical properties of optimized *A. polystachya* methyl ester and *M. pinnata* methyl ester, as well as their 20% and 30% blends have been investigated and compared with OD. The quality of the fuels has been evaluated in a light duty single cylinder diesel engine in the context of performance, combustion and emission characteristics.

5.2 Conclusion

The following conclusions can be drawn from the study:-

1. The Eggshell extracted and developed heterogeneous catalysts basic strength was found 9.8<H_<10.1 which is heigher than other eggshell like quail eggshell. The significance of the catalyst might be in waste management and utilization is biodiesel technology.
    a. Egg CaO catalyst yield was found 57% of raw uncalcined eggshell powder.
    b. Calcium was found as the major element from EDX analysis which was re-confirmed by XRD analysis having CaO and its compound. Thus it has the potentiality as the catalyst.

2. Product yield after the degumming stage, esterification and transesterification stage were recorded 97.12%, 96.53% and 97.5% respectively, which is 91.4% of CAPO. Optimized *A. polystachya* biodiesel physicochemical properties and its blends properties are confirms by the ASTM limit which can play a great role to substitute the fossil diesel.
    a. For both esterification and the transesterification step quadratic model was the suggested and 0.95 desirability of the model was confirmed by the ANOVA analysis.
    b. Only a 0.64% of COV and 0.41% error was found between the predicted yield by model and experimental yield at the optimal condition for esterification and transesterification step respectively, which ensures the model desirability level. Obtained desirability level more than 0.954 is very satisfactory.
    c. Degumming with 3% (v/v) phosphoric acid (H_3PO_4) is compulsory for low-quality *Aphanamixis polystachya* oil before undergoes through the esterification.
    d. A higher percentage of degree of saturation level is the main reason for higher CN and higher oxygen stability. AP provides slightly lower CN and oxygen stability compared to MP, owing 4% lower saturated and 15% higher polyunsaturated FAME.
3. The performance, combustion and emission parameter are deferrers because of engine operating condition and varies a bit between fuel to fuel, owing to their physicochemical properties. HHV, density, viscosity, flash point and cetane number ate the key parameter that is directly responsible for performance, combustion and emission behavior.
    a. AP diesel-biodiesel blends were provided slightly lower BP and higher BSFC (about 1.17-2.09%) compared to OD, mainly owing to their lower HHV, higher density and viscosity. BTE slightly lowered (1.22-0.33%) because of their

relatively poor fuel atomization behavior (low volatility or high flash point) and inferior energy release capability i.e. chemical energy to heat energy.

b. Higher the CN number the higher the combustion quality thus AP blends showed inferior combustion quality than MP blends which refer to shorter ignition delay and shorter combustion duration and peak heat release rate.
c. The average NO emission and CO_2 emission were 2.93-5.47% and 8.61-17.23% higher respectively, found for AP biodiesel blends compared to OD because of higher combustion temperature (high in-cylinder pressure).
d. The CO and HC emissions were reduced to the extent of 13.90-14.27% and 4.03-10.09% for AP biodiesel blends, compared to OD due to the presence of fuel-borne oxygen content in biodiesel.

Beyond the CO_2 emission and oxygen stability, among the all tested fuels, AP20 can be considered as the suitable substitute for petroleum diesel. Further research should be carried out to improve the stability and to find the optimal blending ratio of *Aphanamixis polystachya* biodiesel without sacrificing the engine performance, engine lifetime and green environment.

5.3 Recommendations

Based on this study and above conclusions, the following recommendation can be drawn for the continuation of this study.

- This study only focused on the catalyst extraction thus it is recommended to study on maximizing the surface area improvement through ball milling and basic strength improvement of the Egg CaO by Li or KBr impregnation for biodiesel technology.
- Some other production technology rather than conventional transesterification process is recommended to minimize the reaction time, especially microwave-assisted technology.
- Catalyst recovery and other chemical recovery technolog, as well as the reuse of the catalyst, are recommended for further study.
- As the crude oil possess higher viscosity thus the lubrication, thermal stability and oxidation degradation can be studied. Egg CaO can be utilized as nano-additives to study the improvement of tribological behavior.
- Antioxidant treatment is recommended to improve the oxygen stability of biodiesel and uncontrolled emission as well as the PM and soot emission for further investigation.

REFERENCES

Abedin, M., Imran, A., Masjuki, H., Kalam, M., Shahir, S., Varman, M., & Ruhul, A. (2016). An overview on comparative engine performance and emission characteristics of different techniques involved in diesel engine as dual-fuel engine operation. *Renewable and Sustainable Energy Reviews, 60*, 306-316.

Agarwal, A. K. (2007). Biofuels (alcohols and biodiesel) applications as fuels for internal combustion engines. *Progress in Energy and Combustion Science, 33*(3), 233-271.

Alexander, C., & Hurt, C. (2007). *Biofuels and their impact on food prices*: Purdue University Cooperative Extension Service.

Ali, M. M., Yunus, R., Cheng, C., & Gimbun, J. (2015). Successive optimisation of waste cooking oil transesterification in a continuous microwave assisted reactor. *RSC Advances, 5*(94), 76743-76751.

Allen, C. M., Toulson, E., Hung, D. L., Schock, H., Miller, D., & Lee, T. (2011). Ignition characteristics of diesel and canola biodiesel sprays in the low-temperature combustion regime. *Energy & Fuels, 25*(7), 2896-2908.

Aransiola, E., Ojumu, T., Oyekola, O., Madzimbamuto, T., & Ikhu-Omoregbe, D. (2014). A review of current technology for biodiesel production: state of the art. *Biomass and bioenergy, 61*, 276-297.

Arbab, M. I., Masjuki, H. H., Varman, M., Kalam, M. A., Sajjad, H., & Imtenan, S. (2014). Performance and emission characteristics of a diesel engine fueled by an optimum biodiesel-biodiesel blend. *RSC Advances, 4*(70), 37122-37129.

Atabani, A., Mahlia, T., Masjuki, H., Badruddin, I. A., Yussof, H. W., Chong, W., & Lee, K. T. (2013). A comparative evaluation of physical and chemical properties of biodiesel synthesized from edible and non-edible oils and study on the effect of biodiesel blending. *Energy, 58*, 296-304.

Atabani, A., Silitonga, A., Ong, H., Mahlia, T., Masjuki, H., Badruddin, I. A., & Fayaz, H. (2013). Non-edible vegetable oils: a critical evaluation of oil extraction, fatty acid compositions, biodiesel production, characteristics, engine performance and emissions production. *Renewable and Sustainable Energy Reviews, 18*, 211-245.

Atadashi, I., Aroua, M., & Aziz, A. A. (2010). High quality biodiesel and its diesel engine application: a review. *Renewable and Sustainable Energy Reviews, 14*(7), 1999-2008.

Atadashi, I. M., Aroua, M. K., & Abdul Aziz, A. (2010). High quality biodiesel and its diesel engine application: A review. *Renewable and Sustainable Energy Reviews, 14*(7), 1999-2008.

Ates, F., & Erginel, N. (2016). Optimization of bio-oil production using response surface methodology and formation of polycyclic aromatic hydrocarbons (PAHs) at elevated pressures. *Fuel Processing Technology, 142*, 279-286.

Aydin, H., & Bayindir, H. (2010). Performance and emission analysis of cottonseed oil methyl ester in a diesel engine. *Renewable Energy, 35*(3), 588-592.

Bala, D. D., De Souza, K., Misra, M., & Chidambaram, D. (2015). Conversion of a variety of high free fatty acid containing feedstock to biodiesel using solid acid supported catalyst. *Journal of Cleaner Production, 104*, 273-281.

Balat, M. (2011a). Potential alternatives to edible oils for biodiesel production–A review of current work. *Energy Conversion and Management, 52*(2), 1479-1492.

Balat, M. (2011). Potential alternatives to edible oils for biodiesel production - A review of current work. *Energy Conversion and Management, 52*(2), 1479-1492.

Balat, M. (2011b). Potential alternatives to edible oils for biodiesel production – A review of current work. *Energy Conversion and Management, 52*(2), 1479-1492.

Balat, M., & Balat, H. (2010). Progress in biodiesel processing. *Applied Energy, 87*(6), 1815-1835.

Benjumea, P., Agudelo, J. R., & Agudelo, A. F. (2010). Effect of the degree of unsaturation of biodiesel fuels on engine performance, combustion characteristics, and emissions. *Energy & Fuels, 25*(1), 77-85.

Boehman, A. L., Morris, D., Szybist, J., & Esen, E. (2004). The impact of the bulk modulus of diesel fuels on fuel injection timing. *Energy & Fuels, 18*(6), 1877-1882.

Boro, J., Konwar, L. J., & Deka, D. (2014). Transesterification of non edible feedstock with lithium incorporated egg shell derived CaO for biodiesel production. *Fuel Processing Technology, 122*, 72-78.

Buyukkaya, E., Benli, S., Karaaslan, S., & Guru, M. (2013). Effects of trout-oil methyl ester on a diesel engine performance and emission characteristics. *Energy Conversion and Management, 69*, 41-48.

Can, Ö. (2014). Combustion characteristics, performance and exhaust emissions of a diesel engine fueled with a waste cooking oil biodiesel mixture. *Energy Conversion and Management, 87*, 676-686.

Canakci, M. (2007). Combustion characteristics of a turbocharged DI compression ignition engine fueled with petroleum diesel fuels and biodiesel. *Bioresource technology, 98*(6), 1167-1175.

Canakci, M., & Sanli, H. (2008). Biodiesel production from various feedstocks and their effects on the fuel properties. *Journal of industrial microbiology & biotechnology, 35*(5), 431-441.

Casey, T. (2010). "The Smell of Change is in the Air with Renewable Biodiesel from Sewage". *Scientific American.*

Chakraborty, R., Bepari, S., & Banerjee, A. (2011). Application of calcined waste fish (Labeo rohita) scale as low-cost heterogeneous catalyst for biodiesel synthesis. *Bioresource technology, 102*(3), 3610-3618.

Chen, G., Shan, R., Li, S., & Shi, J. (2015). A biomimetic silicification approach to synthesize CaO-SiO2 catalyst for the transesterification of palm oil into biodiesel. *Fuel, 153*, 48-55.

Chen, Z., Wu, Z., Liu, J., & Lee, C. (2014). Combustion and emissions characteristics of high n-butanol/diesel ratio blend in a heavy-duty diesel engine and EGR impact. *Energy Conversion and Management, 78*, 787-795.

Colucci, J. A., Borrero, E. E., & Alape, F. (2005). Biodiesel from an alkaline transesterification reaction of soybean oil using ultrasonic mixing. *Journal of the American Oil Chemists' Society, 82*(7), 525-530.

Demirbas, A. (2009). Progress and recent trends in biodiesel fuels. *Energy conversion and management, 50*(1), 14-34.

Deng, X., Fang, Z., Liu, Y.-h., & Yu, C.-L. (2011). Production of biodiesel from Jatropha oil catalyzed by nanosized solid basic catalyst. *Energy, 36*(2), 777-784.

Devan, P., & Mahalakshmi, N. (2009). A study of the performance, emission and combustion characteristics of a compression ignition engine using methyl ester of paradise oil–eucalyptus oil blends. *Applied Energy, 86*(5), 675-680.

Di Serio, M., Tesser, R., Pengmei, L., & Santacesaria, E. (2007). Heterogeneous catalysts for biodiesel production. *Energy & Fuels, 22*(1), 207-217.

dos Santos, I. C. F., de Carvalho, S. H. V., Solleti, J. I., de La Salles, W. F., de La Salles, K. T. S., & Meneghetti, S. M. P. (2008). Studies of Terminalia catappa L. oil: Characterization and biodiesel production. *Bioresource Technology, 99*(14), 6545-6549.

Du, W., Xu, Y., Liu, D., & Zeng, J. (2004). Comparative study on lipase-catalyzed transformation of soybean oil for biodiesel production with different acyl acceptors. *Journal of Molecular Catalysis B: Enzymatic, 30*(3), 125-129.

Edward P. Glenn, J. J. B. a. J. W. O. L. Irrigating Crops with Seawater.

Encinar, J., Gonzalez, J., Rodriguez, J., & Tejedor, A. (2002). Biodiesel fuels from vegetable oils: transesterification of Cynara c ardunculus L. oils with ethanol. *Energy & fuels, 16*(2), 443-450.

Fattah, I. R., Masjuki, H., Kalam, M., Wakil, M., Ashraful, A., & Shahir, S. A. (2014). Experimental investigation of performance and regulated emissions of a diesel engine with Calophyllum inophyllum biodiesel blends accompanied by oxidation inhibitors. *Energy Conversion and Management, 83*, 232-240.

Ferdous, K., Deb, A., Ferdous, J., Uddin, M. R., Khan, M. R., & Islam, M. (2014). Aphanamixis polystachya: a potential non-edible source of biodiesel in Bangladesh. *Journal of Chemical Engineering, 28*(1), 45-49.

Fernando, S., Karra, P., Hernandez, R., & Jha, S. K. (2007). Effect of incompletely converted soybean oil on biodiesel quality. *Energy, 32*(5), 844-851.

Fortes, I., & Baugh, P. (2004). Pyrolysis–GC/MS studies of vegetable oils from Macauba fruit. *Journal of analytical and applied pyrolysis, 72*(1), 103-111.

Freedman, B., Pryde, E., & Mounts, T. (1984). Variables affecting the yields of fatty esters from transesterified vegetable oils. *Journal of the American Oil Chemists Society, 61*(10), 1638-1643.

Frei, D., Liebscher, A., Franz, G., Wunder, B., Klemme, S., & Blundy, J. (2008). Trace element partitioning between orthopyroxene and anhydrous silicate melt on the lherzolite solidus from 1.1 to 3.2 GPa and 1,230 to 1,535°C in the model system Na2O–CaO–MgO–Al2O3–SiO2. *Contributions to Mineralogy and Petrology, 157*(4), 473.

Gao, L., Teng, G., Xiao, G., & Wei, R. (2010). Biodiesel from palm oil via loading KF/Ca–Al hydrotalcite catalyst. *Biomass and bioenergy, 34*(9), 1283-1288.

Gardner, B. (2003). Fuel ethanol subsidies and farm price support: Boon or boondoggle? *Work. Pap*(28599).

Gowda, B. (2014). Evaluation of Aphanamixis polystachya (Wall.) R. Parker as a potential source of biodiesel. *Journal of Biochemical Technology, 3*(5), S128-S133.

Granados, M. L., Poves, M. Z., Alonso, D. M., Mariscal, R., Galisteo, F. C., Moreno-Tost, R., . . . Fierro, J. (2007). Biodiesel from sunflower oil by using activated calcium oxide. *Applied Catalysis B: Environmental, 73*(3), 317-326.

Gumus, M., Sayin, C., & Canakci, M. (2012). The impact of fuel injection pressure on the exhaust emissions of a direct injection diesel engine fueled with biodiesel–diesel fuel blends. *Fuel, 95*, 486-494.

Gürü, M., Koca, A., Can, Ö., Çınar, C., & Şahin, F. (2010). Biodiesel production from waste chicken fat based sources and evaluation with Mg based additive in a diesel engine. *Renewable Energy, 35*(3), 637-643.

Habibullah, M., Rizwanul Fattah, I., Masjuki, H., & Kalam, M. (2015). Effects of palm–coconut biodiesel blends on the performance and emission of a single-cylinder diesel engine. *Energy & Fuels, 29*(2), 734-743.

Heywood, J. (1988). *Internal combustion engine fundamentals*: McGraw-Hill Education.

Heywood, J. B. (1988). *Internal combustion engine fundamentals* (Vol. 930): Mcgraw-hill New York.

Heywood, J. B., Higgins, J. M., Watts, P. A., & Tabaczynski, R. J. (1979). *Development and Use of a Cycle Simulation to Predict SI Engine Efficiency and NOx Emissions*.

How, H. G., Masjuki, H. H., Kalam, M. A., & Teoh, Y. H. (2014). An investigation of the engine performance, emissions and combustion characteristics of coconut biodiesel in a high-pressure common-rail diesel engine. *Energy, 69*, 749-759.

Huang, Z., Teh, S. K., Zheng, W., Lin, K., Ho, K. Y., Teh, M., & Yeoh, K. G. (2010). In vivo detection of epithelial neoplasia in the stomach using image-guided Raman endoscopy. *Biosensors and Bioelectronics, 26*(2), 383-389.

Imtenan, S., Masjuki, H., Varman, M., & Fattah, I. R. (2015). Evaluation of n-butanol as an oxygenated additive to improve combustion-emission-performance characteristics of a diesel engine fuelled with a diesel-calophyllum inophyllum biodiesel blend. *RSC Advances, 5*(22), 17160-17170.

Imtenan, S., Masjuki, H., Varman, M., Fattah, I. R., Sajjad, H., & Arbab, M. (2015). Effect of n-butanol and diethyl ether as oxygenated additives on combustion–emission-performance characteristics of a multiple cylinder diesel engine fuelled with diesel–jatropha biodiesel blend. *Energy Conversion and Management, 94*, 84-94.

Imtenan, S., Masjuki, H. H., Varman, M., Kalam, M. A., Arbab, M. I., Sajjad, H., & Ashrafur Rahman, S. M. (2014). Impact of oxygenated additives to palm and jatropha biodiesel blends in the context of performance and emissions characteristics of a light-duty diesel engine. *Energy Conversion and Management, 83*, 149-158.

Jaggernauth-Ali, P., John, E., & Bridgemohan, P. (2015). The application of calcined marlstones as a catalyst in biodiesel production from high free fatty acid coconut oil. *Fuel, 158*, 372-378.

Ji, J., Wang, J., Li, Y., Yu, Y., & Xu, Z. (2006). Preparation of biodiesel with the help of ultrasonic and hydrodynamic cavitation. *Ultrasonics, 44*, e411-e414.

Jonathan, L. (2017). B10 biodiesel is cleaner, better for engines – MPIC Retrieved 09th January, 2017, from http://paultan.org/2017/01/09/b10-biodiesel-is-cleaner-better-for-engines-mpic/

Joshi, G., Rawat, D. S., Lamba, B. Y., Bisht, K. K., Kumar, P., Kumar, N., & Kumar, S. (2015). Transesterification of Jatropha and Karanja oils by using waste egg shell derived calcium based mixed metal oxides. *Energy Conversion and Management, 96*(0), 258-267.

Kafuku, G., Lam, M. K., Kansedo, J., Lee, K. T., & Mbarawa, M. (2010). Croton megalocarpus oil: A feasible non-edible oil source for biodiesel production. *Bioresource Technology*, *101*(18), 7000-7004.

Kahn Ribeiro, S., S. Kobayashi, M. Beuthe, J. Gasca, D. Greene, D. S. Lee, Y. Muromachi, P. J. Newton, S. Plotkin, D. Sperling, R. Wit, , & P. J. Zhou. (2007). Climate Change 2007: Working Group III: Mitigation of Climate Change. In H. K. U. Ranjan Bose (India) (Ed.). Cambridge, United Kingdom and New York, NY, USA.

Kannan, D., Pachamuthu, S., Nabi, M. N., Hustad, J. E., & Løvås, T. (2012). Theoretical and experimental investigation of diesel engine performance, combustion and emissions analysis fuelled with the blends of ethanol, diesel and jatropha methyl ester. *Energy Conversion and Management, 53*(1), 322-331.

Kapilan, N., & Baykov, B. D. (2014). A review on new methods used for the production of biodiesel. *Pet Coal, 56*(1), 62-73.

Karim, M. Z., Chowdhury, Z. Z., Hamid, S. B. A., & Ali, M. E. (2014). Statistical optimization for acid hydrolysis of microcrystalline cellulose and its physiochemical characterization by using metal ion catalyst. *Materials, 7*(10), 6982-6999.

Kawashima, A., Matsubara, K., & Honda, K. (2009). Acceleration of catalytic activity of calcium oxide for biodiesel production. *Bioresource Technology, 100*(2), 696-700.

Kaya, C., Hamamci, C., Baysal, A., Akba, O., Erdogan, S., & Saydut, A. (2009). Methyl ester of peanut (Arachis hypogea L.) seed oil as a potential feedstock for biodiesel production. *Renewable Energy, 34*(5), 1257-1260.

Khan, J. H., Hussain, M. A., & Mujtaba, I. M. (2014). Polypropylene production optimization in fluidized bed catalytic reactor (FBCR): Statistical modeling and pilot scale experimental validation. *Materials, 7*(4), 2440-2458.

Kinoshita, E., Myo, T., Hamasaki, K., & Nishi, S. (2007). Combustion characteristics of diesel engine with coconut oil ethyl ester: SAE Technical Paper.

Knothe, G. (2007). Some aspects of biodiesel oxidative stability. *Fuel Processing Technology, 88*(7), 669-677.

Kouzu, M., Kasuno, T., Tajika, M., Yamanaka, S., & Hidaka, J. (2008). Active phase of calcium oxide used as solid base catalyst for transesterification of soybean oil with refluxing methanol. *Applied Catalysis A: General, 334*(1), 357-365.

Krisnangkura, K. (1986). A simple method for estimation of cetane index of vegetable oil methyl esters. *Journal of the American Oil Chemists Society, 63*(4), 552-553.

Kumar, N., & Chauhan, S. R. (2013). Performance and emission characteristics of biodiesel from different origins: a review. *Renewable and Sustainable Energy Reviews, 21*, 633-658.

Kumar, N., Varun, & Chauhan, S. R. (2013). Performance and emission characteristics of biodiesel from different origins: A review. *Renewable and Sustainable Energy Reviews, 21*(0), 633-658.

Lam, M. K., Lee, K. T., & Mohamed, A. R. (2010). Homogeneous, heterogeneous and enzymatic catalysis for transesterification of high free fatty acid oil (waste cooking oil) to biodiesel: a review. *Biotechnology advances, 28*(4), 500-518.

Lappi, H., & Alén, R. (2011). Pyrolysis of vegetable oil soaps—palm, olive, rapeseed and castor oils. *Journal of Analytical and Applied Pyrolysis, 91*(1), 154-158.

Lapuerta, M., Armas, O., & Rodriguez-Fernandez, J. (2008). Effect of biodiesel fuels on diesel engine emissions. *Progress in energy and combustion science, 34*(2), 198-223.

Lee, H. V., Yunus, R., Juan, J. C., & Taufiq-Yap, Y. H. (2011). Process optimization design for jatropha-based biodiesel production using response surface methodology. *Fuel Processing Technology, 92*(12), 2420-2428.

Lee, S. B., Lee, J. D., & Hong, I. K. (2011). Ultrasonic energy effect on vegetable oil based biodiesel synthetic process. *Journal of Industrial and Engineering Chemistry, 17*(1), 138-143.

Leonard, C. (2007). Not a Tiger, but Maybe a Chicken in Your Tank.

Leung, D., & Guo, Y. (2006). Transesterification of neat and used frying oil: optimization for biodiesel production. *Fuel Processing Technology, 87*(10), 883-890.

Leung, D. Y., Wu, X., & Leung, M. (2010). A review on biodiesel production using catalyzed transesterification. *Applied energy, 87*(4), 1083-1095.

Li, Z., Deng, L., Lu, J., Guo, X., Yang, Z., & Tan, T. (2010). Enzymatic Synthesis of Fatty Acid Methyl Esters from Crude Rice Bran Oil with Immobilized Candida. *Chinese Journal of Chemical Engineering, 18*(5), 870-875.

Lima, D. G., Soares, V. C., Ribeiro, E. B., Carvalho, D. A., Cardoso, É. C., Rassi, F. C., . . . Suarez, P. A. (2004). Diesel-like fuel obtained by pyrolysis of vegetable oils. *Journal of Analytical and Applied Pyrolysis, 71*(2), 987-996.

Lin, L., Ying, D., Chaitep, S., & Vittayapadung, S. (2009). Biodiesel production from crude rice bran oil and properties as fuel. *Applied Energy, 86*(5), 681-688.

Lin, L., Zhou, C., Saritporn, V., Shen, X., & Dong, M. (2011). Opportunities and challenges for biodiesel fuel. *Applied Energy, 88*(4), 1020-1031

Liu, H., Su, L., Shao, Y., & Zou, L. (2012). Biodiesel production catalyzed by cinder supported CaO/KF particle catalyst. *Fuel, 97*, 651-657.

Liu, W., Yin, P., Liu, X., Zhang, S., & Qu, R. (2015). Biodiesel production from the esterification of fatty acid over organophosphonic acid. *Journal of Industrial and Engineering Chemistry, 21*, 893-899.

Lyn, W., & Valdmanis, E. (1968). The effects of physical factors on ignition delay: SAE Technical Paper.

Ma, F., Clements, L. D., & Hanna, M. A. (1999). The effect of mixing on transesterification of beef tallow. *Bioresource Technology, 69*(3), 289-293.

Ma, F., & Hanna, M. A. (1999). Biodiesel production: a review. *Bioresource technology, 70*(1), 1-15.

Madhu, D., Singh, B., & Sharma, Y. C. (2014). Studies on application of fish waste for synthesis of high quality biodiesel. *RSC Advances, 4*(59), 31462-31468.

Maher, K. D., & Bressler, D. C. (2007). Pyrolysis of triglyceride materials for the production of renewable fuels and chemicals. *Bioresource technology, 98*(12), 2351-2368.

Malaysian Biodiesel Association. (Access date 29th December 2016).

Maneechakr, P., Samerjit, J., & Karnjanakom, S. (2015). Ultrasonic-assisted biodiesel production from waste cooking oil over novel sulfonic functionalized carbon spheres derived from cyclodextrin via one-step: a way to produce biodiesel at short reaction time. *RSC Advances, 5*(68), 55252-55261.

Mason, R. L., Gunst, R. F., & Hess, J. L. (2003). *Statistical design and analysis of experiments: with applications to engineering and science* (Vol. 474): John Wiley & Sons.

Meher, L., Dharmagadda, V. S., & Naik, S. (2006). Optimization of alkali-catalyzed transesterification of Pongamia pinnata oil for production of biodiesel. *Bioresource technology, 97*(12), 1392-1397.

Miller, R. G. (2011). Future oil supply: The changing stance of the International Energy Agency. *Energy Policy, 39*(3), 1569-1574.

Mittelbach, M., & Remschmidt, C. (2004). *Biodiesel: the comprehensive handbook*: Martin Mittelbach.

Montgomery, D. C. (2008). *Design and analysis of experiments*: John Wiley & Sons.

Moradi, G., Mohadesi, M., Ghanbari, M., Moradi, M., Hosseini, S., & Davoodbeygi, Y. (2015). Kinetic comparison of two basic heterogenous catalysts obtained from sustainable resources for transesterification of waste cooking oil. *Biofuel Research Journal, 2*(2), 236-241.

Moser, B. R., & Vaughn, S. F. (2010). Coriander seed oil methyl esters as biodiesel fuel: unique fatty acid composition and excellent oxidative stability. *Biomass and bioenergy, 34*(4), 550-558.

Murillo, S., Miguez, J., Porteiro, J., Granada, E., & Moran, J. (2007). Performance and exhaust emissions in the use of biodiesel in outboard diesel engines. *Fuel, 86*(12), 1765-1771.

Murugesan, A., Umarani, C., Chinnusamy, T., Krishnan, M., Subramanian, R., & Neduzchezhain, N. (2009). Production and analysis of bio-diesel from non-edible oils—a review. *Renewable and Sustainable Energy Reviews, 13*(4), 825-834.

Murugesan, A., Umarani, C., Chinnusamy, T. R., Krishnan, M., Subramanian, R., & Neduzchezhain, N. (2009). Production and analysis of bio-diesel from non-edible oils - A review. *Renewable and Sustainable Energy Reviews, 13*(4), 825-834. doi: DOI: 10.1016/j.rser.2008.02.003

Myers, R. H., Montgomery, D. C., & Anderson-Cook, C. M. (2016). *Response surface methodology: process and product optimization using designed experiments*: John Wiley & Sons.

Nabi, M. N., Akhter, M. S., & Shahadat, M. M. Z. (2006). Improvement of engine emissions with conventional diesel fuel and diesel–biodiesel blends. *Bioresource Technology, 97*(3), 372-378.

Nakatani, N., Takamori, H., Takeda, K., & Sakugawa, H. (2009). Transesterification of soybean oil using combusted oyster shell waste as a catalyst. *Bioresource Technology, 100*(3), 1510-1513.

Ndayishimiye, P., & Tazerout, M. (2011). Use of palm oil-based biofuel in the internal combustion engines: performance and emissions characteristics. *Energy, 36*(3), 1790-1796.

Nettles-Anderson, S. L., & Olsen, D. B. (2009). Survey of straight vegetable oil composition impact on combustion properties: SAE Technical Paper.

Niju, S., Begum, K. M. M. S., & Anantharaman, N. (2015). Preparation of biodiesel from waste frying oil using a green and renewable solid catalyst derived from egg shell. *Environmental Progress and Sustainable Energy, 34*(1), 248-254.

Niju, S., Meera, K., Begum, S., & Anantharaman, N. (2014). Modification of egg shell and its application in biodiesel production. *Journal of Saudi Chemical Society, 18*(5), 702-706.

Nik, W. W., Ani, F., & Masjuki, H. (2005). Thermal stability evaluation of palm oil as energy transport media. *Energy Conversion and Management, 46*(13), 2198-2215.

Omidvarborna, H., Kumar, A., & Kim, D.-S. (2015). NO x emissions from low-temperature combustion of biodiesel made of various feedstocks and blends. *Fuel Processing Technology, 140*, 113-118.

Öner, C., & Altun, Ş. (2009). Biodiesel production from inedible animal tallow and an experimental investigation of its use as alternative fuel in a direct injection diesel engine. *Applied Energy, 86*(10), 2114-2120.

Ong, H. C., Masjuki, H. H., Mahlia, T. M. I., Silitonga, A. S., Chong, W. T., & Leong, K. Y. (2014). Optimization of biodiesel production and engine performance from high free fatty acid Calophyllum inophyllum oil in CI diesel engine. *Energy Conversion and Management, 81*, 30-40.

Ozsezen, A. N., & Canakci, M. (2011). Performance and combustion characteristics of alcohol–gasoline blends at wide-open throttle. *Energy, 36*(5), 2747-2752.

Ozsezen, A. N., Canakci, M., & Sayin, C. (2008). Effects of biodiesel from used frying palm oil on the performance, injection, and combustion characteristics of an indirect injection diesel engine. *Energy & Fuels, 22*(2), 1297-1305.

Palash, S. M., Masjuki, H. H., Kalam, M. A., Atabani, A. E., Rizwanul Fattah, I. M., & Sanjid, A. (2015). Biodiesel production, characterization, diesel engine performance, and emission characteristics of methyl esters from Aphanamixis

polystachya oil of Bangladesh. *Energy Conversion and Management, 91*, 149-157.

Park, S. H., Cha, J., & Lee, C. S. (2012). Impact of biodiesel in bioethanol blended diesel on the engine performance and emissions characteristics in compression ignition engine. *Applied Energy, 99*, 334-343.

Park, Y. M., Lee, J. Y., Chung, S.-H., Park, I. S., Lee, S.-Y., Kim, D.-K., . . . Lee, K.-Y. (2010). Esterification of used vegetable oils using the heterogeneous WO 3/ZrO 2 catalyst for production of biodiesel. *Bioresource technology, 101*(1), S59-S61.

Payri, F., Desantes, J. M., & Benajes, J. (2015). Compression Ignition Engines: State-of-the-Art and Current Technologies. Future Trends and Developments. *Handbook of Clean Energy Systems*.

Puhan, S., Saravanan, N., Nagarajan, G., & Vedaraman, N. (2010). Effect of biodiesel unsaturated fatty acid on combustion characteristics of a DI compression ignition engine. *Biomass and bioenergy, 34*(8), 1079-1088.

Raj, F. R. M. S., & Sahayaraj, J. W. (2010). *A Comparative Study over Alternative Fuel (Biodiesel) for Environmental Friendly Emission.* Paper presented at the Recent Advances in Space Technology Services and Climate Change (RSTSCC), Chennai, India.

Rizwanul Fattah, I. M., Kalam, M. A., Masjuki, H. H., & Wakil, M. A. (2014). Biodiesel production, characterization, engine performance, and emission characteristics of Malaysian Alexandrian laurel oil. *RSC Advances, 4*(34), 17787-17796.

Sanford, S. D., White, J. M., Shah, P. S., Wee, C., Valverde, M. A., & Meier, G. R. (2009). Feedstock and Biodiesel Characteristics Report Retrieved 21th January, 2012, from http://www.biodiesel.org/resources/reportsdatabase/reports/gen/20091117_GEN-398.pdf

Sanford, S. D., White, J. M., Shah, P. S., Wee, C., Valverde, M. A., & Meier, G. R. (2009). Feedstock and Biodiesel Characteristics Report Retrieved 21th January, 2012., from From http://www.biodiesel.org/resources/reportsdatabase/reports/gen/20091117_GEN-398.pdf

Sanjid, A., Masjuki, H., Kalam, M., Rahman, S. A., Abedin, M., Reza, M., & Sajjad, H. (2014). Experimental investigation of palm-jatropha combined blend properties, performance, exhaust emission and noise in an unmodified diesel engine. *Procedia Engineering, 90*, 397-402.

Saxena, P., Jawale, S., & Joshipura, M. H. (2013a). A Review on Prediction of Properties of Biodiesel and Blends of Biodiesel. *Procedia Engineering, 51*(0), 395-402.

Saxena, P., Jawale, S., & Joshipura, M. H. (2013b). A review on prediction of properties of biodiesel and blends of biodiesel. *Procedia engineering, 51*, 395-402.

Sayin, C. (2010). Engine performance and exhaust gas emissions of methanol and ethanol–diesel blends. *Fuel, 89*(11), 3410-3415.

Sealand Turbo-Diesel Asia Pte Ltd. (2016). Delphi common rail injectors Retrieved 2nd January 2016, from http://www.turbodiesel.com.sg/proddetail.aspx?ID=30&amp

Selin, R. (2013). The Outlook for Energy: A View to 2040.

Semwal, S., Arora, A. K., Badoni, R. P., & Tuli, D. K. (2011). Biodiesel production using heterogeneous catalysts. *Bioresource technology, 102*(3), 2151-2161.

Şensöz, S., Angın, D., & Yorgun, S. (2000). Influence of particle size on the pyrolysis of rapeseed (Brassica napus L.): fuel properties of bio-oil. *Biomass and Bioenergy, 19*(4), 271-279.

Shahabuddin, M., Kalam, M. A., Masjuki, H. H., Bhuiya, M. M. K., & Mofijur, M. (2012). An experimental investigation into biodiesel stability by means of oxidation and property determination. *Energy, 44*(1), 616-622.

Shahabuddin, M., Liaquat, A. M., Masjuki, H. H., Kalam, M. A., & Mofijur, M. (2013). Ignition delay, combustion and emission characteristics of diesel engine fueled with biodiesel. *Renewable and Sustainable Energy Reviews, 21*, 623-632.

Shancita, I., Masjuki, H., Kalam, M., Reham, S., Ruhul, A., & Monirul, I. (2016). Evaluation of the characteristics of non-oxidative biodiesels: a FAME composition, thermogravimetric and IR analysis. *RSC Advances, 6*(10), 8198-8210.

Sharma, Y. C., & Singh, B. (2009). Development of biodiesel: Current scenario. *Renewable and Sustainable Energy Reviews, 13*(6-7), 1646-1651.

Sharon, H., Karuppasamy, K., Kumar, D. S., & Sundaresan, A. (2012). A test on DI diesel engine fueled with methyl esters of used palm oil. *Renewable Energy, 47*, 160-166.

Shukla, P. C., Gupta, T., Labhsetwar, N. K., & Agarwal, A. K. (2015). Physico-chemical speciation of particulates emanating from Karanja biodiesel fuelled automotive engine. *Fuel, 162*, 84-90.

Sieminski, A. (2014). International Energy Outlook. *Energy Information Administration (EIA)*.

Silitonga, A., Masjuki, H., Mahlia, T., Ong, H., Chong, W., & Boosroh, M. (2013). Overview properties of biodiesel diesel blends from edible and non-edible feedstock. *Renewable and Sustainable Energy Reviews, 22*, 346-360.

Silitonga, A. S., Masjuki, H. H., Mahlia, T. M. I., Ong, H. C., Chong, W. T., & Boosroh, M. H. (2013). Overview properties of biodiesel diesel blends from edible and non-edible feedstock. *Renewable and Sustainable Energy Reviews, 22*(0), 346-360.

Singh, S., & Singh, D. (2010). Biodiesel production through the use of different sources and characterization of oils and their esters as the substitute of diesel: a review. *Renewable and Sustainable Energy Reviews, 14*(1), 200-216.

Singh, S. P., & Singh, D. (2010). Biodiesel production through the use of different sources and characterization of oils and their esters as the substitute of diesel: A review. *Renewable and Sustainable Energy Reviews, 14*(1), 200-216.

Sonntag, N. (1979). Composition and characteristics of individual fats and oils. *Bailey's industrial oil and fat products, 1*, 289-477.

. Stat-Ease Handbook for Experimentesrs. 2016, from http://www.statease.com/pubs/handbk_for_exp_sv.pdf

Takase, N., Nozaki, M., Kato, A., Ozeki, H., Yoshida, M., & Ogura, Y. (2015). Enlargement of foveal avascular zone in diabetic eyes evaluated by en face optical coherence tomography angiography. *Retina, 35*(11), 2377-2383.

Tan, Y. H., Abdullah, M. O., & Nolasco-Hipolito, C. (2015). The potential of waste cooking oil-based biodiesel using heterogeneous catalyst derived from various calcined eggshells coupled with an emulsification technique: A review on the emission reduction and engine performance. *Renewable and Sustainable Energy Reviews, 47*, 589-603.

Teng, W. K., Ngoh, G. C., Yusoff, R., & Aroua, M. K. (2016). Microwave-assisted transesterification of industrial grade crude glycerol for the production of glycerol carbonate. *Chemical Engineering Journal, 284*, 469-477.

Teoh, Y., Masjuki, H., Kalam, M., Amalina, M., & How, H. (2013). Impact of waste cooking oil biodiesel on performance, exhaust emission and combustion characteristics in a light-duty diesel engine: SAE Technical Paper.

Tomasevic, A., & Siler-Marinkovic, S. (2003). Methanolysis of used frying oil. *Fuel Processing Technology, 81*(1), 1-6.

Tsai, W. T., Yang, J. M., Lai, C. W., Cheng, Y. H., Lin, C. C., & Yeh, C. W. (2006). Characterization and adsorption properties of eggshells and eggshell membrane. *Bioresource Technology, 97*(3), 488-493.

U. S. Energy Information Administration. (September 9, 2014). International Energy Outlook 2014, Report Number: DOE/EIA-0484(2014). www.eia.gov/ieo.

Uriarte, F. A. J. (2010). Biofuels from Plant Oils Retrieved 24th January 2012., from http://www.aseanfoundation.org/documents/books/biofuel.pdf

Usta, N. (2005). An experimental study on performance and exhaust emissions of a diesel engine fuelled with tobacco seed oil methyl ester. *Energy Conversion and Management, 46*(15–16), 2373-2386.

Veljković, V. B., Stamenković, O. S., Todorović, Z. B., Lazić, M. L., & Skala, D. U. (2009). Kinetics of sunflower oil methanolysis catalyzed by calcium oxide. *Fuel, 88*(9), 1554-1562.

Viriya-empikul, N., Krasae, P., Puttasawat, B., Yoosuk, B., Chollacoop, N., & Faungnawakij, K. (2010). Waste shells of mollusk and egg as biodiesel production catalysts. *Bioresource technology, 101*(10), 3765-3767.

Vyas, A. P., Verma, J. L., & Subrahmanyam, N. (2010). A review on FAME production processes. *Fuel, 89*(1), 1-9.

Witoon, T. (2011). Characterization of calcium oxide derived from waste eggshell and its application as CO 2 sorbent. *Ceramics International, 37*(8), 3291-3298.

Yan, S., Kim, M., Salley, S. O., & Ng, K. Y. S. (2009). Oil transesterification over calcium oxides modified with lanthanum. *Applied Catalysis A: General, 360*(2), 163-170.

Yücel, Y. (2012). Optimization of biocatalytic biodiesel production from pomace oil using response surface methodology. *Fuel Processing Technology, 99*, 97-102.

Zeng, D., Li, R., Yan, T., & Fang, T. (2014). Perspectives and advances of microalgal biodiesel production with supercritical fluid technology. *RSC Advances, 4*(75), 39771-39781.

Zeng, D., Zhang, Q., Chen, S., Liu, S., Chen, Y., Tian, Y., & Wang, G. (2015). Preparation and characterization of a strong solid base from waste eggshell for

biodiesel production. *Journal of Environmental Chemical Engineering, 3*(1), 560-564.

Zhou, W., Konar, S. K., & Boocock, D. G. (2003). Ethyl esters from the single-phase base-catalyzed ethanolysis of vegetable oils. *Journal of the American Oil Chemists' Society, 80*(4), 367-371.

APPENDIX A

Publications

Published Journal Paper:

Ruhul, A. M., Kalam, M. A., Masjuki, H. H., Rizwanul Fattah, I. M., Reham, S. S., & Rashed, M. M. (2015). State of the art of biodiesel production processes: a review of the heterogeneous catalyst. *RSC Advances*, 5(122), 101023-101044. doi: 10.1039/C5RA09862A [**ISI indexed, Q2**]

Ruhul, A. M., Kalam, M. A., Masjuki, H. H., Alabdulkarem, A., Atabani, A. E., Fattah, I. M. R., & Abedin, M. J. (2016). Production, characterization, engine performance and emission characteristics of *Croton megalocarpus* and *Ceiba pentandra* complementary blends in a single-cylinder diesel engine. *RSC Advances*, 6, 24584 - 24595. doi: 10.1039/C5RA21750D [**ISI indexed, Q2**]

Ruhul, A. M., Abedin, M. J., Rahman, S. A. M., Masjuki, H. H., Alabdulkarem, A., Kalam, M. A., Shanchita, I. (2016). Impact of fatty acid composition and physico-chemical properties of Jatropha and Alexandrian laurel biodiesel blends: An analysis of performance and emission characteristics. *Journal of Cleaner Production*, 133, 1181–1189, doi:10.1016/j.jclepro.2016.06.017 **[ISI indexed, Q1]**

Conference paper:

Ruhul, A. M., Kalam, M. A., Masjuki, H. H., Imtenan, S., Sanjid, A., Teoh, Y. H., & How, H. G. Combustion and emission investigation of Calophyllum inophyllum biodiesel blends in an unmodified diesel engine. Paper presented at the Proceedings of the Australian Combustion Symposium, 2015, Melbourne, Australia.

Ruhul, A. M., Masjuki, H. H., Kalam, M. A., Shahir, S. A., Reham, S. S., & Shancita, I. Biodiesel production, properties and emissions test characteristics of non-edible fuels in Diesel engine. Paper presented at the International Conference on Green Technology, 2016, Kota Kinabalu, Sabah, Malaysia.